Development and application of two-dimensional capillary electrophoresis for online mass spectrometry of CE(SDS)-separated proteins

Dissertation

Zur Erlangung des Doktorgrades der Naturwissenschaften (Dr. rer. nat.)

der Fakultät für Chemie und Pharmazie

der Universität Regensburg

vorgelegt von

Jennifer Römer

aus Steinheim am Albuch

im Mai 2021

Die vorgelegte Arbeit entstand im Zeitraum von Februar 2017 bis Mai 2021 an der Hochschule Aalen in Kooperation mit dem Institut für Analytische Chemie, Chemo- und Biosensorik der naturwissenschaftlichen Fakultät IV Chemie und Pharmazie der Universität Regensburg.

Die Arbeit wurde angeleitet durch Prof. Dr. Frank-Michael Matysik und durchgeführt unter der Leitung von Prof. Dr. Christian Neusüß.

Das Promotionsgesuch wurde eingereicht am: 20.05.2021

Termin des Kolloquiums: 23.07.2021

Der Prüfungsausschuss setzt sich zusammen aus:
Vorsitzender: Prof. Dr. Siavosh Mahboobi
Erstgutachter: Prof. Dr. Frank-Michael Matysik
Zweitgutachter: Prof. Dr. Christian Neusüß
Drittprüfer: Dr. Katja Dettmer-Wilde

"Nothing in life is to be feared, it is only to be understood"

Marie Curie

"Chemie Chemie Ya, Chemie Ya, Chemie Yay,

Chemie Chemie, Chemie Chemie"

Kraftklub

Danksagung

Diese Arbeit wäre ohne die Hilfe und Unterstützung von vielen Menschen nicht entstanden. Deshalb möchte ich mich hiermit bei einigen von ihnen aus tiefstem Herzen bedanken.

Der erste Dank geht an Prof. Dr. Christian Neusüß. Ich bin unglaublich dankbar, dass du mir die Möglichkeit gegeben hast, sich dieser Aufgabe anzunehmen. Danke für die zahlreichen Diskussionen und guten Ideen, die stets einen anderen Blick auf das Ganze erlaubten und dadurch sehr wertvoll wurden. Danke, dass ich so viel von dir lernen durfte.

Des Weiteren möchte ich mich aufrichtig bei Prof. Dr. Frank-Michael Matysik für seine Unterstützung und die Aufnahme als Doktorand bedanken.

Ein großes Dankeschön geht an den Prüfungsausschuss, der sich neben Herrn Prof. Dr. Neusüß und Herrn Prof. Dr. Matysik, aus dem Vorsitzenden Herrn Prof. Dr. Mahboobi und der Drittprüferin Frau Dr. Dettmer-Wilde zusammensetzte. Herzlichen Dank, dass Sie sich dazu bereit erklärt haben, diese Arbeit zu begutachten und das Kolloquium durchzuführen.

Vielen Dank an Dr. Bernd Moritz und Dr. Steffen Kiessig, mit denen die Zusammenarbeit stets eine Bereicherung war. Zudem möchte ich mich bei F. Hoffmann-La Roche Ltd. für die finanzielle Unterstützung dieser Arbeit bedanken.

Einen besonderen Dank geht an alle Mitglieder der Fakultät Chemie an der Hochschule Aalen und der Arbeitsgruppe von Prof. Dr. Neusüß. Vielen Dank für die unglaublich tolle Zeit an der Hochschule, die durch euch zu einem besonderen Abschnitt meines Lebens wurde. Vielen Dank an Dr. Cristina Montealegre, die mir den Einstieg durch ihre herzliche Art und ihre Vorarbeit unglaublich erleichterte. Danke an Oliver Höcker, der nicht nur bei technischen Problemen eine große Hilfe war und durch seine offene und in sich ruhende Art oft vieles relativierte. Vielen Dank an Dr. Kevin Jooß, der durch sein Fachwissen und der Leidenschaft für die Wissenschaft sehr prägend war. Einen großen Dank geht an Dr. Jens Meixner, der nicht nur während der intensiven Laborzeit, sondern auch auf so vielen Ebenen zur großen Hilfe wurde. Tausend Dank an Alexander Stolz, von dem ich so viel lernen durfte und es eine Freude war mit ihm zu arbeiten - danke für die wertvollen Beiträge zu dieser Arbeit. Vielen Dank auch an Johannes Schlecht, für die tollen Diskussionen und die hilfreichen Beiträge zur Arbeit. Ihr seid alle zu einem wichtigen Teil meines Lebens geworden und ich bin sehr dankbar euch als Freunde zu haben.

Ganz besonders möchte ich auch meinen Freunden außerhalb der Hochschule danken - für ihr großes Verständnis und ihre Unterstützung in all den Jahren. Dank euch war der Ausgleich zwischen Arbeit und Leben perfekt.

Der größte Dank geht an meine Familie. An meine Geschwister Richard, Nora und Steffi für die unglaubliche Bereicherung in meinem Leben - ohne euch wäre alles halb so schön. Vielen Dank Marc für die jahrelange Unterstützung und Geduld auf dem gesamten Weg - das werde ich dir nie vergessen. Meinen allergrößten Dank, aus tiefstem Herzen, geht an meine Eltern Renate und Gerhard - danke für eure bedingungslose Unterstützung in jedem Lebensbereich. Ohne euch hätte ich das alles nicht geschafft - ihr seid und bleibt meine größten Vorbilder. Diese Arbeit ist für euch.

Table of contents

List of publications

Peer-reviewed papers included in this thesis

Online mass spectrometry of CE(SDS)-separated proteins by two-dimensional capillary electrophoresis

Römer, J., Montealegre, C., Schlecht, J., Kiessig, S., Moritz, B., and Neusüß, C. (2019). Anal. Bioanal. Chem. 411, 7197–7206; DOI: 10.1007/s00216-019-02102-8

Abstract

Sodium dodecyl sulfate-polyacrylamide gel electrophoresis (SDS-PAGE) is the fundamental technique for protein separation by size. Applying this technology in capillary format, gaining high separation efficiency in a more automated way, is a key technology for size separation of proteins in the biopharmaceutical industry. However, unequivocal identification by online mass spectrometry (MS) is impossible so far, due to strong interference in the electrospray process by SDS and other components of the SDS-MW separation gel buffer. Here, a heart-cut two-dimensional electrophoretic separation system applying an electrically isolated valve with an internal loop of 20 nL is presented. The peak of interest in the CE(SDS) separation is transferred to the CZE-MS, where electrospray-interfering substances of the SDS-MW gel are separated prior to online electrospray ionization mass spectrometry. An online SDS removal strategy for decomplexing the protein-SDS complex is implemented in the second dimension, consisting of the co-injection of organic solvent and cationic surfactant. This online CE(SDS)-CZE-MS system allows MS characterization of proteoforms separated in generic CE(SDS), gaining additional separation in the CZE and detailed MS information. In general, the system can be applied to all kinds of proteins separated by CE(SDS). Here, we present results of the CE(SDS)-CZE-MS system on the analysis of several biopharmaceutical relevant antibody impurities and fragments. Additionally, the versatile application spectrum of the system is demonstrated by the analysis of extracted proteins from soybean flour. The online hyphenation of CE(SDS) resolving power and MS identification capabilities will be a powerful tool for protein and mAb characterization.

Improved CE(SDS)-CZE-MS method utilizing an 8-port nanoliter valve

Römer, J., Kiessig, S., Moritz, B., and Neusüß, C. (2021). Electrophoresis, 42, 374-380; DOI: 10.1002/elps.202000180

Abstract

Capillary sieving electrophoresis utilizing SDS (CE(SDS)) is one of the most applied methods for the analysis of antibody (mAb) size heterogeneity in the biopharmaceutical industry. Inadequate peak identification of observed protein fragments is still a major issue. In a recent publication, we introduced an electrophoretic 2D system, enabling online mass spectrometric detection of generic CE(SDS)-separated peaks and identification of several mAb fragments. However, an improvement regarding system stability and handling of the approach was desired. Here, we introduce a novel 8-port valve in conjunction with an optimized decomplexation strategy. The valve contains four sample loops with increased distances between the separation dimensions. Thus, successively coinjection of solvent and cationic surfactant without any additional detector in the second dimension is enabled, simplifying the decomplexation strategy. Removal efficiency was optimized by testing different volumes of solvents as presample and cationic surfactant as postsample zone. 2D measurements of the light and heavy chain of the reduced NIST mAb with the 8-port valve and the optimized decomplexation strategy demonstrates the increased robustness of the system. The presented novel set-up is a step toward routine application of CE(SDS)-CZE-MS for impurity characterization of proteins in the biopharmaceutical field.

Online top-down mass spectrometric identification of CE(SDS)-separated antibody fragments by two-dimensional capillary electrophoresis

Römer, J., Stolz, A., Kiessig, S., Moritz, B., and Neusüß, C. (2021). accepted by the Journal of Pharmaceutical and Biomedical Analysis; DOI: 10.1016/j.jpba.2021.114089

Abstract

Size heterogeneity analysis by capillary sieving electrophoresis utilizing sodium dodecyl sulfate (CE(SDS)) with optical detection is a major method applied for release and stability testing of monoclonal antibodies (mAbs) in biopharmaceutical applications. Identification of mAb-fragments and impurities observed with CE(SDS) is of outstanding importance for the assessment of critical quality attributes and development of the analytical control system. Mass spectrometric (MS) detection is a powerful tool for protein identification and characterization. Unfortunately, CE(SDS) is incompatible with online MS-hyphenation due to strong ionization suppression of SDS and other separation buffer components. Here, we present a comprehensive platform for full characterization of individual CE(SDS)-separated peaks by CE(SDS)-capillary zone electrophoresis-top-down-MS. The peak of interest is transferred from the first to the second dimension via an 8-port valve to remove MS-incompatible components. Full characterization of mAb byproducts is performed by intact mass determination and fragmentation by electron transfer dissociation, higher-energy collisional dissociation, and ultraviolet photodissociation. This enables online determination of intact mass as well as sequence verification of individual CE(SDS)-separated peaks simultaneously. A more substantiated characterization of unknown CE(SDS) peaks by exact localization of modifications without prior digestion is facilitated. High sensitivity is demonstrated by successful mass and sequence verification of low abundant, unknown CE(SDS) peaks from two stressed mAb samples. Good fragmentation coverages are obtained by MS^2, enabling unequivocal identification of these mAb-fragments. Also, the differentiation of reduced/non-reduced intra-protein disulfide bonds is demonstrated. In summary, a reliable and unambiguous online MS^2 identification of unknown compounds of low-abundant individual CE(SDS) peaks is enabled.

Publications not included in this thesis

Coupling of capillary electromigration techniques to mass spectrometry

Neusüß, C., Römer, J., Höcker, O., Jooß, K. (2018). in Capillary Electromigration Separation Methods. Elsevier Inc. DOI: 10.1016/B978-0-12-809375-7.00012-5

Recent advances in capillary electrophoresis mass spectrometry: Instrumentation, methodology and applications

Stolz, A., Jooß, K., Höcker, O., Römer, J., Schlecht, J., Neusüß, C., (2019). Electrophoresis, 40, 79–112; DOI: 10.1002/elps.201800331

Aus einfachem Abschätzen wird vielfaches Messen

Römer, J., Kiessig, S., Moritz, B., and Neusüß, C. (2020). LABO

Capillary Zone Electrophoresis-Top-Down Tandem Mass Spectrometry for In-Depth Characterization of Hemoglobin Proteoforms in Clinical and Veterinary Samples

Stolz, A., Hedeland, Y., Salzer, L., Römer, J., Heiene, R., Leclercq, L., Cottet, H., Bergquist, J., and Neusüß, C. (2020). Anal. Chem., 92, 10531-10539; DOI: 10.1021/acs.analchem.0c01350

Patent

Valve for transferring at least one fluid

Neusüß, C., Römer J., F. Hoffman-La Roche AG (2020). International application number: PCT/EP2020/054474. Munich, Germany. European Patent Office

Abstract

A valve for transferring at least one fluid is disclosed. The valve comprises: -at least one stator, wherein the stator comprises a plurality of ports, the ports comprising a plurality of groups of ports, the plurality of groups of ports comprising a first group of at least two first ports, a second group of at least two second ports and a third group of at least two third ports; -at least one rotor, wherein the rotor comprises a plurality of channels, the channels comprising at least one first channel and at least one second channel; and -at least one actuator, wherein the actuator is operably connectable to the rotor; wherein the actuator is configured to rotate the rotor into at least one loading orientation, wherein in the loading orientation one or both of the following situations are present: a) the first channel is connected to the first ports such that a first fluid is transferable via at least one of the first ports into the first channel; b) the second channel is connected to the second ports such that a second fluid is transferable via at least one of the second ports into the second channel; wherein the actuator is further configured to rotate the rotor into at least one first injection orientation and into at least one second injection orientation, wherein in the first injection orientation the first channel is connected to the third ports and the first fluid is transferable from the first channel into at least one of the third ports, wherein in the second injection orientation the second channel is connected to the third ports and the second fluid is transferable from the second channel into at least one of the third ports.

Conference contributions

List of oral presentations

2018

2^{nd} Joint CE- and FFE-Forum, Karlsruhe-Berghausen (DE),
Title: CE(SDS)-CZE-MS for the analysis of proteins and monoclonal antibodies
10 - 11. October 2018

2019

48^{th} International Symposium on High-Performance Liquid Phase Separations and Related Techniques, University of Milano-Bicocca, Milan (IT)
Title: CE(SDS)-CZE-MS for the analysis of proteins including monoclonal antibodies
16 - 20. June 2019

2020

30. Doktorandenseminar des Arbeitskreises Separation Science der GDCh-Fachgruppe Analytische Chemie, Hohenroda (DE),
Title: Online mass spectrometry of CE(SDS)-separated proteins by two-dimensional capillary electrophoresis
11 - 14. January 2020

36^{th} International Symposium on Microscale Separations and Bioanalysis, Online Conference,
Title: Online mass spectrometry of CE(SDS)-separated proteins by two-dimensional capillary electrophoresis
27 - 30. September 2020

List of poster presentations

2018

Analytical Technologies in the Biopharmaceutical Industry Europe, Barcelona (ES),
Title: CE(SDS)-CZE-MS for the Analysis of Monoclonal Antibodies
6 - 9. March 2018
(CASSS student travel grant)

Declaration of collaboration

The presented research in this thesis was partly obtained in cooperation with other researchers. In accordance with § 8 Abs. 1 Satz 2 Ziff. 7 of the *Ordnung zum Erwerb des akademischen Grades eines Doktors der Naturwissenschaften (Dr. rer. nat.) an der Universität Regensburg vom 18. Juni 2009 (Änderungssatzung vom 26. Februar 2014)*, these collaborations are described within this section.

4.1 Online mass spectrometry of CE(SDS)-separated proteins by two-dimensional capillary electrophoresis

Two-dimensional experiments and data evaluation has been performed by the author (C^4D signal, NIST mAb, soybean proteins, and mAb4 partly (Figure 4.8: b.1 -b.3))) and Cristina Montealegre (mAb1, mAb2, mAb3, and mAb4 partly (Figure 4.8: a.1-a.3)). SDS-MW-gel buffer optimization and one-dimensional measurements of mAb4 were performed by Johannes Schlecht. The original draft was written by the author, Cristina Montealegre and Johannes Schlecht. Review & editing was done by Steffen Kiessig , Bernd Moritz and Christian Neusüß. Steffen Kiessig and Bernd Moritz acquired funding and conceived the approach, and Christian Neusüß supervised the project and conceived the approach.

4.2 Improved CE(SDS)-CZE-MS method utilizing an 8-port nanoliter valve

The author and Christian Neusüß developed the 8-port nanoliter valve. VICI AG International contributed to realization and manufacturing. Conceptualization, investigation, experiments, data evaluation, visualization, and writing (original draft) have been performed solely by the author. Funding acquisition and writing (review & editing) were made by Steffen Kiessig and Bernd Moritz. Christian Neusüß contributed to conceptualization, writing (review & editing), and supervision.

4.3 Online top-down mass spectrometric identification of CE(SDS)-separated antibody fragments by two-dimensional capillary electrophoresis

Conceptualization, investigation, experiments, data evaluation, visualization, and writing (original draft) have been performed primarily by the author. Alexander Stolz contributed to conceptualization, investigation, HPLC-MS experiments, data evaluation, visualization, and writing (original draft). Funding acquisition and writing (review & editing) were made by Steffen Kiessig and Bernd Moritz. Christian Neusüß contributed to conceptualization, writing (review & editing), and supervision.

List of abbreviations

^{1}D	First dimension
1D	One-dimensional
^{2}D	Second dimension
2D	Two-dimensional
AGC	Automatic gain control
ALS	Acid labile surfactant
BGE	Background electrolyte
BPE	Base peak electropherogram
CE	Capillary electrophoresis
CE(SDS)	Capillary sieving electrophoresis with sodium dodecyl sulfate
CID	Collision-induced dissociation
CIEF	Capillary isoelectric focusing
CPA	Corrected peak area
CTAB	Cetyltrimethylammonium bromide
CZE	Capillary zone electrophoresis
C^{4}D	Capacitively coupled contactless conductivity detection
DAD	Diode array detector
DTT	Dithiothreitol
EIE	Extracted ion electropherogram
EDTA	Ethylenediaminetetraacetic acid
ESI	Electrospray ionization
ETD	Electron transfer dissociation
EOF	Electroosmotic flow

Fab	Antigenbinding fragment
FAc	Formic acid
Fc	Fragment crystallizable
FS	Fused silica
HAc	Acetic acid
HC	Heavy chain
HCD	Higher-energy collisional dissociation
HCl	Hydrochloric acid
HPLC	High-performance liquid chromatography
ID	Inner diameter
IdeS	Immunoglobulin-degrading enzyme of Streptococcus pyogenes
Ig	Immunoglobulin
IPA	2-Propanol
LC	Light chain
LIF	Laser-induced fluorescence
LOD	Limit of detection
mAb	Monoclonal antibody
MALDI	Matrix-assisted laser desorption ionization
MS	Mass spectrometry
MS^1	Full scan mass spectrometry
MS^2	Tandem mass spectrometry
MW	Molecular weight
m/z	Mass-to-charge
NaOH	Sodium hydroxide

NIST	National Institute of Standard and Technologies
OD	Outer diameter
PAEK	Polyaryletherketone
PEEK	Polyether ether ketone
PTFE	Polytetrafluoroethylene
PTM	Post-translational modification
PVA	Polyvinylalcohol
RP-HPLC	Reversed-phase high-performance liquid chromatography
RSD	Relative standard deviation
SDS	Sodium dodecyl sulfate
SDS-PAGE	Sodium dodecyl sulfate-polyacrylamide gel electrophoresis
SEC	Size-exclusion chromatography
SI	Supporting information
SL	Sheath liquid
TDMS	Top-down mass spectrometry
TOF	Time-of-flight
Tris	Tris(hydroxymethyl)aminomethane
UV	Ultraviolet light
UVPD	Ultraviolet photodissociation
VIS	Visible light

1 Introduction

Medical treatment has changed distinctly in the last decades. Especially, biopharmaceuticals like monoclonal antibodies (mAbs) have tremendously gained importance [1]. Compared to so-called small-molecule pharmaceuticals, new therapeutic modalities, more efficient treatment, and better compatibility are enabled due to their higher specificity [2, 3]. Besides these benfits, there are also challenges coming along, such as extensive development, production, purification, and quality control of these complex biopharmaceuticals [3, 4]. To assure safety and efficacy, a detailed characterization of these molecules with various analytical methods is required [5, 6]. For size heterogeneity and purity analysis, sodium dodecyl sulfate (SDS) in capillary format (CE(SDS)), also known as capillary gel electrophoresis, is the method of choice. Compared to size exclusion chromatography and the widespread slab gel approach, CE(SDS) offers a superior separation efficiency in a range of 10 - 200 kDa [7, 8]. As a result of the commonly used optical detection like laser-induced fluorescence or ultraviolet-visible detection, this technique's main drawback is the missing peak identification. In contrast, mass spectrometric detection would allow an unambiguous identification, thus providing additional valuable information. Due to interfering compounds in the SDS-separation gel buffer and resulting signal suppression, direct hyphenation of CE(SDS) with mass spectrometry (MS) is hindered [9]. So far, peak assignment has been only attempted by spiking experiments or fraction collection, with extensive sample preparation and further analytical approaches [10, 11]. Online hyphenation of several MS-incompatible CE methods was demonstrated by the research group of Prof. Neusüß by a two-dimensional capillary electrophoretic separation system [12–17]. Here, the peak of interest is transferred from the first MS-interfering to the second MS-compatible CE separation dimension by a heart-cut approach via a 4-port-nanoliter valve. Hence, interfering compounds are separated from the analyte in the second dimension, and mass spectrometric characterization is allowed.
This thesis describes the first online hyphenation of generic CE(SDS) separation with MS, implementing a second electrophoretic separation combined with a previously developed SDS-protein decomplexation [18]. Proof of principle and characterization of this two-dimensional separation system is demonstrated by analyzing several mAbs and soybean proteins. Further technical improvements like the development of an 8-port nanoliter valve and decomplexation optimization resulted in higher system robustness. Additionally, detailed characterization and unambiguous identification of CE(SDS)-separated species were enabled by combining the two-dimensional system with top-down MS. For a better understanding of this work, a short introduction to the theory of proteins and biopharmaceuticals is given. Furthermore, the applied separation techniques and detection systems are described. Finally, the hyphenation of these techniques is presented with a summary of the state of the art, leading to the here described electrophoretic two-dimensional separation system.

2 Theory

2.1 Proteins and monoclonal antibodies

2.1.1 Structure of peptides and proteins

Proteins are the most abundant biological macromolecules and present in every cell. Depending on their structure, they have different shapes and functions. Every protein is based on 20 amino acids. These amino acids have a common basic structure of a carboxyl and an amino group located on the α-carbon. The difference of these amino acids can be found in the side chain (here R). This side-chain defines the physical and chemical properties of amino acids. The carboxyl group of one and the amino group of another amino acid can form by the loss of water a covalent bond, the so-called peptide bond (see Figure 2.1).

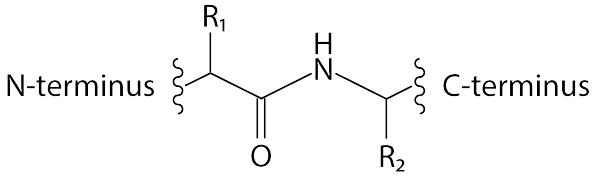

Figure 2.1: Peptide of two amino acids

By repeating this condensation reaction, the amino acid chain increases. Depending on the number of covalently bond amino acids, they are named oligopeptides ($<$ 10 amino acids), polypeptides ($>$ 10 amino acids), or proteins ($\gg$ 100 amino acids). The differentiation of the terms polypeptide and protein is not well-defined, but in general, polypeptide is used for molecules smaller than 10 kDa and protein for molecules bigger than 10 kDa [19]. The amino acid sequence is representing the primary structure of peptides and proteins. In the sub-level of these peptide chains, sub-structures with a high geometrical order like α-helix and β-sheets are defined as secondary structure. The coordination through non-covalent interactions or covalent bonds of these sub-structures within a polypeptide chain presents the tertiary structure. Proteins can consist of single or multiple polypeptide chains. If a protein is composed of more than one polypeptide chain, the coordination of these polypeptide chains is representing the quarternary structure of a protein. They can be coordinated to each other through non-covalent interactions or covalent bonds, like disulfide bonds. An example of a polypeptide chain protein with disulfide bonds is a monoclonal antibody (mAb) [19].

2.1.2 Structure of monoclonal antibodies

There are five different isotypes of immunoglobulins (Ig): IgA, IgD, IgE, IgG, and IgM. Here, mAbs of the IgG class represent with around 80% the majority of human mAbs. Most

approved therapeutic mAbs are part of the IgG class as well [20]. IgGs consist of four polypeptides, two light chains (LC, each $\sim$25 kDa), and two heavy chains (HC, each $\sim$ 50 kDa), as displayed in Figure 2.2. Each LC and HC has intra disulfide bonds and different domains. There are constant domains (for HC: CH1, CH2, CH3, and for LC: CL) responsible for recognizing and binding the effector. On the CH2 domain N-glycosylation is present increasing stability and binding properties [21]. Besides these constant domains, there are variable domains (for HC: VH and for LC: VL) representing the antigen-binding regions. The LC and HC, as well as both HCs are linked via inter disulfide bonds to each other. For this reason, intact mAbs have a high molecular mass of around 150 kDa [3, 6].

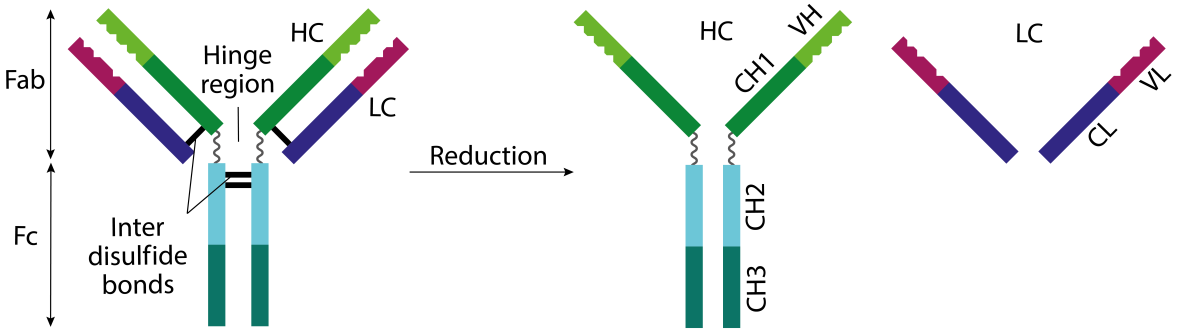

Figure 2.2: Basic structure of an intact and reduced mAb (IgG)

The complexity and high mass of intact mAbs can be challenging, especially for mass spectrometric analysis. Therefore, intact mAbs can be dissociated into their HCs and LCs by reducing the disulfide bonds with dithiothreitol (DTT), β-mercaptoethanol, or tris(2-Carboxyethyl) phosphine hydrochloride [22]. Besides disulfide bond reduction, proteolytic cleavages in the hinge region can be applied using papain or endopeptidase (immunoglobulin-degrading enzyme of Streptococcus pyogenes (IdeS)) resulting in antigen-binding fragments (Fab) and crystallizable fragments (Fc) or $(Fab')_2$ and Fc/2 fragments, respectively [6, 23, 24]. Through additional reduction, $F(ab)_2$ is cleaved into LC and Fd fragment [23]. These resulting fragments have a size of around 25 kDa, accessible for further mass spectrometric experiments like middle-down approaches.

First in vitro mAbs were produced in 1975 from mouse cells (murine) by Köhler and Milstein [25]. Utilizing these murine mAbs as therapeutics for humans generate an immune response, and the mAb is inactivated. Therefore, regions of this original murine mAb were substituted by human mAb domains to decrease undesired immune response. Depending on the regions that are exchanged, they are called chimeric (murine variable domain, human constant domain) or humanized (additional part of murine variable domains are replaced). In the last years, fully human mAbs are becoming more important and are developed as well [20, 26].

2.1.3 Therapeutic relevance of monoclonal antibodies

In the last decade, biopharmaceutical proteins like mAbs gained more and more attention as therapeutics. Until May 2021, there are 104 mAb-based proteins approved as therapeutics either by the US Food and Drug Administration or European Medicines Agency. Of these 104 released mAb-based proteins, 73 were approved since 2011, and additional 18 mAb-based proteins are currently reviewed by these agencies [27]. These numbers show the massive interest in utilizing mAbs as therapeutics. One of the main reasons is their target selectivity, eliminating unnecessary exposures to non-targeted organs that can be observed employing chemotherapeutics. Therefore, therapeutic mAbs are defined as well-tolerated drugs [3]. There are several mAbs and related biopharmaceuticals on the market for the treatment of autoimmune, cardiovascular, and infectious diseases, as well as cancer and chronic inflammation [20, 28]. Therapeutic activity of a mAb is mainly related to its sequence and the resulting tertiary and quaternary structure. Additional, post-translational modifications (PTMs) such as glycosylation, glycation, oxidation, deamidation, and disulfide bond formation play an essential role. The relative elaborated production, complex structure of mAbs, undesired PTMs, and storage-related degradation can lead to heterogeneity in the protein structure [3, 4].

2.1.4 Characterization and analysis of monoclonal antibodies

Detailed characterization and stability control of mAbs is essential to assure efficacy, safety, and therapeutic activity. Besides identification of impurities and characterization of the mAb, the analysis of its heterogeneity is of outstanding importance. This includes identification of mAb variants and fragments, especially for monitoring and understanding the production and stability of mAbs. Modification and degradation can occur when proteins are exposed to external stress factors such as temperature or pH changes, mechanical stress, or light exposure during production, storage, or shipment [29]. Known modifications, such as variations in the amino acid sequence or PTMs can induce changes in hydrophobicity, higher-order structure, glycosylation, charge, and size. Especially for the analysis of complex mAb structures and related modifications, various analytical techniques are required.
There are several well-established techniques based on chromatographic [30] and electrophoretic separations [31, 32] for mAb analysis [6, 33]. Combining a variety of orthogonal separation techniques can help to cope with analytical challenges. Changes in hydrophobicity, such as oxidation of methionine or tryptophan, are mainly analyzed by hydrophobic interactions chromatography [34] and peptide mapping using reversed-phase high-performance liquid chromatography (RP-HPLC) [6, 35]. Deamidation, isomerization, and glycation can lead to charge heterogeneities. These modifications can be analyzed by ion-exchange

chromatography, isoelectric focusing, and capillary zone electrophoresis (CZE) [36, 37]. Size variants can be observed when fragmentation or aggregation occurs. Size-exclusion chromatography (SEC) is mainly utilized to characterize aggregates [7]. Due to better resolution compared to SEC, sodium dodecyl sulfate-polyacrylamide electrophoresis (SDS-PAGE) is one of the most established methods separating protein fragments according to their hydrodynamic radius, frequently equated to protein size, under denaturing conditions [38, 39]. This technique has been effectively transferred into the capillary format (capillary sieving electrophoresis utilizing SDS as an anionic surfactant, CE(SDS)), gaining better separation resolution, linearity, precision, and robustness compared to the slab gel approach [8]. Additionally, CE(SDS) allows online detection by ultraviolet light (UV) or laser-induced fluorescence (LIF), hence, quantification is possible (see chapter 2.2.2).
Besides these separation techniques, MS has become of outstanding importance for protein identification and characterization (see chapter 2.3). Utilizing MS, the protein's intact mass, information about amino acid sequence, PTMs, protein fragments, and impurities can be obtained. For the analysis of biopharmaceuticals, mass spectrometers capable of detecting a wide mass-to-charge (m/z) range combined with a high mass resolution are the instruments of choice, such as Time-of-flight (TOF) or Orbitrap mass spectrometers. Furthermore, tandem mass spectrometric (MS^2) experiments are becoming more and more important for the analysis of complex mAb structures [33].

2.2 Electrophoretic separations

The basic principle of electrophoretic separations is the migration of charged analytes in an electrical field. This separation can be applied in different formats, such as slab gels, fused silica capillaries, and microfluidic chips. Additionally, there is a wide variety of separation modes utilizing different separation mechanisms. The first observation of electrophoretic mobility of proteins, here egg albumin, utilizing a U-tube and fluorescence detection was presented in 1923 by Svedberg and Jette [40]. First measurements were performed with an improved U-tube set-up of egg albumin at different pH levels by Scott and Svedberg one year later, known as the moving-boundary method [41]. Arne Tiselius focused on improving protein separation by utilizing UV absorption for detection [42, 43]. In the year 1937, after further set-up improvements, Tiselius demonstrated with the separation of serum the first separation of proteins by electrophoresis [44] and was awarded with the Nobel Prize in chemistry for his work in 1948.

2.2.1 Capillary zone electrophoresis

Stellan Hertjén transferred the separation in capillary format (3 mm quartz tubes) to minimize convection, which allowed separation without an anti convection medium like gels. This method was introduced as free zone electrophoresis and can be seen as the hour of birth of capillary electrophoresis [45]. Emerging interest for this method started as Jorgenson and Lukacs utilized capillaries with a smaller inner diameter (ID) of 75 μm in combination with a sensitive absorbance detector [46]. Due to the increase of the surface-area-to-volume ratio, Joule heating resulting from electric current flowing through a conductor, can be dissipated more effectively.

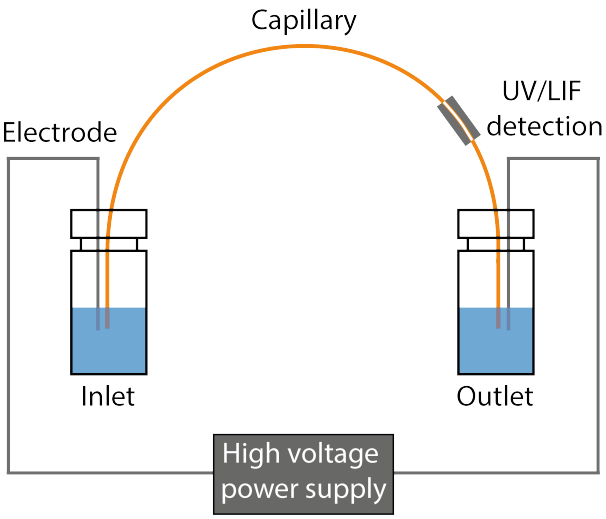

Figure 2.3: Capillary electrophoresis set-up with UV or LIF detection

Therefore, higher separation voltage application was enabled, leading to better separation efficiency and resolution. Today, capillary electrophoretic separations are still performed in fused silica capillaries. Regarding CZE, the capillary is filled and placed in an electrically conductive liquid, called background electrolyte (BGE) (see Figure 2.3). In this BGE, electrodes are positioned to apply high voltage up to 30 kV. Analytes are migrating according to their charge in the direction of the anode or cathode, respectively. The separation of analytes depends on their velocity in the electric field and can be stated as in equation 2.1.

$$v = \mu_e \cdot E \tag{2.1}$$

with v = Ion velocity
μ_e = Electrophoretic mobility
E = Applied electric field

The electrophoretic mobility μ_e of molecules is related to their charge and size, as shown in equation 2.2.

$$\mu_e = \frac{q}{6\pi\eta r} \tag{2.2}$$

with μ_e = Electrophoretic mobility
q = Ion charge
η = Solution viscosity
r = Ion radius

This equation reveals that small and highly charged analytes have a higher mobility than larger and less charged analytes. For this reason, they migrate faster in an electric field. In fact, the electrophoretic mobility μ_e is additional depending on the degree of ionization of the analyte and results in the effective electrophoretic mobility μ_{eff} as shown in equation 2.3.

$$\mu_{eff} = \mu_e \cdot \alpha_i \tag{2.3}$$

with μ_{eff} = Effective electrophoretic mobility
μ_e = Electrophoretic mobility
α_i = Degree of ionization

The degree of ionization can be influenced by the pH of the BGE. Therefore, the selectivity of analytes can be regulated by the chosen BGE. Besides the effective electrophoretic mobility, the migration of analytes can be influenced by the capillary wall. Bare fused silica capillaries have silanol groups on the capillary surface. At slightly acidic pH and above, the silanol groups are deprotonated and thus negatively charged. Here, an accumulation of protons along this negatively charged surface takes place, and the so-called static "Stern layer" and a mobile diffuse double-layer is formed. By applying a positive voltage, the diffuse double-layer moves towards the cathode, and a flow in the capillary, the so-called electroosmotic flow (EOF), is generated. Due to this flow, uncharged analytes can be detected at the cathode. If the EOF is higher than the migration velocity of negatively charged analytes, they can be detected as well [47].
For some applications, especially protein analysis, adsorption to the bare fused silica wall can be observed based on electrostatic and hydrophobic interactions. This adsorption can result in a loss of reproducibility, broad peaks, or even total protein adsorption with no peak detection at all. There are several strategies to avoid this phenomenon, depending on the kind of interaction that is occurring. If the predominant interaction is electrostatic, a modification of the BGE, like adjusting the pH or the ionic strength, can be utilized. At low pH, capillary wall's silanol groups are protonated and uncharged, and the protein is positively charged if the pH is below its isoelectric point. If a BGE with a high pH is applied, the silanol groups are deprotonated and negatively charged, while proteins are uncharged or negatively charged as well. Thus, in theory, electrostatic interactions are reduced. Nevertheless, utilizing BGEs at extreme pH ranges can influence protein stability and separation, while some electrostatic and hydrophobic interactions may still occur. By increasing the ionic strength of the BGE, protein-wall interaction can be suppressed. The disadvantage here is the increase of Joule heating due to higher conductivity, resulting in peak broadening or the necessity of lowering the separation voltage. Additionally, low salt content in the BGE is more beneficial for the hyphenation with MS.
A much more suitable strategy to decrease protein-wall interactions is the application of capillary coatings. It allows more degrees of freedom regarding separation conditions and method development. There is a huge variety of capillary coatings. In general, they can be categorized in static (adsorbed or covalently bound to the capillary wall) and covalent (present in the BGE) coatings. Here, silanol groups of the fused silica capillary are covered with neutrally or even positively charged molecules or polymers. Hence, direct wall-analyte interaction is prevented. Another effect utilizing neutral or positively charged coating is that the EOF is close to zero or reversed, respectively [48]. Hence, an improved separation can be facilitated.

2.2.2 Capillary sieving electrophoresis

SDS-PAGE is one of the most utilized analytical tools for protein purification and size-based separation [38, 39]. An excess of SDS is added to the protein, and a negatively charged protein-SDS complex is formed that covers the former protein charge. SDS binds in general in a constant ratio of 1.4 g to 1.0 g of protein. Therefore, protein-SDS complexes have a similar charge/size ratio. In theory, they migrate according to their hydrodynamic radius, frequently equated to protein size, through a slab gel, often cross-linked polyacrylamide gel, by applying voltage.

Capillary sieving electrophoresis utilizing SDS, here referred to as CE(SDS), can be seen as translation of SDS-PAGE into capillary format following the same separation principle [49]. First separations of membrane proteins that were solubilized with SDS were presented by Hjertén [50]. He was utilizing capillaries (ID 0.05 - 0.20 mm) with polyacrylamide gel as sieving matrix and online UV-detection. Protein separation with following molecular weight determination using SDS-PAGE in capillary format was done by Cohen and Karger [51]. One of the drawbacks of these techniques, both in slab gel and capillary format, is that the migration velocity depends not only on the hydrodynamic radius. The binding constant of SDS to protein can vary depending on the protein structure. For example, protein glycosylation and acidic side chains can lower SDS-protein binding, resulting in slower migration and molecular weight over-estimation [52, 53]. Therefore, mass estimation of proteins via SDS-PAGE and CE(SDS) needs to be handled carefully. Nevertheless, the main application of CE(SDS) in the biopharmaceutical industry is not mass determination of protein fragments, rather than general separation of these [49].

CE(SDS) can be seen as a further development regarding separation efficiency and automatization [8]. Instead of using cross-linked separation gels, water-soluble linear or slightly branched polymers are utilized as separation gels inside the capillary [54]. Hence, automatization and higher reproducibility can be achieved by frequent replacement of the separation gel. Due to the high separation gel viscosity, analytes are mainly injected via electrokinetic injection. Here, the capillary inlet is positioned into the sample vial, and voltage is applied for several seconds. For separation, both ends of the capillary are placed in vials filled with separation gel-buffer and voltage in reversed polarity up to 15 kV is applied. The separation is monitored online via UV absorption or LIF detection. Therefore, time-intense fixation and staining of proteins is lapsed compared to SDS-PAGE analysis. Additionally, online detection enables quantification of CE(SDS)-separated peaks, which is an important feature for biopharmaceutical applications. Another key benefit is the availability of commercial separation kits that allow an excellent reproducibility. For these reasons, CE(SDS) has become an important analytical method for impurity and stability control of biopharmaceuticals, especially for mAbs. There are two analytical modes in CE(SDS) that are performed.

One is the intact protein analysis for the determination of impurities and covalently bound aggregates [49]. Another mode is the analysis of the reduced protein. Here, disulfide bonds are reduced prior to analysis, and the LCs and HCs of a mAb are obtained. This reduced mode is utilized for the determination of glycan occupancy and size-based fragments as well. Still, identification of observed unknown fragments and their resulting peaks remains a challenge. The standard procedure for identification is the addition of known fragments to the sample and comparison of migration times and peak intensities. This comparison can give a rough hint, but an unequivocal identification is not facilitated.

2.3 Mass spectrometry

2.3.1 Electrospray ionization

For the access to mass spectrometric detection, analytes need to be present in the gas phase and charged. There are several ion sources with different approaches, depending on the analytes' state of aggregation, mass, and other physical properties. Furthermore, ion sources can be categorized depending on the pressure operation mode (under atmospheric pressure or high vacuum). Electrospray ionization (ESI) is the most utilized ionization process under atmospheric pressure for analytes in the liquid phase, such as present in HPLC or CE separations. Here, solute analytes are guided through the spray capillary, as seen in Figure 2.4.

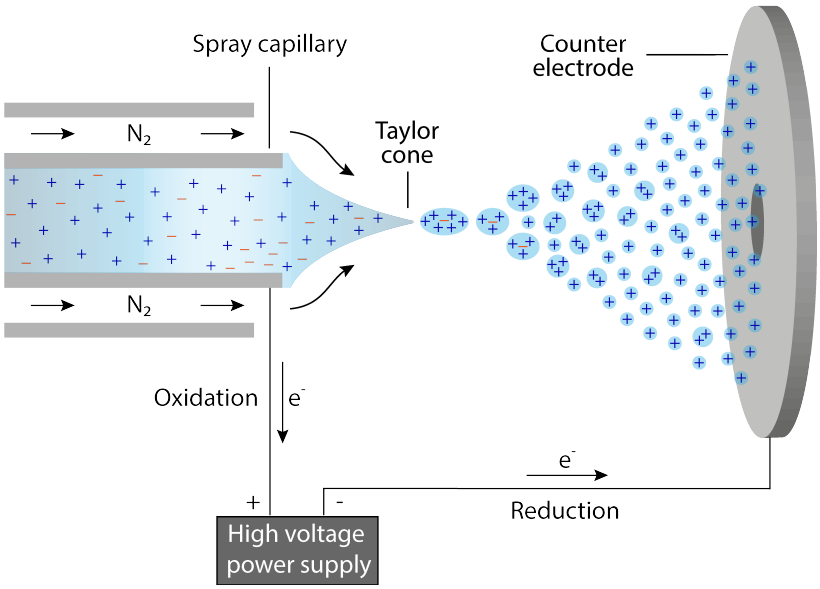

Figure 2.4: Electrospray process

A potential of 3-4 kV is applied between the spray capillary and a counter electrode. Nebulizing gas like nitrogen is utilized to facilitate the spraying process. Analytes are sprayed in a spray chamber with an additional heated nitrogen flow to support solvent evaporation and ion formation. On the spray capillary tip, the so-called Taylor cone is formed. On the tip of this Taylor cone, charged droplets are released when the electrostatic force is higher than the surface tension. For beneficial charged droplet formation, presence of organic solvents and charged additives, such as volatile acids for positive ionization mode, can be supportive. The sprayed charged droplets' size is reduced by evaporation until the surface tension is lower than the charge repulsion inside these droplets. Then the so-called coulomb fission takes place, where smaller and more stable droplets are formed. This mechanism is repeated until only charged analytes are present in the gas phase. A small part of these charged

analytes enters the mass spectrometer and first vacuum stage through the transfer capillary. All in all, this ion formation is a soft ionization method, where almost no fragmentation is observed. Additionally, multiply charged ions are formed, resulting in m/z-regions that are easily accessible and in a good operating mass range of mass spectrometers. Therefore, ESI is the ionization technique of choice for high molecular mass analytes such as proteins [55].

2.3.2 Time-of-flight mass spectrometry

The main constituent part of a TOF mass spectrometer is, besides the ionization source and the ion transfer, the flight tube (as seen in Figure 2.5). In this field-free flight tube ions travel after acceleration with a certain drift velocity depending on their m/z-ratio.

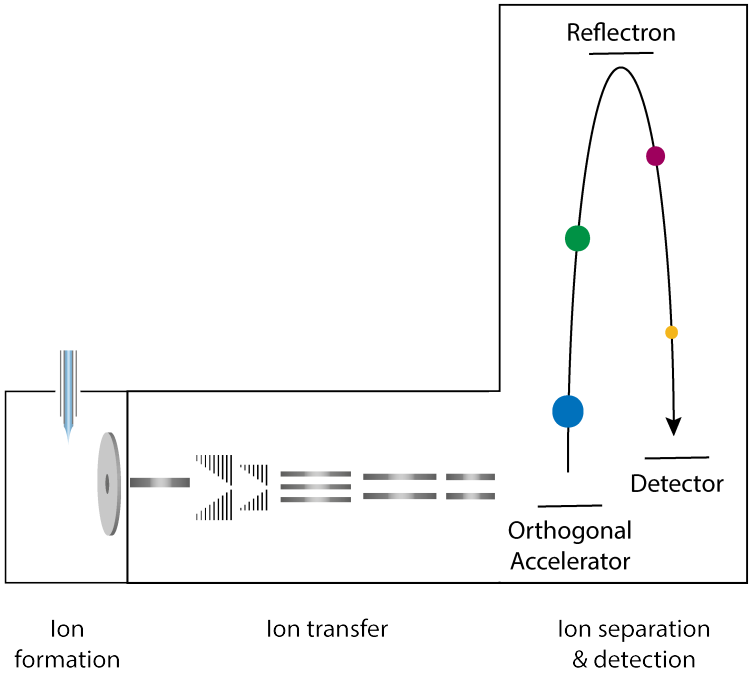

Figure 2.5: Schematic of a Time-of-flight mass spectrometer

Ions that enter the TOF flight tube experience an acceleration pulse, that is ideally orthogonal to the ion transfer to ensure acceleration direction's starting velocity is close to zero. Here, the electric potential energy (E_{el}) resulting from the acceleration is converted into kinetic energy (E_{kin}), and can be equated as indicated in equation 2.4.

$$e \cdot z \cdot U = E_{el} = E_{kin} = \frac{1}{2} m \cdot v^2 \tag{2.4}$$

with e = Elementary charge
z = Charge
U = Acceleration voltage
E_{el} = Electric potential energy
E_{kin} = Kinetic energy
m = Mass
v = Velocity

After transformation, equation 2.5 demonstrates that the resulting ion velocity depends on their m/z-ratio. Ions with a lower m/z-ratio will travel faster through the drift tube than ions with higher m/z-ratios.

$$v = \sqrt{\frac{2 \cdot e \cdot z \cdot U}{m}} \tag{2.5}$$

Due to the fact, that the separation length of the flight tube and the acceleration voltage are kept constant, the equation can be simplified. By substituting velocity through distance per time, equation 2.6 demonstrates the correlation between measured time from starting pulse to detection and the m/z-ratio of the analyte. Therefore, the measurement of the flight time allows the determination of the m/z-ratio of analytes.

$$t^2 = \frac{s^2}{2 \cdot e \cdot U} \frac{m}{z} \tag{2.6}$$

with t = Transfer time
s = Length of flight tube

Benefits of TOF instruments are seen, besides measurement of the complete mass spectra, in precise mass accuracy and constant high mass resolving power over the total mass range. Additionally, they have a high sensitivity due to reasonable transmission rates and duty cycles, and high spectral acquisition rates. Therefore, they are utilized in a brought field of applications and are especially suitable for protein analysis [55].

2.3.3 Orbitrap mass spectrometry and top-down analysis

Another essential mass analyzer is the Orbitrap. It is a Fourier Transform instrument and provides a high mass resolving power (depending on m/z). The main set-up of the Orbitrap consists of a spindle-like shaped central electrode and two symmetrical outer electrodes, as seen in Figure 2.6. Between these electrodes, a potential is set. Once ions are captured in the trap, they start rotating around the central electrode with an additional harmonic axial oscillation. The frequency of this oscillation is inversely proportional to the square root of the detected ions' m/z ratio and is generating an image current. By detecting this image current, the mass spectrum can be calculated by Fourier transformation [55–57].

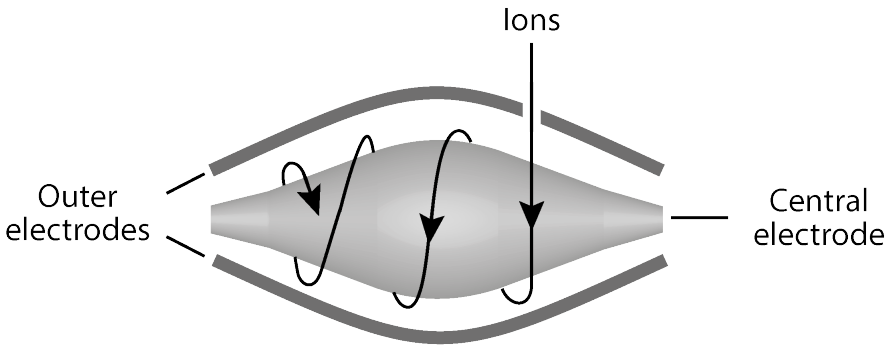

Figure 2.6: Orbitrap set-up and detection principle

Hybrid instruments, combining the high resolving Orbitrap mass analyzer with quadrupoles, (linear) ion traps, and a c-trap, allow the selection, storage, and scan with high mass accuracy of ions. Additional implementation of different fragmentation techniques expands the application field enormously into the field of proteomics. Fragmentation of intact proteins in the MS, also known as top-down analysis, leads to characteristic protein and peptide fragments. By measuring the exact mass of these fragments with the high mass resolution of the Orbitrap and comparing these masses with calculated theoretical masses, fragment ions can be assigned to the protein's primary structure. Top-down analysis aims to generate many different protein fragments to cover the whole sequence for protein and PTM identification. This fragmentation is addressed in the Orbitrap hybrid instruments by combining different fragmentation technologies. The latest generation of hybrid orbitrap mass analyzers provide fragmentation options like collision-induced dissociation (CID), higher-energy collisional dissociation (HCD), electron transfer dissociation (ETD), and ultraviolet photodissociation (UVPD). CID and HCD are based on the collision of selected ions with a neutral collision gas (argon, helium, nitrogen). By cleaving the amide-bond, proteins and peptides result in b- and y-type ions (see Figure 2.7) [55, 58].

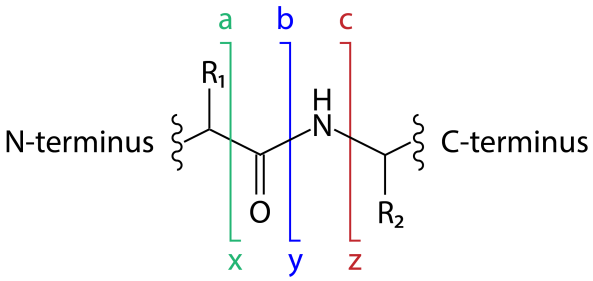

Figure 2.7: Fragment ions of peptides and proteins

ETD fragmentation is generated by the electron transfer from radical anions, most often fluoranthene radical anions, to the precursor ions. Peptide and protein fragments are generated by amine-bond cleavage, resulting in c- & z-type fragments. The preservation of fragile PTMs on proteins and resulting ions is an additional benefit when utilizing ETD [58, 59]. UVPD is induced by photon adsorption of the precursor ions. These photons are introduced via UV light irradiation by laser pulses. Through photon adsorption, ions get excited to a higher energy state, and fragmentation is occurring. Besides b- and y-type ions, a-, x-, c- and z-type ions are generated. This diverse fragmentation obtained with UVPD, providing unique a- and x-ions, contributes valuable information for sequence coverage and protein identification [60].

2.4 Hyphenation and two-dimensional separation

2.4.1 Capillary electrophoresis mass spectrometry

Hyphenation of electrophoretic separation with MS is a growing field, but still not as widespread as the hyphenation of chromatographic separations with MS. One crucial step towards wider application of CE-MS is, besides enhancement of measurement stability and reproducibility, the development of a suitable and robust interface hyphenating CE with MS. Compared to HPLC-ESI sprayer, CE-ESI sprayer have an additional connection, where the so-called sheath liquid (SL), mostly a mixture of organic solvent and water, is introduced. The SL has three major tasks: first, it is closing the electric circuit to the CE, second, it increases the low flow coming from the CE to an ESI compatible level, and third, the organic solvent supports evaporation. These requirements were fulfilled by the introduction of the triple tube sprayer commercialized by Agilent, representing the most utilized CE-MS sprayer. It is known for its high robustness and spray stability, due to a high flow of SL. Nevertheless, this high flow leads to a considerable dilution of analytes, and a correlated sensitivity loss is observed utilizing this type of CE-MS sprayer. To circumvent this low sensitivity, further improvements regarding interfacing have become a significant research field. An additional benefit of further CE-MS interfacing development is the access to different types of mass spectrometers. The triple tube sprayer from Agilent is designed for Bruker and Agilent MS, where the sprayer is on ground. For hyphenation with a different type of ion source where the voltage is applied directly on the sprayer like utilized at the Orbitrap MS from Thermo, modifications in the set-up are required. This compatibility is the second reason for further development of CE-MS interfacing in the last years [61].
In our research group, a nanoflow SL interface (see Figure 2.8) was developed, which was utilized for the hyphenation of the two-dimensional (2D) system with the Orbitrap MS (see chapter 4.3) [62]. Here, an etched separation capillary is placed together with an additional capillary for SL delivery in a glass emitter. Through a cross piece, either a grounding or spray voltage can be applied, therefore, a flexible application on different kind of MS sources is allowed. Further benefits can be seen in the increased sensitivity than achieved with the triple tube sprayer. Additionally, better handling and higher flexibility in method development is obtained than with other porous-tip sheathless interfaces [63].
Besides technical CE-MS hyphenation, separation method compatibility is a significant point. Separation current restrictions by ESI-source instrumentation, limiting separation conditions, need to be considered. Many applications utilize BGEs with high salt content and non-volatile components. To avoid MS contamination, ionization suppression and adduct formation, the BGE and other additives need to be volatile. As volatile BGEs, formic acid (FAc), acetic acid (HAc), their ammonium salts, and ammonium carbonate buffer are commonly utilized [64].

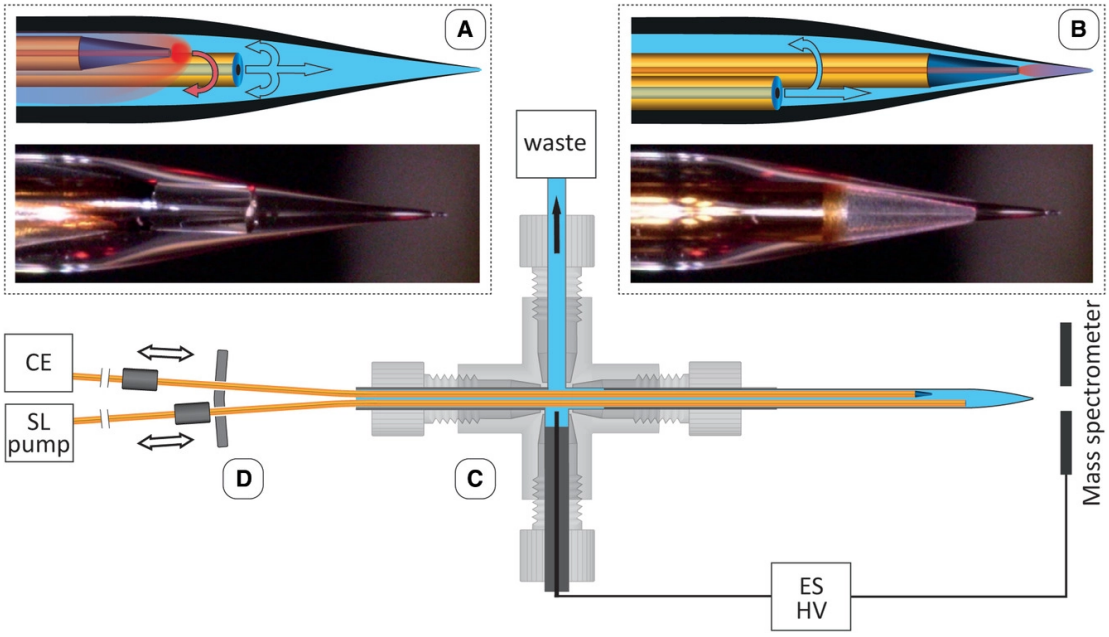

Figure 2.8: Schematic of the nanoflow sheath liquid interface with a two capillary approach [62]

2.4.2 Sample preparation of SDS-containing proteins prior to MS

Mass spectrometric analysis of SDS-separated proteins (in slab gel or in capillary format) is mandatory for identification of species. Matrix-assisted laser desorption ionization (MALDI) MS for protein [65] and peptide [66] analysis is feasible in presence of SDS concentrations of $> 0.3\%$. In contrast, SDS concentrations above 0.01% can be adverse for HPLC-ESI-MS analysis of proteins [67] due to known electrospray suppression [9]. As a result of the strong SDS–protein interaction [68], a separation of the complex solely by one-dimensional (1D) online MS-hyphenated chromatographic or electrophoretic separation techniques is not applicable. Therefore, most of the sample preparation strategies are focusing on offline sample clean-up of SDS containing protein samples prior to mass spectrometric analysis. The chosen SDS-removal method depends on the applied MS approach. Hence, either peptides resulting from protein digest (peptide mapping) or intact protein (intact mass) are purified.

In the last years, SDS-removal strategies for peptides were mainly performed by ion-exchange columns implemented in HPLC-systems [69, 70], in-gel digestion including extraction [71] or filter-aided sample preparation [72]. For intact protein purification regarding SDS, approaches like electric filtration [73], cross flow filtration [74], affinity spin columns [75], and precipitation by organic solvents [76], like acetone [67], or potassium chloride [77] are often utilized. In all these approaches, a compromise between protein recovery and SDS depletion is essential for further mass spectrometric protein analysis [78]. Most of the described

SDS-depletion protocols of intact proteins are labor-intense offline approaches and imply the need of high sample volumes in the range of several microliter. Other straightforward or even online approaches focus on SDS-removal prior to MS by the addition of cyclodextrin to the sample [79], the addition of cetyltrimethylammonium bromide (CTAB) during electrospray ionization by fused-droplet [80], microfluidic free-flow zone electrophoresis [81] or electrokinetic separation with a multi capillary device combined with ACN-rich extraction solution [82]. Nevertheless, the removal of only low SDS concentrations (3 mM for peptides [79, 82] and 10 mM [80] for proteins) is possible, or a high sample amount [81] is required in these presented methods.

2.4.3 Mass spectrometric analysis of CE(SDS)-separated proteins

CE(SDS) provides a high separation efficiency, especially compared to SEC [83], but online hyphenation with MS for peak characterization is not feasible due to the MS incompatible buffer components and its high viscosity. Besides tris(hydroxymethyl)aminomethane (Tris), glycerol, and ethylenediaminetetraacetic acid (EDTA), the commercial SDS-MW gel buffer applied in CE(SDS) contains non-volatile components like SDS, dextran and boric acid [84]. Nevertheless, several approaches try to overcome this challenge and obtain mass spectrometric information of CE(SDS)-separated proteins despite these non-compatible SDS-MW-gel buffer components.

Fraction collection of the peak of interest can generally be one solution but is not always feasible or associated with a high dilution due to the low volumes employed in CE separations. Especially for CE(SDS), fraction collection is hindered due to the high viscosity of the SDS-MW-gel buffer. Only Lu et al. described direct fraction collection of CE(SDS)-separated proteins on a poly(tetrafluoroethylene) membrane with following MALDI-MS analysis after complex offline clean-up [85]. Other approaches apply first RPLC fraction collection [11] or RPLC and GELFrEE fraction collection [10] with additional MS and CE(SDS) analysis to correlate unknown SDS-peaks. Besides the high effort, different selectivities are given, and the transfer and translation of the obtained results to the findings gained with the generic CE(SDS) separation can be inadequate. Another solution can be the reduction or even substitution of the interfering compounds, like replacing SDS with an acid labile surfactant [86, 87], but is often accompanied by a decline or even loss of separation efficiency. Additionally, a total replacement of all MS-interfering components of the SDS-MW-gel buffer while keeping the high separation efficiency has not been developed so far. Furthermore, the modification or replacement of a well characterized generic separation method in the biopharmaceutical industry is very unlikely, due to the high effort of method validation. Hence, the major goal is to keep the validated CE(SDS) separation and combine it with MS detection. This online hyphenation of generic CE(SDS) with MS has not been shown so far.

2.4.4 Two-dimensional capillary electrophoretic separation

Several validated CE methods, mainly applied in the pharmaceutical industry, utilize non-volatile BGEs or other MS-interfering additives. Examples are methods for analyzing mAb charge- and size-heterogeneity, like capillary isoelectric focusing, CE(SDS) and CZE based on an ϵ -aminocaproic acid buffer. To keep the high separation efficiency of validated methods and obtain online mass spectrometric information, 2D separation techniques can be applied [88]. Besides the advantage of increasing the separation efficiency and peak capacity by introducing an additional separation, 2D systems can be utilized to separate ESI-interfering compounds prior to MS detection. Here, the basic idea is to keep the original MS-incompatible separation method in the first dimension (^{1}D) and hyphenate it to an MS-compatible separation dimension employed as second dimension (^{2}D). This can be done by offline or online hyphenation of these two separation dimensions. As described before, fraction collection can be utilized for offline hyphenation with MS, but it has also been applied for offline hyphenation of separations [89, 90]. Nevertheless, besides the laborious effort, it is restricted regarding limit of detection arising from the dilution of few nanoliter fractions in several microliters collection buffer. For this reason, the online hyphenation is preferred for capillary-based electrophoretic separations.

Compared to online hyphenation of chromatographic separations, the online 2D approach with electrophoretic separations implicate some additional challenges. Here, a suitable interface between the separation dimensions, which preserves high voltages and is suitable for transferring small volumes as employed in CE applications, is of outstanding importance. General approaches realizing online electrophoretic 2D separations are described in detail elsewhere [91, 92]. Focusing on CE-CE hyphenation, 2D separations were shown among others by employing flow gating interfaces [93], microdialysis junction [94, 95], quartz coupling elements [96], and microfluidic devices [97, 98]. None of these approaches was utilized for online CE(SDS) hyphenation to mass spectrometry so far. For the 2D CE(SDS)-CZE separation, the hyphenation needs to be appropriate regarding the high viscose SDS-MW gel buffer. For this reason, two fully independent separation dimensions are mandatory, with a defined sample transfer volume from the ^{1}D to the ^{2}D.

Therefore, our research group developed another approach to fulfill these requirements in the form of a 4-port nanoliter valve [12], as seen in Figure 2.9. The here presented valve is commercially available, consisting of a stator for capillary connections and a rotor with a sample loop (here 4 nL, 10 nL, or 20 nL) and two short cuts (6 nL). By aligning the stator and rotor, the sample loop and one of the short cuts connect two capillaries each. Therefore, two fully independent separation dimensions can be used. The rotor can be switched with an electric microactuator into two positions. For this reason, it is possible to have the sample loop either in the ^{1}D or switching it into the ^{2}D to transfer the peak of interest.

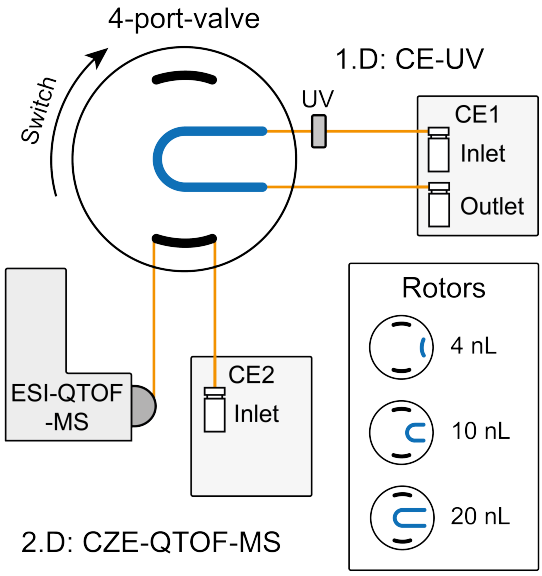

Figure 2.9: General scheme of the two-dimensional capillary electrophoresis set-up hyphenated with Q-TOF-MS [88]

With this set-up, it was possible to demonstrate various applications, combining MS interfering separations in the ^{1}D with an MS-compatible CZE separation in the ^{2}D hyphenated to a Q-TOF-MS [13–17].

To utilize CE(SDS) as the ^{1}D with the here presented valve approach, an additional SDS-protein decomplexation needed to be implemented in this 2D separation. As described in the previous chapter, mainly offline approaches for SDS depletion are common, and only a few online approaches are reported. None of these approaches was utilized to obtain online mass spectrometric information of CE(SDS)-separated proteins. Hence, an in-capillary decomplexation strategy was developed in our research group, consisting of the pre-injection of an organic solvent as presample zone and a cationic surfactant as postsample zone [18]. The combination of CE(SDS) separation in the ^{1}D with this decomplexation strategy in the ^{2}D was demonstrated for the first time for several mAb fragments by Cristina Montealegre [99].

This thesis focuses on measurements of mAb fragments, application to other protein samples, and validation of the 4-port valve for CE(SDS) applications. Additional, technical and method related improvements of the 2D set-up were performed, resulting in an 8-port valve approach and an improved decomplexation strategy. This new approach was evaluated and applied for top-down identification and characterization of unknown mAb fragments.

References

(1) Walsh, G. (2018). Biopharmaceutical benchmarks 2018. *Nat. Biotechnol. 36*, 1136–1145.

(2) Kesik-Brodacka, M. (2018). Progress in biopharmaceutical development. *65*, 306–322.

(3) Crommelin, D. J. A., Sindelar, R. D., and Meibohm, B., *Pharmaceutical Biotechnology: Fundamentals and Applications*, 5th ed. 2019, 2019.

(4) Liu, H., Gaza-Bulseco, G., Faldu, D., Chumsae, C., and Sun, J. (2008). Heterogeneity of monoclonal antibodies. *J. Pharm. Sci. 97*, 2426–2447.

(5) Staub, A., Guillarme, D., Schappler, J., Veuthey, J.-L., and Rudaz, S. (2011). Intact protein analysis in the biopharmaceutical field. *J. Pharm. Biomed. Anal. 55*, 810–822.

(6) Beck, A., Wagner-Rousset, E., Ayoub, D., van Dorsselaer, A., and Sanglier-Cianférani, S. (2013). Characterization of therapeutic antibodies and related products. *Anal. Chem. 85*, 715–736.

(7) Goyon, A., Fekete, S., Beck, A., Veuthey, J.-L., and Guillarme, D. (2018). Unraveling the mysteries of modern size exclusion chromatography - the way to achieve confident characterization of therapeutic proteins. *J. Chromatogr., B: Anal. Technol. Biomed. Life Sci. 1092*, 368–378.

(8) Shi, Y., Li, Z., and Lin, J. (2012). Advantages of CE-SDS over SDS-PAGE in mAb purity analysis. *Anal. Methods 4*, 1637.

(9) Rundlett, K. L., and Armstrong, D. W. (1996). Mechanism of signal suppression by anionic surfactants in capillary electrophoresis-electrospray ionization mass spectrometry. *Anal. Chem. 68*, 3493–3497.

(10) Kubota, K., Kobayashi, N., Yabuta, M., Ohara, M., Naito, T., Kubo, T., and Otsuka, K. (2017). Identification and characterization of a thermally cleaved fragment of monoclonal antibody-A detected by sodium dodecyl sulfate-capillary gel electrophoresis. *J. Pharm. Biomed. Anal. 140*, 98–104.

(11) Wang, W.-H., Cheung-Lau, J., Chen, Y., Lewis, M., and Tang, Q. M. (2019). Specific and high-resolution identification of monoclonal antibody fragments detected by capillary electrophoresis-sodium dodecyl sulfate using reversed-phase HPLC with top-down mass spectrometry analysis. *mAbs 11*, 1233–1244.

(12) Kohl, F. J., Montealegre, C., and Neusüß, C. (2016). On-line two-dimensional capillary electrophoresis with mass spectrometric detection using a fully electric isolated mechanical valve. *Electrophoresis 37*, 954–958.

(13) Hühner, J., and Neusüß, C. (2016). CIEF-CZE-MS applying a mechanical valve. *Anal. Bioanal. Chem. 408*, 4055–4061.

(14) Neuberger, S., Jooß, K., Ressel, C., and Neususs, C. (2016). Quantification of ascorbic acid and acetylsalicylic acid in effervescent tablets by CZE-UV and identification of related degradation products by heart-cut CZE-CZE-MS. *Anal. Bioanal. Chem. 408*, 8701–8712.

(15) Hühner, J., Jooß, K., and Neusüß, C. (2017). Interference-free mass spectrometric detection of capillary isoelectric focused proteins, including charge variants of a model monoclonal antibody. *Electrophoresis 38*, 914–921.

(16) Jooß, K., Hühner, J., Kiessig, S., Moritz, B., and Neusüß, C. (2017). Two-dimensional capillary zone electrophoresis-mass spectrometry for the characterization of intact monoclonal antibody charge variants, including deamidation products. *Anal. Bioanal. Chem. 409*, 6057–6067.

(17) Montealegre, C., and Neusüß, C. (2018). Coupling imaged capillary isoelectric focusing with mass spectrometry using a nanoliter valve. *Electrophoresis 39*, 1151–1154.

(18) Sanchez-Hernandez, L., Montealegre, C., Kiessig, S., Moritz, B., and Neusüß, C. (2016). In-capillary approach to eliminate SDS interferences in antibody analysis by capillary electrophoresis coupled to mass spectrometry. *Electrophoresis 38*, 1044–1052.

(19) Nelson, D. L., and Cox, M. M., *Lehninger Biochemie: Mit 131 Tabellen*, 4., vollständig überarbeitete und erweiterte Auflage, Übersetzung der 5. amerikanischen Auflage, korrigierter Nachdruck; Springer-Lehrbuch; Springer: Berlin and Heidelberg, 2011.

(20) Keizer, R. J., Huitema, A. D. R., Schellens, J. H. M., and Beijnen, J. H. (2010). Clinical pharmacokinetics of therapeutic monoclonal antibodies. *Clin. Pharmacokinet. 49*, 493–507.

(21) Shepard, H. M., Phillips, G. L., D Thanos, C., and Feldmann, M. (2017). Developments in therapy with monoclonal antibodies and related proteins. *17*, 220–232.

(22) Thermo Fisher Scientific Reducing and Denaturing Reagents, `https://www.thermofisher.com/de/de/home/life-science/protein-biology/protein-labeling-crosslinking/protein-modification/reducing-agents-protein-disulfides.html`.

(23) An, Y., Zhang, Y., Mueller, H.-M., Shameem, M., and Chen, X. (2014). A new tool for monoclonal antibody analysis. *mAbs 6*, 879–893.

(24) Sjögren, J., Olsson, F., and Beck, A. (2016). Rapid and improved characterization of therapeutic antibodies and antibody related products using IdeS digestion and subunit analysis. *Analyst 141*, 3114–3125.

(25) Köhler, G., and Milstein, C. (1975). Continuous cultures of fused cells secreting antibody of predefined specificity. *Nature 256*, 495–497.

(26) Steinitz, M. (2009). Three decades of human monoclonal antibodies: past, present and future developments. *Hum. Antibodies 18*, 1–10.

(27) Antibody Society Antibody therapeutics approved or in regulatory review in the EU or US `https://www.antibodysociety.org/resources/approved-antibodies/`.

(28) Chames, P., van Regenmortel, M., Weiss, E., and Baty, D. (2009). Therapeutic antibodies: successes, limitations and hopes for the future. *Br. J. Pharmacol. 157*, 220–233.

(29) Hawe, A., Wiggenhorn, M., van de Weert, M., Garbe, J. H. O., Mahler, H.-C., and Jiskoot, W. (2012). Forced degradation of therapeutic proteins. *J. Pharm. Sci. 101*, 895–913.

(30) D'Atri, V., Fekete, S., Clarke, A., Veuthey, J.-L., and Guillarme, D. (2019). Recent Advances in Chromatography for Pharmaceutical Analysis. *Anal. Chem. 91*, 210–239.

(31) Lechner, A., Giorgetti, J., Gahoual, R., Beck, A., Leize-Wagner, E., and François, Y.-N. (2019). Insights from capillary electrophoresis approaches for characterization of monoclonal antibodies and antibody drug conjugates in the period 2016–2018. *J. Chromatogr., B: Anal. Technol. Biomed. Life Sci. 1122-1123*, 1–17.

(32) Zhao, S. S., and Chen, D. D. Y. (2014). Applications of capillary electrophoresis in characterizing recombinant protein therapeutics. *Electrophoresis 35*, 96–108.

(33) Fekete, S., Guillarme, D., Sandra, P., and Sandra, K. (2016). Chromatographic, Electrophoretic, and Mass Spectrometric Methods for the Analytical Characterization of Protein Biopharmaceuticals. *Anal. Chem. 88*, 480–507.

(34) Haverick, M., Mengisen, S., Shameem, M., and Ambrogelly, A. (2014). Separation of mAbs molecular variants by analytical hydrophobic interaction chromatography HPLC: overview and applications. *mAbs 6*, 852–858.

(35) Graf, T., Heinrich, K., Grunert, I., Wegele, H., Haberger, M., Bulau, P., and Leiss, M. (2020). Recent advances in LC-MS based characterization of protein-based biotherapeutics - mastering analytical challenges posed by the increasing format complexity. *J. Pharm. Biomed. Anal. 186*, 113251.

(36) Vlasak, J., and Ionescu, R. (2008). Heterogeneity of monoclonal antibodies revealed by charge-sensitive methods. *Curr. Pharm. Biotechnol. 9*, 468–481.

(37) Moritz, B. et al. (2015). Evaluation of capillary zone electrophoresis for charge heterogeneity testing of monoclonal antibodies. *J. Chromatogr., B: Anal. Technol. Biomed. Life Sci. 983-984*, 101–110.

(38) Shapiro, A. L., Viñuela, E., and V. Maizel, J. (1967). Molecular weight estimation of polypeptide chains by electrophoresis in SDS-polyacrylamide gels. *Biochem. Biophys. Res. Commun. 28*, 815–820.

(39) Laemmli, U. K. (1970). Cleavage of structural proteins during the assembly of the head of bacteriophage T4. *Nature 227*, 680–685.

(40) Svedberg, T., and Jette, E. R. (1923). The cataphoresis of proteins. *J. Am. Chem. Soc. 45*, 954–957.

(41) Scott, N. D., and Svedberg, T. (1924). Measurements of the mobility of egg albumin at different acidities. *J. Am. Chem. Soc. 46*, 2700–2707.

(42) Svedberg, T., and Tiselius, A. (1926). A new method for determination of the mobility of proteins. *J. Am. Chem. Soc. 48*, 2272–2278.

(43) Tiselius, A., *The moving-boundary method of studying the electrophoresis of proteins: Inaugural Dissertation Upsala*, IV; 7, Vol. 4; Nova Acta Regiae Societatis Scientiarum Upsaliensis: 1930.

(44) Tiselius, A. (1937). A new apparatus for electrophoretic analysis of colloidal mixtures. *Trans. Faraday Soc. 33*, 524.

(45) Hjertén, S. (1967). Free zone electrophoresis. *Chromatog. Rev. 9*, 122–219.

(46) Jorgenson, J. W., and Lukacs, K. D. (1981). Zone electrophoresis in open-tubular glass capillaries. *Anal. Chem. 53*, 1298–1302.

(47) Agilent Technologies, *High Performance Capillary Electrophoresis: A Primer*, 2nd ed., 2018.

(48) Huhn, C., Ramautar, R., Wuhrer, M., and Somsen, G. W. (2010). Relevance and use of capillary coatings in capillary electrophoresis-mass spectrometry. *Anal. Bioanal. Chem. 396*, 297–314.

(49) Sänger-van de Griend, C. E. (2019). CE-SDS method development, validation, and best practice-An overview. *Electrophoresis 40*, 2361–2374.

(50) *Electrophoresis '83: Advanced methods, biochemical and clinical applications ; proceedings of the International Conference on Electrophoresis, Tokyo, Japan, May 9 - 12, 1983 ; [annual meeting of the International Society of Electrophoresis*; Hirai, H., Ed.; de Gruyter: Berlin, 1984.

(51) Cohen, A. S., and Karger, B. L. (1987). High-performance sodium dodecyl sulfate polyacrylamide gel capillary electrophoresis of peptides and proteins. *J. Chromatogr., A 397*, 409–417.

(52) Guan, Y., Zhu, Q., Huang, D., Zhao, S., Jan Lo, L., and Peng, J. (2015). An equation to estimate the difference between theoretically predicted and SDS PAGE-displayed molecular weights for an acidic peptide. *5*, 13370.

(53) Tran, N. T., Cabanes-Macheteau, M., and Taverna, M. In *Carbohydrate Analysis by Modern Chromatography and Electrophoresis*; Journal of Chromatography Library, Vol. 66; Elsevier: 2002, pp 691–785.

(54) Zhu, Z., Lu, J. J., and Liu, S. (2012). Protein separation by capillary gel electrophoresis: A review. *Anal. Chim. Acta 709*, 21–31.

(55) Gross, J. H., *Mass Spectrometry: A Textbook*; Springer International Publishing: Cham and s.l., 2017.

(56) Eliuk, S., and Makarov, A. (2015). Evolution of Orbitrap Mass Spectrometry Instrumentation. *8*, 61–80.

(57) Hecht, E. S., Scigelova, M., Eliuk, S., and Makarov, A. In *Encyclopedia of Analytical Chemistry*, Meyers, R. A., Ed.; Wiley: 2006; Vol. 3, pp 1–40.

(58) Mander, L., *Comprehensive natural products II: Chemistry and biology*; Elsevier: Amsterdam, 2010.

(59) Siuti, N., and Kelleher, N. L. (2007). Decoding protein modifications using top-down mass spectrometry. *Nat. Methods 4*, 817–821.

(60) Julian, R. (2017). The Mechanism behind Top-Down UVPD Experiments: Making Sense of Apparent Contradictions. *J. Am. Soc. Mass Spectrom. 28*, 1823–1826.

(61) Lindenburg, P. W., Haselberg, R., Rozing, G., and Ramautar, R. (2015). Developments in Interfacing Designs for CE–MS: Towards Enabling Tools for Proteomics and Metabolomics. *Chromatographia 78*, 367–377.

(62) Höcker, O., Knierman, M., Meixner, J., and Neusüß, C. (2020). Two capillary approach for a multifunctional nanoflow sheath liquid interface for capillary electrophoresis-mass spectrometry. *Electrophoresis*, DOI: 10.1002/elps.202000169.

(63) Höcker, O., Montealegre, C., and Neusüß, C. (2018). Characterization of a nanoflow sheath liquid interface and comparison to a sheath liquid and a sheathless porous-tip interface for CE-ESI-MS in positive and negative ionization. *Anal. Bioanal. Chem. 410*, 5265–5275.

(64) Pantůcková, P., Gebauer, P., Bocek, P., and Krivánková, L. (2009). Electrolyte systems for on-line CE-MS: detection requirements and separation possibilities. *Electrophoresis 30*, 203–214.

(65) Amado, F. M. L., Santana-Marques, M. G., Ferrer-Correia, A. J., and Tomer, K. B. (1997). Analysis of Peptide and Protein Samples Containing Surfactants by MALDI-MS. *Anal. Chem. 69*, 1102–1106.

(66) Tummala, R., and Limbach, P. A. (2004). Effect of sodium dodecyl sulfate micelles on peptide mass fingerprinting by matrix-assisted laser desorption/ionization mass spectrometry. *Rapid Commun. Mass Spectrom. 18*, 2031–2035.

(67) Botelho, D., Wall, M. J., Vieira, D. B., Fitzsimmons, S., Liu, F., and Doucette, A. (2010). Top-down and bottom-up proteomics of SDS-containing solutions following mass-based separation. *J. Proteome Res. 9*, 2863–2870.

(68) Chattoraj, D. K., Biswas, S. C., Mahapatra, P. K., and Chatterjee, S. (1999). Standard free energies of binding of solute to proteins in aqueous medium. Part 2. Analysis of data obtained from equilibrium dialysis and isopiestic experiments. *Biophys. Chem. 77*, 9–25.

(69) Vissers, J. P. C., Chervet, J.-P., and Salzmann, J.-P. (1996). Sodium Dodecyl Sulphate Removal from Tryptic Digest Samples for On-line Capillary Liquid Chromatography/-Electrospray Mass Spectrometry. *Biol. Mass Spectrom. 31*, 1021–1027.

(70) Sun, D., Wang, N., and Li, L. (2012). Integrated SDS removal and peptide separation by strong-cation exchange liquid chromatography for SDS-assisted shotgun proteome analysis. *J. Proteome Res. 11*, 818–828.

(71) Shevchenko, A., Tomas, H., Havlis, J., Olsen, J. V., and Mann, M. (2006). In-gel digestion for mass spectrometric characterization of proteins and proteomes. *Nat. Protoc. 1*, 2856–2860.

(72) Wiśniewski, J. R., Zougman, A., Nagaraj, N., and Mann, M. (2009). Universal sample preparation method for proteome analysis. *Nat. Methods 6*, 359–362.

(73) Kachuk, C., Faulkner, M., Liu, F., and Doucette, A. A. (2016). Automated SDS Depletion for Mass Spectrometry of Intact Membrane Proteins though Transmembrane Electrophoresis. *J. Proteome Res. 15*, 2634–2642.

(74) Kim, K. H., Compton, P. D., Tran, J. C., and Kelleher, N. L. (2015). Online matrix removal platform for coupling gel-based separations to whole protein electrospray ionization mass spectrometry. *J. Proteome Res. 14*, DOI: 10.1021/pr501331q.

(75) Hengel, S. M., Floyd, E., Baker, E. S., Zhao, R., Wu, S., and Paša-Tolić, L. (2012). Evaluation of SDS depletion using an affinity spin column and IMS-MS detection. *Proteomics 12*, 3138–3142.

(76) Tubaon, R. M., Haddad, P. R., and Quirino, J. P. (2017). Sample Clean-up Strategies for ESI Mass Spectrometry Applications in Bottom-up Proteomics: Trends from 2012 to 2016. *Proteomics 17*, DOI: 10.1002/pmic.201700011.

(77) Carraro, U., Rizzi, C., and Sandri, M. (1991). Effective recovery by KCl precipitation of highly diluted muscle proteins solubilized with sodium dodecyl sulfate. *Electrophoresis 12*, 1005–1010.

(78) Kachuk, C., Stephen, K., and Doucette, A. (2015). Comparison of sodium dodecyl sulfate depletion techniques for proteome analysis by mass spectrometry. *J. Chromatogr., A 1418*, 158–166.

(79) Quirino, J. P. (2017). Sodium dodecyl sulfate removal during electrospray ionization using cyclodextrins as simple sample solution additive for improved mass spectrometric detection of peptides. *Anal. Chim. Acta 1005*, 54–60.

(80) Shieh, I.-F., Lee, C.-Y., and Shiea, J. (2005). Eliminating the interferences from TRIS buffer and SDS in protein analysis by fused-droplet electrospray ionization mass spectrometry. *J. Proteome Res. 4*, 606–612.

(81) Kinde, T. F., Lopez, T. D., and Dutta, D. (2015). Electrophoretic extraction of low molecular weight cationic analytes from sodium dodecyl sulfate containing sample matrices for their direct electrospray ionization mass spectrometry. *Anal. Chem. 87*, 2702–2709.

(82) Tubaon, R. M., Haddad, P. R., and Quirino, J. P. (2018). Membrane-Free Electrokinetic Device Integrated to Electrospray-Ionization Mass Spectrometry for the Simultaneous Removal of Sodium Dodecyl Sulfate and Enrichment of Peptides. *Anal. Chem. 90*, 10122–10127.

(83) Dada, O. O., Rao, R., Jones, N., Jaya, N., and Salas-Solano, O. (2017). Comparison of SEC and CE-SDS methods for monitoring hinge fragmentation in IgG1 monoclonal antibodies. *J. Pharm. Biomed. Anal. 145*, 91–97.

(84) Liu, Y., Reddy, P., Ratnayake, C. K., and Koh, E. V. Methods and compositions for capillary electrophoresis (CE): United States Patent pat., US 7,381,317 B2, 2004.

(85) Lu, J. J., Zhu, Z., Wang, W., and Liu, S. (2011). Coupling sodium dodecyl sulfate-capillary polyacrylamide gel electrophoresis with matrix-assisted laser desorption ionization time-of-flight mass spectrometry via a poly(tetrafluoroethylene) membrane. *Anal. Chem. 83*, 1784–1790.

(86) Ross, A. R. S., Lee, P. J., Smith, D. L., Langridge, J. I., d. Whetton, A., and Gaskell, S. J. (2002). Identification of proteins from two-dimensional polyacrylamide gels using a novel acid-labile surfactant. *Proteomics 2*, 928–936.

(87) König, S., Schmidt, O., Rose, K., Thanos, S., Besselmann, M., and Zeller, M. (2003). Sodium dodecyl sulfate versus acid-labile surfactant gel electrophoresis: comparative proteomic studies on rat retina and mouse brain. *Electrophoresis 24*, 751–756.

(88) Schlecht, J., Jooß, K., and Neusüß, C. (2018). Two-dimensional capillary electrophoresis-mass spectrometry (CE-CE-MS): coupling MS-interfering capillary electromigration methods with mass spectrometry. *Anal. Bioanal. Chem. 410*, 6353–6359.

(89) Helmja, K., Borissova, M., Knjazeva, T., Jaanus, M., Muinasmaa, U., Kaljurand, M., and Vaher, M. (2009). Fraction collection in capillary electrophoresis for various stand-alone mass spectrometers. *J. Chromatogr., A 1216*, 3666–3673.

(90) Santos, B., Simonet, B. M., Ríos, A., and Valcárcel, M. (2007). Integrated 2-D CE. *Electrophoresis 28*, 1345–1351.

(91) Kohl, F. J., Sánchez-Hernández, L., and Neusüß, C. (2015). Capillary electrophoresis in two-dimensional separation systems: Techniques and applications. *Electrophoresis 36*, 144–158.

(92) Kler, P. A., Sydes, D., and Huhn, C. (2015). Column-coupling strategies for multi-dimensional electrophoretic separation techniques. *Anal. Bioanal. Chem. 407*, 119–138.

(93) Michels, D. A., Hu, S., Dambrowitz, K. A., Eggertson, M. J., Lauterbach, K., and Dovichi, N. J. (2004). Capillary sieving electrophoresis-micellar electrokinetic chromatography fully automated two-dimensional capillary electrophoresis analysis of Deinococcus radiodurans protein homogenate. *Electrophoresis 25*, 3098–3105.

(94) Mohan, D., and Lee, C. S. (2002). On–line coupling of capillary isoelectric focusing with transient isotachophoresis–zone electrophoresis: A two–dimensional separation system for proteomics. *Electrophoresis 23*, 3160–3167.

(95) Yang, C., Zhang, L., Liu, H., Zhang, W., and Zhang, Y. (2003). Two-dimensional capillary electrophoresis involving capillary isoelectric focusing and capillary zone electrophoresis. *J. Chromatogr., A 1018*, 97–103.

(96) Bowerbank, C. R., and Lee, M. L. (2001). Comprehensive isotachophoresis-capillary zone electrophoresis using directly inserted columns having different diameters with a periodic counterflow and dual ultraviolet detectors. *J. Micro. Sep. 13*, 361–370.

(97) Lu, J. J., Wang, S., Li, G., Wang, W., Pu, Q., and Liu, S. (2012). Chip-capillary hybrid device for automated transfer of sample preseparated by capillary isoelectric focusing to parallel capillary gel electrophoresis for two-dimensional protein separation. *Anal. Chem. 84*, 7001–7007.

(98) Kler, P. A., Posch, T. N., Pattky, M., Tiggelaar, R. M., and Huhn, C. (2013). Column coupling isotachophoresis–capillary electrophoresis with mass spectrometric detection: Characterization and optimization of microfluidic interfaces. *J. Chromatogr., A 1297*, 204–212.

(99) Römer, J., Montealegre, C., Schlecht, J., Kiessig, S., Moritz, B., and Neusüß, C. (2019). Online mass spectrometry of CE (SDS)-separated proteins by two-dimensional capillary electrophoresis. *Anal. Bioanal. Chem. 411*, 7197–7206.

3 Experimental

In this chapter, essential materials, chemicals, and instruments used in this work are listed. In addition, assembly and handling of both utilized nanoliter valves are described. Main focus is on the development and utilization of the 8-port valve and resulting improvements of the total 2D set-up. Furthermore, optimization of the decomplexation strategy by spiking experiments is explained. More detailed information can be found in each section of the results and discussions.

3.1 Materials and chemicals

The main consumables and materials are listed in the following table 1.

Table 1: List of consumables

Consumables	Supplier
Fused silica capillaries (OD = 363 μm; ID = 50 μm)	Polymicro (Phoenix, USA)
Borosilicate emitter (5.5 cm length, OD = 1 mm, tip ID = 30 μm)	BioMedical Instruments (Zöllnitz, Germany)
1.5 mL Crimp Neck Vials N11 0.1 mL Micro inserts 0.3 mL Micro inserts	Macherey-Nagel (Düren, Germany)
SDS-MW gel buffer	AB Sciex (Darmstadt, Germany)
Precision wipes (low-lint)	Kimtech Science (Kent, United Kingdom)

All aqueous solutions were prepared with ultrapure water prepared in-house (18 MΩ cm at 25°C, SG Ultra Clear UV from Siemens Water Technologies, Günzburg, Germany). Following chemicals in table 2 were applied for sample preparation and experiment performance.

Table 2: List of most often used chemicals

Chemicals	Abbreviation	Supplier
Acetic acid (glacial, 100%)	HAc	Carl Roth (Karlsruhe, Germany)
Acetonitrile (HPLC-MS grade)	ACN	Carl Roth (Karlsruhe, Germany)
1-Butanol (HPLC grade)	BuOH	Merck (Darmstadt, Germany)
Cetyltrimethylammoniumbromide ($\geq$ 99%)	CTAB	Sigma Aldrich (Steinheim, Germany)
Dithiothreitol ($\geq$ 99.5%)	DTT	Sigma Aldrich (Steinheim, Germany)
ESI-TOF Tuning Mix		Agilent Technologies (Waldbronn, Germany)
Ethanol (HPLC grade)	EtOH	Fisher Scientific (Schwerte, Germany)
Formic acid ($\geq$ 98%)	FAc	Carl Roth (Karlsruhe, Germany)
Glutaraldehyde solution (50% in water)	CHO	Sigma Aldrich (Steinheim, Germany)
Hydrochloric acid (37%)	HCl	Merck (Darmstadt, Germany)
Methanol (HPLC-MS grade)	MeOH	Carl Roth (Karlsruhe, Germany)
NIST antibody	NIST mAb	National Institute of Standards and Technology (Gaithersburg, USA)
Poly(vinyl alcohol) ($\geq$ 99%, average MW 89,000–98,000)	PVA	Sigma Aldrich (Steinheim, Germany)
2-Propanol (HPLC-MS grade)	IPA	Carl Roth (Karlsruhe, Germany)
Sodium dodecyl sulfate (10% in water)	SDS	Sigma Aldrich (Steinheim, Germany)
Sodium hydroxide ($\geq$ 99%)	NaOH	Merck (Darmstadt, Germany)
Soybean flour		Alnatura
Tris(hydroxymethyl)aminomethane ($\geq$ 99%)	Tris	Sigma Aldrich (Steinheim, Germany)
Urea		Merck (Darmstadt, Germany)

3.2 Instruments

For experiment performance, several instruments were utilized. The most important ones can be found in the following table 3.

Table 3: List of instruments

Instrument	Supplier
G1600 HP^{3D}CE	Agilent Technologies (Waldbronn, Germany)
4-port nanoliter valve	VICI AG International (Schenkon, Switzerland)
8-port nanoliter valve	VICI AG International (Schenkon, Switzerland)
ECD2600 EX UV-VIS detector	ECOM spol. s r.o., (Prague, Czech Republic)
TraceDec C^{4}D detector	Innovative Sensor Technologies (Strasshof, Austria)
Syringe pump	Cole-Parmer (Vernon Hills, USA)
Compact mass spectrometer	Bruker (Bremen, Germany)
Orbitrap Fusion Lumos mass spectrometer	Thermo Fisher Scientific (San Jose, USA)
G1607A sheath liquid interface	Agilent Technologies (Waldbronn, Germany)
Thermomixer	Eppendorf (Wesseling-Berzdorf, Germany)
Centrifuge	Eppendorf (Wesseling-Berzdorf, Germany)

3.3 Assembly and handling of 4- and 8-port nanoliter valve

The nanoliter valve consists of a metal body that is connected to an electric microactuator (4-port valve: two-position; 8-port valve: multi-position) with a clamp ring (see Figure 3.1 a)). The rotor with the sample loops is placed on top of a movable part of the metal body (see Figure 3.1 b)). The stator, where capillaries can be connected with fittings, is placed on top of the metal body, positioned through two metal pins, and fixed with two additional screws (see Figure 3.1 c)).

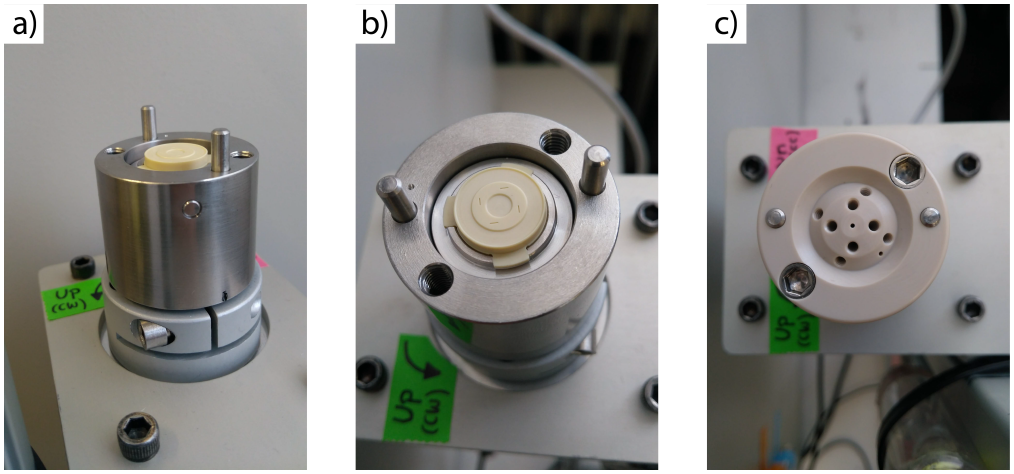

Figure 3.1: Set-up of the 8-port valve a) Side view of metal body fixed on electric microactuator with rotor b) top view of metal body with rotor c) top view of metal body with fixed stator

Alignment of the stator channels with the sample loops on the rotor is of outstanding importance to avoid leakage inside the valve. For the 4-port valve, alignment is done by a mechanical stop. Positioning of the 8-port valve is performed by the serial communication and programming according to the manual [1]. Due to the small channel dimensions (100 μm bore size) of the nanoliter valves, they are prone to clogging when small particles are introduced by capillary connection or from liquids that are flushed through. For the release of clogged channels, high-pressure flush with water or NaOH (up to 3 bar) or air (up to 5 bar) was applied through the capillaries first. If clogging could not be removed by high pressure flush, a total disassembly of the valve, extensive cleaning with a wire and ultrasonic bath, drying, and reassembly is necessary. To prevent this time consuming cleaning, introduction of particles was reduced to a minimum. First, capillaries used for the analysis were cut, and the tip was polished with a ceramic cutter. Here, it is essential to obtain a flat tip, to optimize the connection between capillaries and channels of the valve, hence minimize the resulting dead volume. After polishing and before connecting to the stator, water was flushed through the capillaries with a syringe connected via an adapter to remove possible particles inside and at the capillary tip. After this procedure, capillary

ends were thread through the fittings and cleaned again with a low-lint wipe dipped in isopropanol. All solutions and liquids used for the 2D analysis were prepared frequently and degassed for 15 min before use to reduce crystals and air bubbles.

3.4 Development and comparison of 8-port nanoliter valve

One essential part of this work was the design and implementation of an optimized valve to improve system robustness and simplify handling. The 4-port nanoliter valve utilized for the first publication was commercially obtained from VICI AG International without any modification. The stator has four ports for capillary connections. The rotor has one main loop with a volume of 20 nL (also 4 nL and 10 nL available), as shown in Figure 3.2 a). Additionally, there are two smaller loops with a volume of around 6.7 nL, where only one can be used due to the two-position limitation. Based on the correlation of the applicable separation voltage, the so-called breakdown voltage, and the material's thickness, here the distance between loops, a higher distance between loops is beneficial. The distance between the main loop and the smaller loop is about 0.85 mm. Therefore, one of the main obstacles with this valve was measurement instability due to observed current leakage and limited applicable separation voltage of $\pm$ 15 kV. To increase the applicable voltage and reduce current leakage, distances between the loops were increased: for 10 nL and 20 nL loops to 3.14 mm (Figure 3.2 b) and 3.2 c)) and for 40 nL loops to 2.11 mm, see Figure 3.2 d).

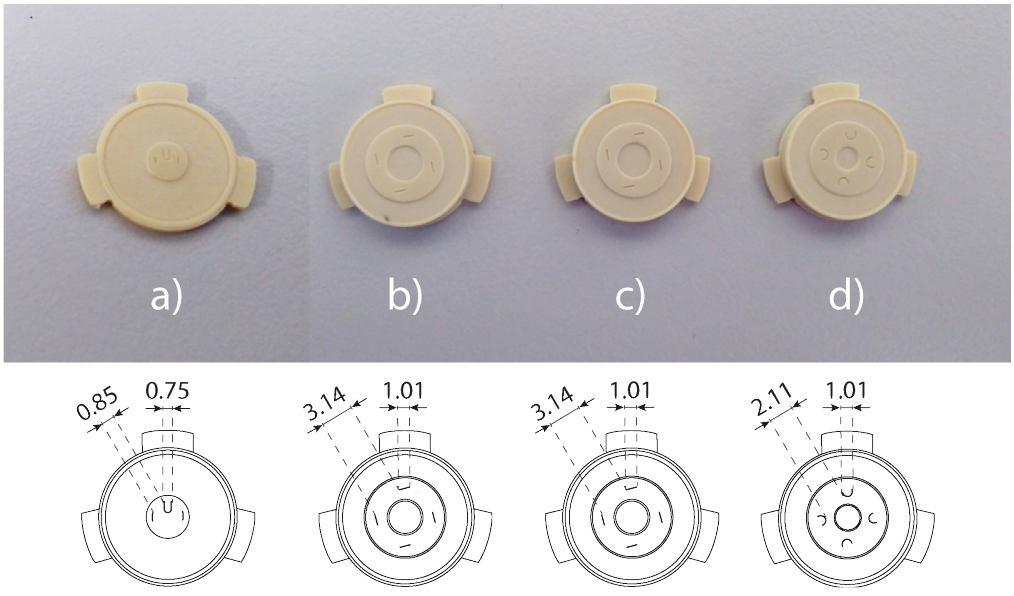

Figure 3.2: Rotor pictures and related drawings of a) 4-port valve (20 nL loop) b) 8-port valve (10 nL loops) c) 8-port valve (20 nL loops) d) 8-port valve (40 nL loops)

Besides the increased distances between the loops, the 8-port valve rotor has an additional loop compared to the rotor of the 4-port valve. These four loops are symmetrically arranged and have all the same geometry and volume. With the high flexibility of the multi-position actuator employed with the 8-port nanoliter valve, the loops on the rotor can be transferred to each of the four dimensions. The stator is adapted to the geometry of the rotor loops, and 360 μm fittings are utilized for capillary connection. This gives the possibility to connect eight capillaries to obtain four independent dimensions, compared to the 4-port nanoliter valve with only four capillary connections and two dimensions. Therefore, it is possible to vary between the loops and utilize two of them for the pre- and postsample zone transfer into the ^{2}D for the decomplexation. This allows a more precise positioning of both zones in relation to the SDS-protein zone in the ^{2}D without the need for a capacitively coupled contactless conductivity detector (C^{4}D).
Additional to the commonly applied rotor made of a polyaryletherketone/polytetrafluoroethylene based composite, two additional rotor materials (pure polytetrafluoroethylene and pure hydrocarbon) were tested to reduce material abrasion of the stator (made of polyether ether ketone) and improve tightness to lower the risk of leakage inside the valve.

3.5 Further development of two-dimensional system set-up

The set-up of the 2D system was adopted at the beginning of this work, as shown in Figure 3.3 a). By replacing the UV-detector TIDAS CCD UV/NIR detector (J&M Analytik AG, Essingen, Germany; see Figure 3.3 a)) with ECD2600 EX UV-VIS detector (ECOMspol. s r.o., Prague, Czech Republic; see Figure 3.3 b)), signals with a higher S/N-ratio could be obtained and handling simplified.

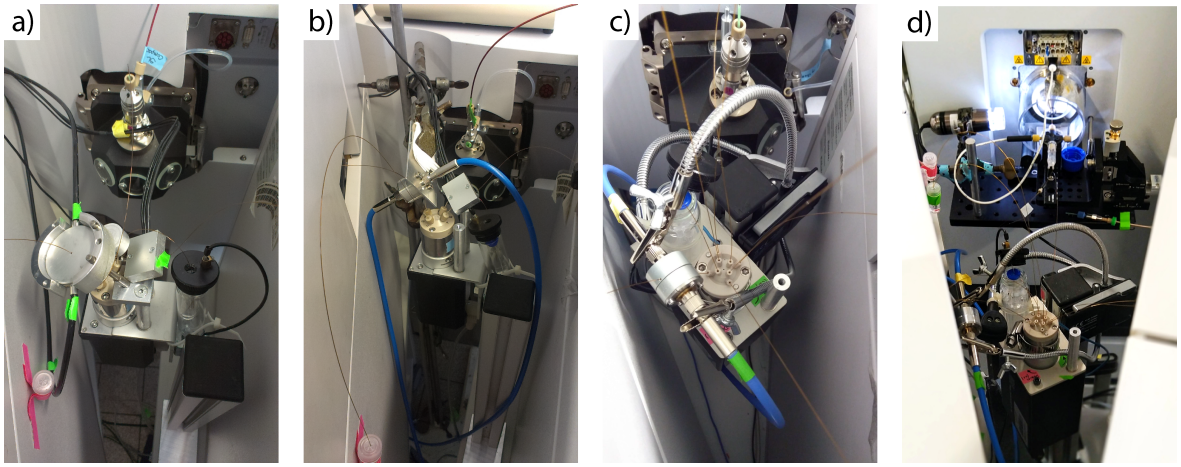

Figure 3.3: Set-up of the 2D system with a) 4-port valve as adopted at the beginning b) 4-port valve with implemented new UV-detector c) 8-port valve and additional improvement of UV-holder d) 8-port valve with nanoflow sheath liquid interface

Experiments for the first publication [2] (see chapter 4.1) were performed with the set-up as shown in Figure 3.3 a) and 3.3 b). For higher flexibility and more robustness, the holder for the UV detector was replaced as seen in Figure 3.3 c). This set-up was utilized for the second publication [3] (see chapter 4.2). The same set-up was hyphenated with the Orbitrap MS for the top-down experiments [4] via the nanoflow sheath liquid interface (see chapter 4.3), as shown in Figure 3.3 d).

3.6 Optimization of decomplexation by spiking experiments

Due to frequently observed current instabilities after incapillary decomplexation in the ^{2}D adapted from Sanchez-Hernandez et al. [5], offline spiking experiments were performed. First, different ratios of CTAB (0.4% in methanol : water (1:1); n = 11 mM), former utilized as postsample zone, and 0.3% SDS-solution (in water; n = 10 mM) were mixed. As it can be seen in Figure 3.4, for all ratios, precipitation could be observed. Slightly less precipitation was observed for the excess of SDS (Figure 3.4 a), but was not applicable for the intended use of SDS removal. Strongest precipitation was observed at the ratio of 1:1 (as seen in Figure (3.4 c)).

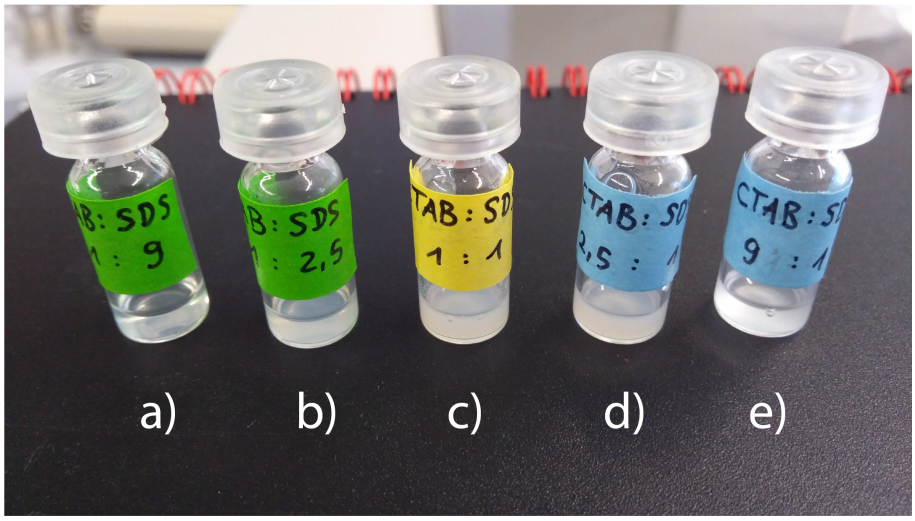

Figure 3.4: Spiking experiments with different ratios of CTAB (0.4% in methanol : water (1:1)) and 10% SDS-solution a) 1:9 b) 1:2.5 c) 1:1 d) 2.5:1 e) 9:1

By the addition of methanol, which was utilized as presample zone before, precipitations were still observed (see Figure 3.5 b)). Primarily, intense precipitation was seen by replacing the SDS-solution with SDS-MW gel buffer (Figure 3.5 a)). Here, besides SDS, dextran, Tris, glycerol, EDTA, and boric acid are present.

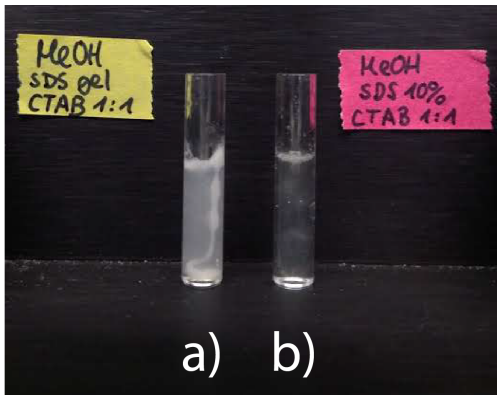

Figure 3.5: Spiking experiments with equal volumes of methanol, CTAB (0.4% in methanol : water (1:1)) and a) SDS-MW gel buffer or b) 10% SDS-solution

To increase the solubility and to keep the molar CTAB : SDS ratio at 1:1, different organic solvents (hexane, octanol, ethanol, and butanol) were tested to replace methanol as presample zone and solvent for CTAB. Here, no precipitation was observed with the addition of butanol. For this reason, several mixtures with different ratios of water, butanol, ethanol/methanol were tested to find an appropriate solvent solution for CTAB with no precipitation by the addition of SDS-MW gel buffer. Finally, a clear solution was obtained by solving CTAB in a mixture of water : ethanol : butanol with a ratio of 2:2:1. Comparing the old decomplexation mixture with methanol (see Figure 3.6 a)) with the new decomplexation mixture with water : ethanol : butanol (see Figure 3.6 b)), precipitation could be clearly reduced. For this reason, water as presample zone and CTAB (0.4% in water : ethanol : butanol (2:2:1)) as postsample zone were tested and compared to the old approach regarding removal efficiency in 2D experiments in the second publication (see chapter 4.2).

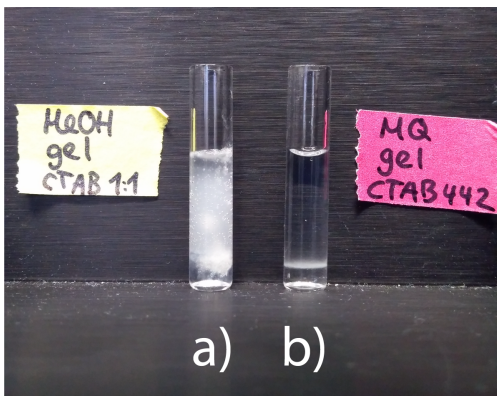

Figure 3.6: Spiking experiments with equal volumes of SDS-MW gel buffer and a) methanol and CTAB (0.4% in methanol : water (1:1)) and b) water and CTAB (0.4% in water : ethanol : butanol (2:2:1))

References

(1) VICI AG International Universal Electric Actuator Instruction Manual: Models EUH, EUD, and EUT: Firmware revisions CT and previous.

(2) Römer, J., Montealegre, C., Schlecht, J., Kiessig, S., Moritz, B., and Neusüß, C. (2019). Online mass spectrometry of CE (SDS)-separated proteins by two-dimensional capillary electrophoresis. *Anal. Bioanal. Chem. 411*, 7197–7206.

(3) Römer, J., Kiessig, S., Moritz, B., and Neusüß, C. (2020). Improved CE(SDS)-CZE-MS method utilizing an 8-port nanoliter valve. *Electrophoresis 42*, 374–380.

(4) Römer, J., Stolz, A., Kiessig, S., Moritz, B., and Neusüß, C. (2021). Online top-down mass spectrometric identification of CE(SDS)-separated antibody fragments by two-dimensional capillary electrophoresis. *J. Pharm. Biomed. Anal. 201*, 114089.

(5) Sanchez-Hernandez, L., Montealegre, C., Kiessig, S., Moritz, B., and Neusüß, C. (2016). In-capillary approach to eliminate SDS interferences in antibody analysis by capillary electrophoresis coupled to mass spectrometry. *Electrophoresis 38*, 1044–1052.

4 Results and Discussion

4.1 Online mass spectrometry of CE(SDS)-separated proteins by two-dimensional capillary electrophoresis

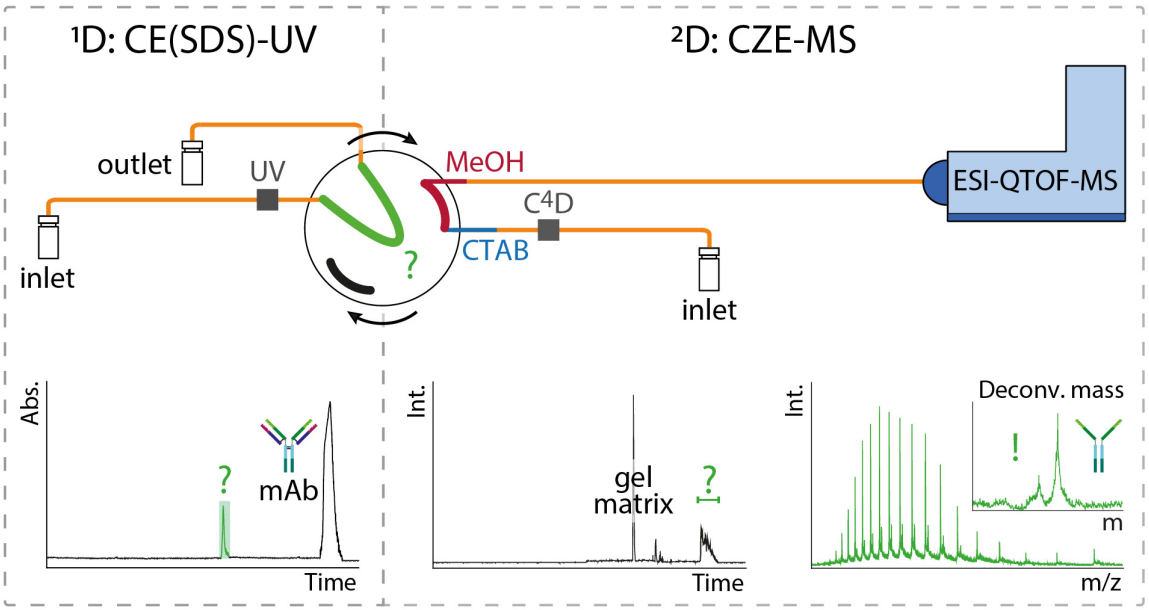

Figure 4.1: Graphical abstract: Set-up and principle of the two-dimensional approach

This chapter has been published and adapted with permission from:

Römer, J., Montealegre, C., Schlecht, J., Kiessig, S., Moritz, B., and Neusüß, C. (2019). Anal. Bioanal. Chem. 411, 7197–7206; DOI: 10.1007/s00216-019-02102-8

4.1.1 Abstract

Sodium dodecyl sulfate-polyacrylamide gel electrophoresis (SDS-PAGE) is the fundamental technique for protein separation by size. Applying this technology in capillary format, gaining high separation efficiency in a more automated way, is a key technology for size separation of proteins in the biopharmaceutical industry. However, unequivocal identification by online mass spectrometry (MS) is impossible so far, due to strong interference in the electrospray process by SDS and other components of the SDS-MW separation gel buffer. Here, a heart-cut two-dimensional electrophoretic separation system applying an electrically isolated valve with an internal loop of 20 nL is presented. The peak of interest in the CE(SDS) separation is transferred to the CZE-MS, where electrospray-interfering substances of the SDS-MW gel are separated prior to online electrospray ionization mass spectrometry. An online SDS removal strategy for decomplexing the protein-SDS complex is implemented in the second dimension, consisting of the co-injection of organic solvent and cationic surfactant. This online CE(SDS)-CZE-MS system allows MS characterization of proteoforms separated in generic CE(SDS), gaining additional separation in the CZE and detailed MS information. In general, the system can be applied to all kinds of proteins separated by CE(SDS). Here, we present results of the CE(SDS)-CZE-MS system on the analysis of several biopharmaceutical relevant antibody impurities and fragments. Additionally, the versatile application spectrum of the system is demonstrated by the analysis of extracted proteins from soybean flour. The online hyphenation of CE(SDS) resolving power and MS identification capabilities will be a powerful tool for protein and mAb characterization.

4.1.2 Introduction

Sodium dodecyl sulfate-polyacrylamide gel electrophoresis (SDS-PAGE) is the fundamental technique for protein separation by size, widely used in biochemistry, biotechnology, molecular biology, and other life sciences. For quantitative purposes, this technique is often applied in capillary format (CE(SDS)). It enables highly resolved protein size separation in an automated way based on nanoliter sample injection. Generally, ultraviolet (UV) or laser-induced fluorescence (LIF) detection systems are used in these CE(SDS) methods [1]. As such, it has emerged as a key technology in the biopharmaceutical field for quality control of protein biotherapeutics to evaluate size heterogeneity, purity, and stability [2–5]. Biotechnologically produced proteins, especially monoclonal antibodies (mAb), gain steadily more attention as therapeutics. Impurities and degradation products of mAb which may affect drug quality and efficacy [6, 7] need to be well characterized. However, this is challenging due to size and potential heterogeneity of these molecules. Thus, various analytical techniques are commonly applied [6, 8, 9], where CE-based methods are applied for most biopharmaceuticals released

in recent years. Most widespread CE technique for quantitation of highly resolved size-related impurities is CE(SDS). The most relevant studies of CE(SDS) for mAb analysis have been reviewed by Gahoual et al. [10].

The unequivocal identification and characterization of the unknown signals and impurities in CE(SDS) are challenging. Mass spectrometry (MS) is the key technology in protein characterization. However, direct coupling of CE(SDS) with electrospray ionization mass spectrometry (ESI-MS) is prevented due to strong suppression effects of SDS [11] and other components of the SDS-MW separation gel in the electrospray ionization process. As a first step, the SDS-protein complex needs to be cleaved. There are several offline approaches for decomplexing SDS-protein complexes prior to MS analysis, as reviewed by Kachuk et al. [12]. An in-capillary decomplexation method enables the release of protein by CZE in the electric field, assisted by an organic and cationic surfactant plug [13]. An online SDS-removal strategy has not been applied to CE(SDS)-separated proteins so far. Only matrix-assisted laser desorption ionization mass spectrometry (MALDI) has been applied for the analysis of CE(SDS)-separated proteins after complex offline clean-up [14]. Spiking experiments or correlation between CE(SDS) peaks and MS analysis have been used for identification purposes as well [15, 16]. To the best of our knowledge, an online mass spectrometric characterization of CE(SDS)-separated peaks has not been reported so far.

In general, there are several options for the direct MS hyphenation of incompatible CE separation methods [17]. Most of these strategies compromise separation efficiency and ESI-MS sensitivity. This is the case for simply reducing, replacing, or omitting the MS incompatible electrolytes. There were some approaches, replacing SDS with an acid labile surfactant (ALS) in slab gel electrophoresis, revealing not the same separation performance than with SDS [18, 19]. Root et al. improved protein size separation with ALS in microchip electrophoresis [20]. Still, MS-interfering sieving polymer was used and MS hyphenation not performed. Regarding the SDS-MW gel buffer, the ESI-interfering compounds boric acid, SDS, and dextran [21] have not been adequately substituted at the same separation performance. Choosing another ionization method can be an additional approach for the direct MS hyphenation of incompatible CE separation methods. Nevertheless, an ionization method for the direct hyphenation of CE(SDS) with MS that is not affected by the SDS-MW gel compounds and suitable for protein ionization has not been developed so far.

In order to maintain the original separation method and sensitive ESI-MS performance, two-dimensional (2D) or multidimensional separation systems can be used for the online coupling of non-MS-compatible systems (first dimension, ^{1}D), where the second dimension (^{2}D) is used for separating interfering matrix from the analyte of interest. Most common multidimensional methods are combining chromatographic techniques like HPLC or GC [22]. However, the coupling of capillary-based electrophoretic techniques is difficult due to the

small volumes to be transferred (mid-nanoliter range) and the strong electrical fields used. Thus, relatively few techniques have been developed [22–25]. We introduced a 4-port valve with an internal loop for direct coupling of two capillary-based electrophoretic techniques [26]. This set-up provides a high degree of flexibility in the combination of two separation techniques due to the distinct partition of the two dimensions. In this way, two-dimensional capillary zone electrophoresis (CZE), CZE-CZE-MS, with the 4-port valve has been applied for the identification of degradation products from tablets containing ascorbic acid and acetylsalicylic acid [27] and for the characterization of charge heterogeneities of intact antibodies [28]. Online coupling of capillary isoelectric focusing (CIEF) with CZE-MS detection could be demonstrated for the characterization of proteins including antibodies [29, 30]. Additionally, imaged capillary isoelectric focusing (iCIEF) was hyphenated with MS via the 4-port valve, gaining accurate masses of the main isoform and the main acidic and basic variant of a mAb [31].
Here, we present a method for the hyphenation of generic CE(SDS) with ESI-MS in a CE(SDS)-CZE-MS system. Aware of the high impact for the biopharmaceutical field, we characterized fragments and impurities of several antibodies in detail. By analyzing a bispecific antibody with two different light chains, it is pointed out that the system is not only useful for the separation of the SDS-protein complex and other MS-interfering compounds from the SDS-MW gel, but also provides a second separation dimension. To demonstrate the broad field of application of the CE(SDS)-CZE-MS system, we characterized main peaks of proteins extracted from soybean flour.

4.1.3 Materials and methods

Chemicals and samples

Methanol, 2-propanol (each LC-MS grade), acetic acid, and formic acid were obtained from Carl Roth GmbH und Co. KG (Karlsruhe, Germany). Sodium hydroxide and hydrochloric acid were purchased from Merck (Darmstadt, Germany). Dithiothreitol (DTT), SDS (10% in water), cetyltrimethylammonium bromide (CTAB), glutaraldehyde solution (50% in water), poly(vinyl alcohol) (PVA) ($\geq$ 99%, average MW 89,000–98,000), and tris(hydroxymethyl)aminomethane (Tris) were obtained from Sigma Aldrich (Steinheim, Germany). All solutions were prepared using ultrapure water (18 MΩ cm at 25 °C, SG Ultra Clear UV from Siemens Water Technologies, USA). ESI Tuning mix solution was acquired from Agilent Technologies (Waldbronn, Germany). SDS-MW gel buffer was from Sciex (AB Sciex, Darmstadt, Germany). Sample solutions of four mAbs (mAb1–4) were provided by F. Hoffmann-La Roche (Basel, Switzerland). The NIST mAb was obtained from the National Institute of Standards and Technology (Gaithersburg, USA). Soybean flour

from Alnatura was obtained from a local store. All samples were diluted in SDS solution. Reduction of the mAbs were carried out adding 1 M DTT and heating during 5 min at 70 °C in a Thermomixer (Eppendorf, Wesseling-Berzdorf, Germany), followed by centrifugation at 14,100 g during 45 s (Eppendorf, Wesseling-Berzdorf, Germany). MAb1 and 4 were unstressed (stored at 2-8 °C only). MAb2 and mAb3 were subjected to stress conditions. The stress conditions for mAb3 were 3 months at 25 °C and 14 days at 60 °C. MAb2 was stressed at 40 °C for 12 weeks.

First dimension: CE(SDS)-UV

The ^{1}D was performed in an Agilent HP^{3D}CE instrument (Agilent Technologies, Waldbronn, Germany) with ChemStation software for instrument control and a grounded external electrode as the outlet of this ^{1}D. Fused silica capillaries from Polymicro (Polymicro Technologies, Phoenix, AZ, USA) with 50 μm ID were used with capillary lengths of 35 cm (from inlet to valve) and 15 cm (from valve to outlet). Capillaries were conditioned prior use by flushing 0.1 M NaOH, 0.1 M HCl, and water at 2 bar for 3 min each, and SDS-MW gel buffer at 2 bar for 20 min. Due to the low dielectric strength of the valve material, the maximum applicable voltage is limited as described in our previous work [26] and was set to $-$ 15 kV for the separation. Additional external UV detection was performed by a detection cell and a TIDAS CCD UV/NIR detector (J&M Analytik AG, Essingen, Germany) or an ECD2600 EX UV-VIS detector (ECOM spol. s r.o., Prague, Czech Republic) at 200 nm wavelength. A detection window was created 4.5 cm to the valve in the first capillary of the ^{1}D where the UV cell was positioned. When the CE(SDS) peak was observed with the UV detector, the velocity was calculated using the migration time and the effective length of the capillary. The time for the CE(SDS) peak to reach the sample loop in the valve was determined by the migration velocity and the distance from the external detector to the middle of the sample loop.

Four-port nanoliter valve

A four-port valve with an internal 20 nL sample loop was purchased from VICI AG International (Schenkon, Swiss) including a two-position electric microactuator. All used rotors, stators, nuts, and ferrules for the valve were purchased from VICI. A technical note with more information about the general valve design and the performance of the interface has been published in the research group [26]. Shortly, the valve can be switched manually by an electric actuator in two positions. The valve has a sample loop and two independent short cuts. Ferrules and nuts are used to tightly connect the 365 μm OD capillaries to the valve interface. The materials selected for the valve, polyether ether ketone (PEEK) for the stator and Valcon E® (polyaryletherketone (PAEK)/polytetrafluoroethylene (PTFE)-based composite) for the rotor, are non-conductive materials, which simplifies the

approach avoiding the need of isolating the valve from the electric circuit. In contrast to other standard background electrolytes, the SDS-MW gel buffer is more likely to escape from the valve loop probably due to its low surface tension. When current instability occurs, proper performance of the 2D system was assured by removing leakage drops between rotor and stator.

Second dimension: CZE-C^4D-ESI-MS

An Agilent CE instrument ($HP^{3D}CE$) was used as ^2D. PVA-coated capillaries were applied, prepared in-house as described elsewhere [27]. Total capillary lengths were 38 cm for both capillaries. As MS-compatible volatile background electrolyte, 1 M acetic acid was utilized. Separation voltage was set to + 10 kV. An orthogonal electrospray interface (ESI, model G1607A from Agilent Technologies) was used for coupling of CE and MS. For MS detection, a Compact Q-TOF (Bruker Daltonics, Bremen, Germany) was employed. MS control and data analysis were carried out using Data Analysis software (Bruker, Bremen, Germany). Electrospray ionization was performed in positive ion mode (4.5 kV). The flow rate of dry gas was 4.0 L/min at a temperature of 170 °C with a nebulizer gas pressure of 0.2 bar. Good ionization efficiency for several mAb fragments was achieved by using 2-propanol:water (50:50, v/v) with 0.2% (v/v) formic acid as sheath liquid. It was delivered with a flow rate of 0.24 mL/h by a syringe pump (Cole-Parmer®, IL, USA) equipped with a 5 mL syringe (5MDF-LL-GT, SGE Analytical Science, Melbourne, Australia). Spectra were acquired in a mass range of m/z 700–3500. Internal calibration of the MS at the end of each analysis was made to improve mass accuracy [28].

SDS-removal strategy optimization

Based on our previous work related with the in-capillary strategy to remove SDS from a mAb sample [13], zones of methanol and a cationic surfactant, here CTAB, were placed at the valve prior transferring the peak of interest from the first to the second dimension. The SDS-removal strategy in the 2D system was adapted and optimized by using the reduced mAb1 diluted in SDS-MW gel buffer. The sample was transferred to the ^2D by using the sample loop of the valve as injector (no separation over the ^1D). To understand the requirements of the 2D system, different volumes of methanol and cationic surfactants and their position in respect to the sample were tested. A contactless conductivity detector (C^4D) as intermediate detection (TraceDec® from Innovative Sensor Technologies, Strasshof, Austria) located 4 cm in front of the valve allows determining the precise time for the zones to be in the desired position. A decrease in the conductivity was registered as a negative peak corresponding to the zones of methanol and methanol:water (solvent for the cationic surfactant) passing through the C^4D sensor (Figure 4.2).

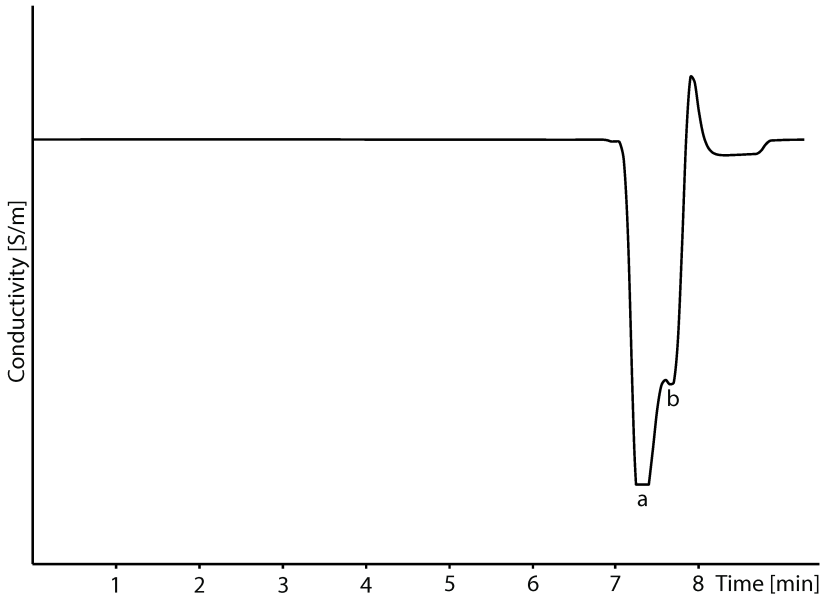

Figure 4.2: C^4D signal obtained in the 2D. During the positioning of methanol (50 mbar for 10 s, corresponding to peak a) and cationic surfactant (0.4% (w/v) CTAB in methanol: water (50:50, v/v), 50 mbar for 20 s, corresponding to peak b) for the SDS removal strategy this C^4D signal is obtained

Therefore, the C^4D detection can be used for methanol and CTAB positioning at the same time that the separation in the ^1D takes place. Thus, the SDS-protein complex does not wait for a long time in the sample loop and the analysis time for a complete 2D run is reduced. Optimal conditions were 50 mbar for 12 s methanol plus 50 mbar for 20 s 0.4% (v/v) CTAB as the most flexible and efficient conditions. In this way, sufficient methanol before and CTAB after the sample are assured considering the small short-cut of the valve in the ^2D (approx. volume of one-third of the sample loop, $\sim$ 6.7 nL).

Soybean protein extraction and reduction

Soybean proteins were extracted from 30 mg defatted soybean flour by the addition of 1 mL Tris buffer (50 mM Tris [pH 7.5], 10 mM DTT, 0.1% SDS) and shaking for 30 min at room temperature. After centrifugation for 10 min at 14,100 g, 95 μl of the supernatant was spiked with 0.4% (v/v) SDS and reduced with 4 mM DTT at 70 °C for 10 min.

Limit of detection

For the limit of detection (LOD) determination of the 2D system, the NIST mAb light chain (LC) was measured at different concentrations (see Figure 4.3). Here, 1 mg/mL, 0.3 mg/mL, 0.1 mg/mL, and 0.03 mg/mL of the intact NIST mAb were reduced as described before and measured with the CE(SDS)-CZE-MS system (n = 3).

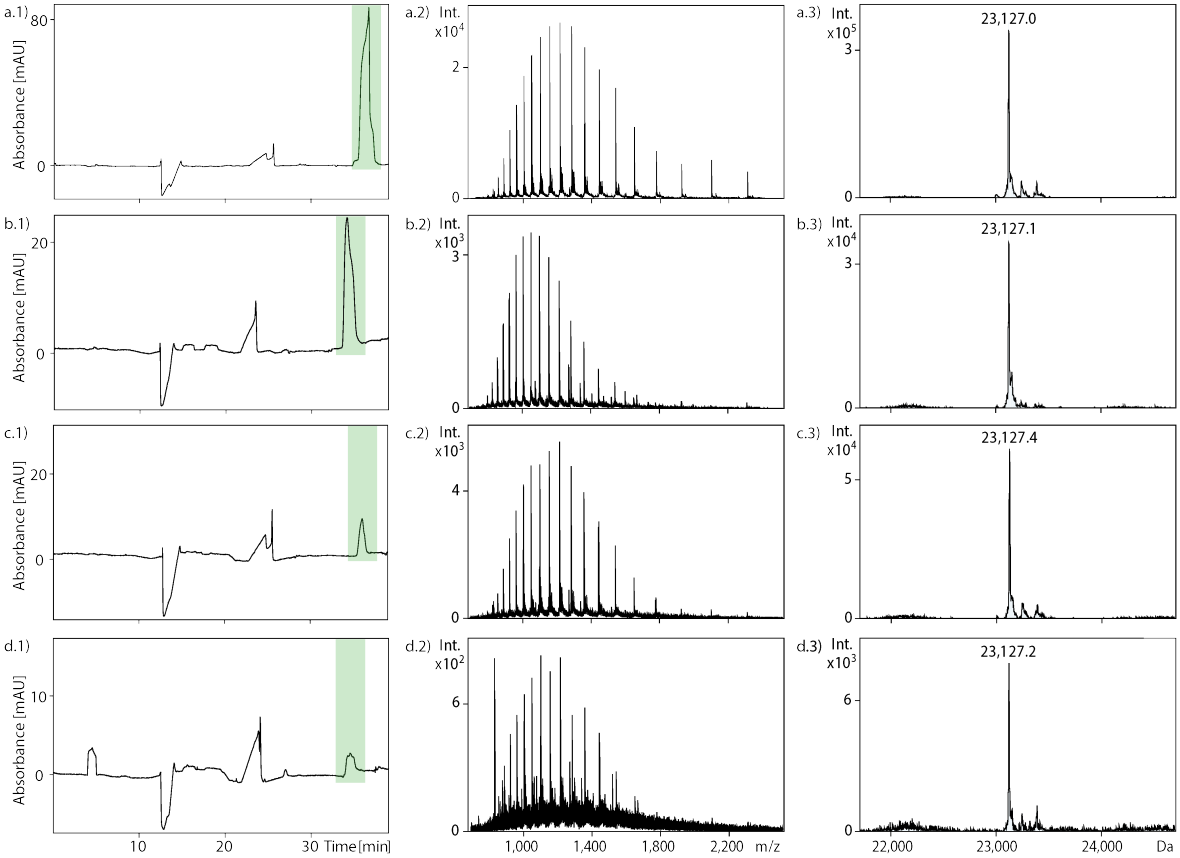

Figure 4.3: Dilution experiments with LC of NIST mAb with the CE(SDS)-CZE-MS system. a) CE(SDS)-UV separation of reduced NIST mAb at different concentrations (a.1 1.0 mg/mL, b.1 0.3 mg/mL, c.1 0.1 mg/mL and d.1 0.03 mg/mL using −15 kV for 60 s injection) and the corresponding ^{2}D CZE-MS result illustrated by the raw mass spectra (a.2 - d.2) and the deconvoluted mass spectra of each concentration level (a.3 - d.3). Results were obtained using methanol/water (50:50, v/v) with 0.5% (v/v) formic acid as sheath liquid. Other conditions as in Figure 4.4

SDS-MW gel buffer optimization

The SDS-MW gel buffer optimization was performed using a PA 800 plus Pharmaceutical Analysis System (Beckman Coulter, Brea, CA, USA) with 32 Karat 10.1 software. Different concentrations of the components and several additives (polyalcohols, organic solvents, cellulose derivatives, carboxylic and dicarboxylic acids, amino acids, and other zwitterionic compounds) were investigated to improve resolution and separation for the different LCs and further underlying species of the bispecific mAb4. Optimized buffer composed of 0.6 M Tris-borate (pH 8.1), 0.1% (w/v) SDS, 5% (v/v) 2-propanol, 10% (w/v) and dextran (MW 1,500,000–2,800,000).

4.1.4 Results and discussion

Setup and principle

Two CE instruments are used as the inlet for the ^{1}D and ^{2}D and connected to the nanoliter valve, with the outlet of the ^{2}D connected to the MS detector (Figure 4.4). A UV detector is implemented in ^{1}D as intermediate detection system to allow precise peak cutting. Common separation profiles of immunoglobulin G1 mAbs can be achieved in the first (CE(SDS)) dimension, as demonstrated for a reduced mAb (mAb1), with LC and heavy chain (HC) as the main peaks (Figure 4.4 b). When transferring a fraction of the CE(SDS) into the second dimension containing a 1 M acetic acid electrolyte, it was not possible to separate the SDS-protein complex in the CZE; thus, no peaks in the MS could be obtained (data not shown). Therefore, the SDS-protein complex needs to be efficiently destroyed while keeping the protein zone narrow. This can be achieved by an in-capillary decomplexing strategy for SDS-protein complexes that was developed in our group [13]. It is based on the hydrodynamic co-injection of methanol and a positively charged surfactant like CTAB and has been implemented in this 2D set-up (materials and methods). For the exact positioning of these plugs, a C^{4}D is placed in front of the valve in the second dimension (see Figure 4.4 a and Figure 4.2). The selected valve allows performing the CE(SDS) separation and the positioning of the zones in the ^{2}D simultaneously (Figure 4.4 a). After the peak of interest from the ^{1}D arrived in the valve loop (determined by UV detection) and the plugs of methanol and CTAB were positioned in the ^{2}D, the separation voltage is stopped in the ^{1}D and the valve is switched from position A to B (Figure 4.4 a, c). Voltage is applied in the ^{2}D until the protein peak is detected in the MS. The BPE shows that the first peaks, corresponding to components from the SDS-MW gel matrix as Tris-SDS and CTAB-SDS complexes, and the peak from the LC of mAb1 are clearly separated (Figure 4.4 d). In this way, MS characterization from CE(SDS)-separated peaks can be assured and high-quality MS spectra allow data interpretation.

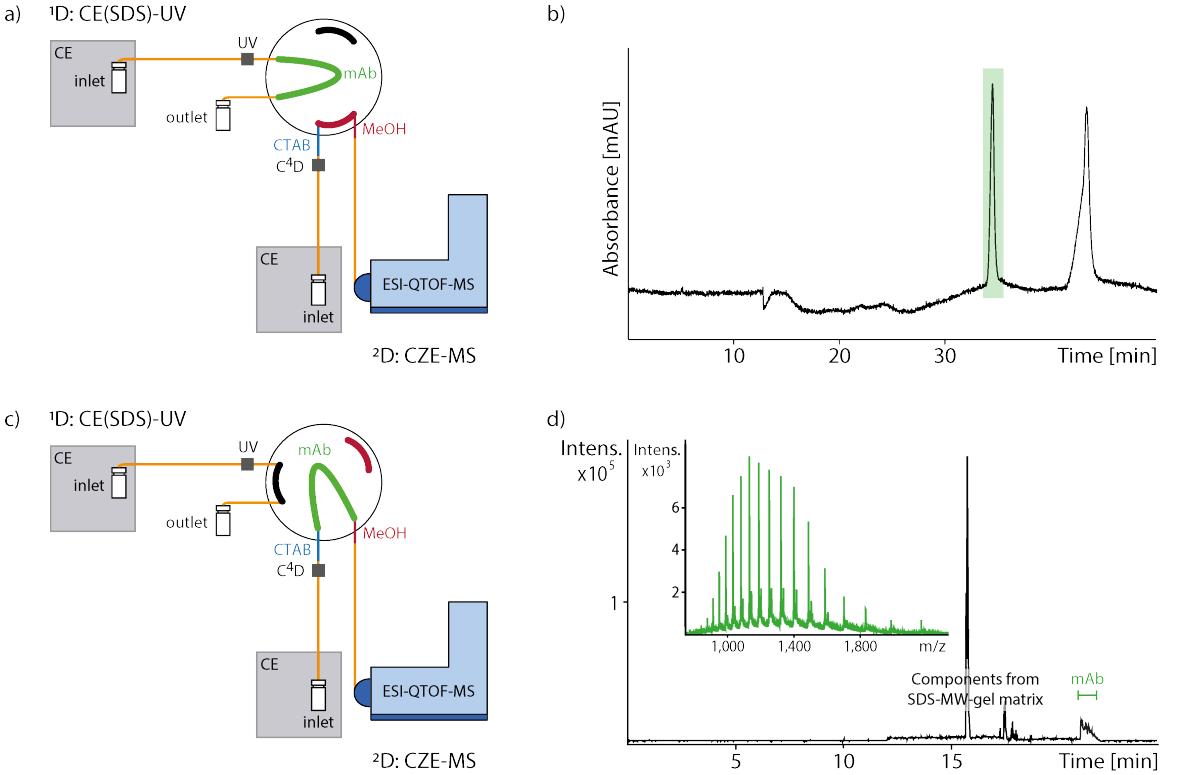

Figure 4.4: Set-up and workflow of the CE(SDS)-CZE-MS system. a) Detailed scheme of position A in the nanoliter valve, where the reduced mAb1 is separated in the ^{1}D CE(SDS). The positioning of methanol (red) and cationic surfactant (blue) in the ^{2}D is done simultaneously for the SDS removal. b) CE(SDS)-UV separation from the reduced mAb1 in the ^{1}D. c) Detailed scheme of position B where the peak of interest from mAb1 is transferred to the ^{2}D in between the zones of methanol and cationic surfactant. d) Base peak electropherogram (BPE) showing the ^{2}D CZE-MS separation of the transferred peak from the interfering components of the SDS-MW gel buffer and its raw mass spectrum. Conditions ^{1}D: 50 μm ID fused silica capillary, SDS-MW gel buffer, separation voltage -15 kV, UV detection 200 nm. Conditions ^{2}D: 50 μm ID PVA-coated capillary, 1 M acetic acid as separation buffer, separation voltage + 10 kV. MS conditions: positive ion mode (4.5 kV), dry gas 4.0 L/min at 170 °C, nebulizer 0.2 bar, sheath liquid 2-propanol:water (50:50, v/v) with 0.2%(v/v) formic acid with a flow rate of 3.3 μL/min, mass range 700-3500 m/z. SDS-removal strategy applied in the ^{2}D: 50 mbar for 12 s methanol plus 50 mbar for 20 s 0.4% (w/v) CTAB in methanol:water (50:50, v/v)

Validation of CE(SDS)-CZE-MS system

Good repeatability can be obtained in the ^{1}D for migration time (relative standard deviation (RSD) 2.6% n = 8), which is similar to commercial 1D systems [2]. Repeatability of signal intensity was determined for the LC of mAb1 (c = 2.3 mg/mL, n = 3), obtaining RSD values of 16% for the extracted ion electropherogram (EIE) from the eight most abundant m/z signals. The charge-deconvoluted masses show a standard deviation of 0.1 Da. Interday precision was tested (n = 14) and RSD values of 18% for the signal intensity of the EIE were obtained. A standard deviation of 0.9 Da for the deconvoluted masses was specified.

To further optimize the repeatability and interday precision, the general automation of the 2D system would be beneficial. Here, the peak cutting process, the plug positioning, and valve switching are estimated to be more reproducible, robust, and less error-prone then. Another possible improvement is seen in the adaptation of the commercially used valve to our application. But overall, reproducibility in-between several series of measurements is given, when the 2D system is set-up in the same manner as described before. The LOD of the 2D system was determined with the LC of the NIST mAb in different concentrations between 0.03 and 1.0 mg/mL (see Figure 4.3). It was possible to obtain meaningful MS spectra down to the lowest concentration. The sample with a concentration of 0.03 mg/mL resulted in an S/N of 11.3–35.2 regarding the EIE from the eight most abundant m/z signals. Therefore, a LOD of the 2D system for the LC is estimated to be between 0.003 and 0.008 mg/mL. This allows the characterization of impurities of a mAb in this mass region below the level of 1%, which has been proven as presented in the following paragraph. With increasing molecular weight of the proteins, a rise of the sample concentration is required to obtain the same MS spectrum intensity and quality. The enhancement of MS signal intensity in higher mass regions could be addressed by the hyphenation via a nanoflow sheath liquid interface [32].

Analysis of mAbs with CE(SDS)-CZE-MS system

As mention before, the main application of the CE(SDS)-CZE-MS system is seen in the biopharmaceutical field, analyzing mAbs. Therefore, the determination of low-level impurities of a thermal stressed intact mAb (mAb2) with the 2D system is shown (Figure 4.5). The CE(SDS) profile of the intact mAb2 showed three peaks in the low molecular weight region. Notably, CE(SDS) peak 1 (0.5 of the total corrected peak area [%CPA] of the total peak area) revealed four main peaks in the MS spectrum ($n = 3$). These masses can be attributed to the cleavage of a PSS motif between the constant heavy chain 2 (CH2) and CH3 domains of mAb2. Cleavage can occur either after the proline or after the adjacent serine. In addition, mAb2 consists of two different heavy chains (HC1 and HC2), i.e., peaks 1A (12,982.3 $\pm$ 0.2 Da) and 1C (13,069.1 $\pm$ 0.2 Da) are related to the cleavage of HC1, whereas peaks 1B (12,999.4 $\pm$ 0.3 Da) and 1D (13,086.5 $\pm$ 0.7 Da) are related to the cleavage of HC2. The mass difference of both peak doublets ($\sim$ 87 Da) can be attributed to serine. Other smaller peaks associated with possible oxidation products ($+$ 16 Da) from peak 1B and peak 1D are also resolved. The CE(SDS) peak 2 (1.1%CPA, $n = 3$) revealed two peaks in MS; peak 2A (23,599.8 $\pm$ 0.5 Da) can be attributed to the LC of mAb2. Peak 2B (23,813.9 $\pm$ 0.6 Da) could not be identified so far. As it can be seen in Figure 4.5: peak 3 in the CE(SDS) separation (0.6%CPA) consists of the main peak with a shoulder. When transferred and analyzed by MS ($n = 5$), two different distributions with three main

peaks each and with a mass difference of about 467 Da were found (peaks 3A, B, C; and peaks 3D, E, F, respectively). The mass differences between the peaks of each distribution can be attributed to the cleavage of a RSTSE motif between the CH1 and variable heavy chain (VH) domains of mAb2. Cleavages between the constant and variable domains have also been reported elsewhere [33, 34].

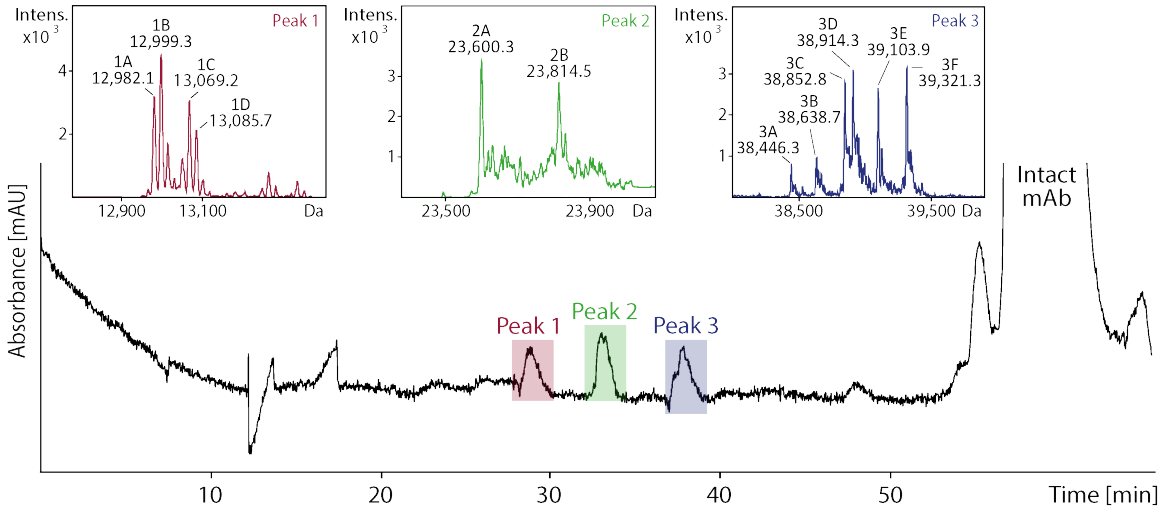

Figure 4.5: Analysis of antibody fragments with the CE(SDS)-CZE-MS system. CE(SDS)-UV separation of non-reduced mAb2 with the deconvoluted mass spectra obtained in the ^{2}D for peak 1 (red), peak 2 (green), and peak 3 (blue). Results for peak 1 and peak 2 obtained using an injection of − 10 kV for 40 s (6.8 mg/mL in 1% (v/v) SDS) and for peak 3 − 10 kV for 80 s (13 mg/mL in 2% (v/v) SDS). Other conditions are as in Figure 4.4

The LC is still linked to the resulting fragments since the cysteine that forms the disulfide bridge to the LC is preceding the HC cleavage site. As for peak 1, each cleavage site results in one peak for each of the two HCs of the molecule. Peaks 3A (38,446.3 ± 2.4 Da) and 3D (38,914.3 ± 0.3 Da) result from the C-terminal cleavage at the arginine of the RSTSE motif. In analogy, peaks 3B (38,636.9 ± 2.1 Da) and 3E (39,103.9 ± 1.7 Da) can be attributed to C-terminal cleavage after the threonine of this motif. C-terminal cleavage at glutamate causes peaks 3C (38,852.1 ± 1.6 Da) and 3F (39,320.0 ± 0.9 Da). The mass differences between peaks 3A and 3B and between peaks 3D and 3F (approx. 191 Da) result from an additional serine and threonine (ST from the RSTSE motif), whereas the differences between peaks 3B and 3C and between peaks 3E and 3F (approx. 216 Da) result from an additional serine and glutamate (SE from the RSTSE motif). Data from SEC-MS and RP-HPLC-MS measurements agree well with the presented CE(SDS)-CZE-MS results. Overall, twelve mass peaks resulting from three SDS peaks could be explained in detail with our novel CE(SDS)-CZE-MS system. This demonstrates that the resolution of generic CE(SDS) separations and the common used spiking experiments for identification are not sufficient.

To further confirm the value of the CE(SDS)-CZE-MS system for extensive characterization of protein biopharmaceuticals, we applied the system to another intact mAb (Figure 4.6).

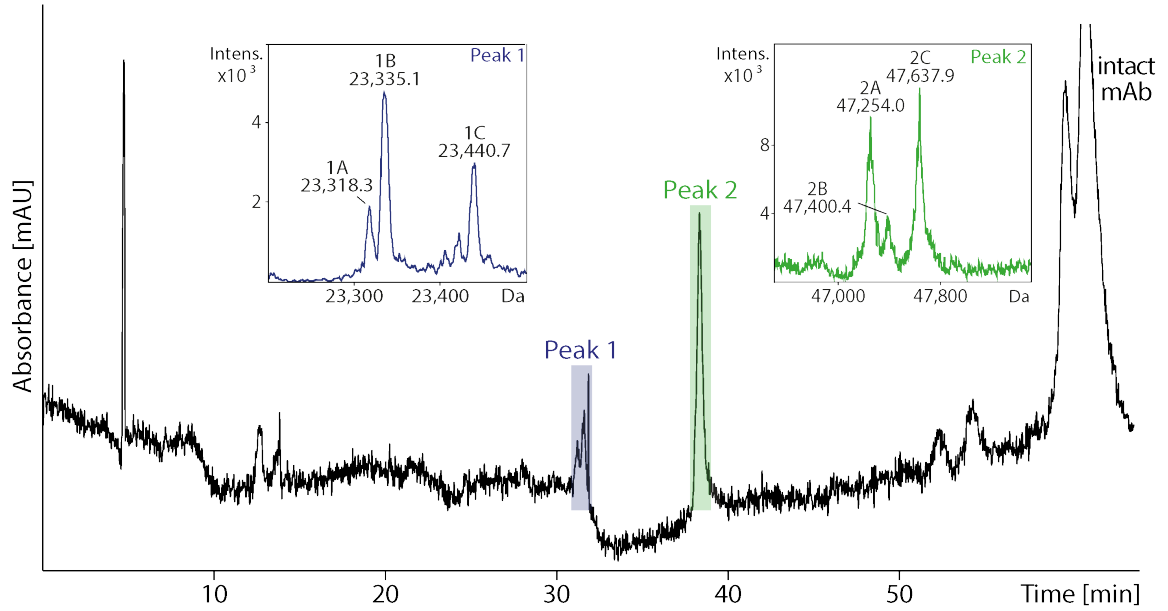

Figure 4.6: Analysis of antibody fragments with the CE(SDS)-CZE-MS system. CE(SDS)-UV separation of non-reduced mAb3 with the deconvoluted mass spectra obtained in the ^{2}D for peak 1 (blue) and peak 2 (green). Results obtained using an injection of − 10 kV for 80 s (2.3 mg/mL in 0.2% (v/v) SDS). Other conditions are as in Figure 4.4

Different low-level proteoforms of mAb3 were successfully transferred from the CE(SDS) and analyzed online by MS, providing valuable information for mAb characterization. As IgG1, this mAb3 has four inter and 12 intra disulfide bridges (two in each LC and four in each HC). Figure 4.6: shows the electrophoretic separation of the non-reduced mAb3 obtained by CE(SDS) using the external UV detection of the 2D system. The intact mAb is the main peak with other smaller peaks attributed to various mAb proteoforms. In the first instance, double peak 1 was transferred (n = 6). It represents 2% in peak area and migrates in the region of the LC; thus, similar molecular weight is expected. Mass signals, peak 1B (23,335.8 ± 1.0 Da) and peak 1C (23,439.4 ± 1.5 Da), were detected, with peak 1C identified as reduced LC (23,438.9 Da). Peak 1B has a difference of 103.7 Da in comparison with peak 1C, which could be correlated with a loss of the C-terminal cysteine of the LC. Peak 1A (23,317.9 ± 0.7 Da) is a small peak with a difference of 17.8 Da regarding peak 1B, possibly associated with a loss of water. In the case of peak 2, similar mass to HC or the fragment antigen binding (Fab) could be expected due to the migration time in the CE(SDS). Interestingly, two main peaks were observed in MS: peak 2A (47,253.1 ± 0.7 Da, n = 4) and peak 2C (47,638.2 ± 0.7 Da, n = 4). Peak 2C can be attributed to the reduced Fab fragment. In the case of peak 2A, a difference of 385.1 Da is observed. Possible cleavage

of the last three amino acids of Fab in the hinge region (K-T-H, 366.2 Da) including a loss of water can be likely an explanation for this peak [35]. In fact, due to its high flexibility, modifications and cleavages can often occur in the hinge region [36]. A small peak, peak 2B (47,400.4 $\pm$ 2.5 Da), was observed with a difference of 237.8 Da with respect to peak 2C and could be attributed with a cleavage of only two of the last amino acids (T-H, 238.2 Da), but the low intensity and the complex peak shape impeded precise data interpretation. The analyses of the mAbs demonstrate the high value of the CE(SDS)-CZE-MS system for the analysis and extensive characterization of protein biopharmaceuticals. The system allows a profound insight into underlying molecular structures for each CE(SDS) peak.

Analysis of bispecific mAb with CE(SDS)-CZE-MS system

A major drawback of the commercial SDS-MW gel buffer is the low resolving power for different LCs of bispecific antibodies (see Figure 4.7 a).

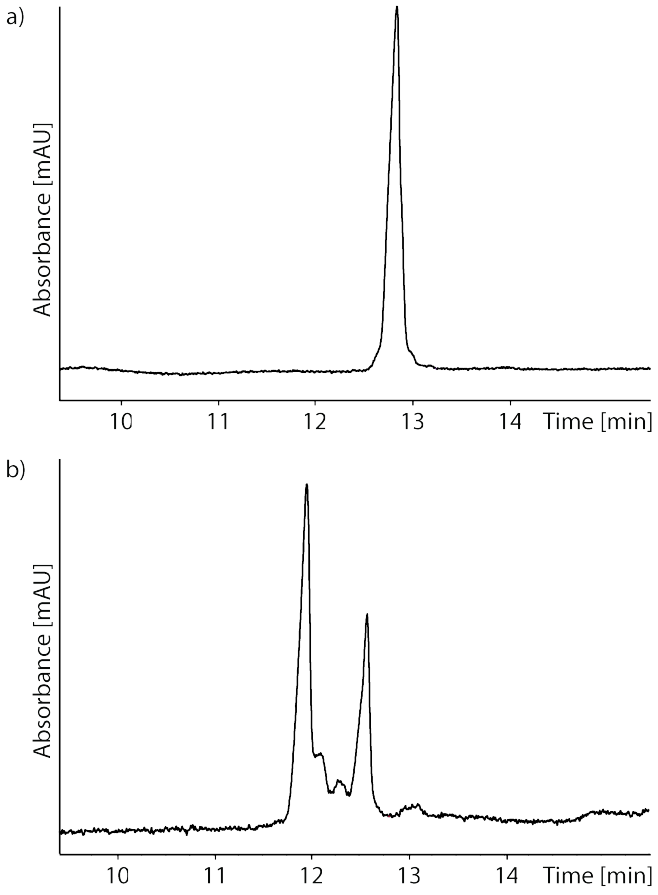

Figure 4.7: CE(SDS)-UV analysis of reduced bispecific antibody. Results obtained in 1D CE(SDS)-UV, for the separation of the two LCs of the reduced bispecific mAb4 with the commercial SDS-MW-gel buffer (a) and with the optimized SDS-MW-gel buffer (b). Conditions: concentration 0.15 mg/mL, injection – 5 kV for 30 s, separation voltage – 15 kV, capillary 50 μm ID and length 31 cm (eff. 21 cm), UV-detection: 214 nm

Beyond the possibility to remove interfering compounds, the ^{2}D can be used to gain separation efficiency, i.e., to separate proteins that are co-migrating in CE(SDS). We analyzed a bispecific mAb (mAb4) that consists of two different LC structures that showed a mass difference of around 1.6 kDa. With the commercial SDS-MW gel buffer, a separation of these LCs could not be achieved in the ^{1}D CE(SDS) (Figure 4.8 a.1). By transferring this peak of the non-separated LCs into the second CZE-MS dimension, the separation and MS characterization of these LCs was possible (Figure 4.8 a.2 and a.3). This demonstrates the gain in separation efficiency with the 2D system.

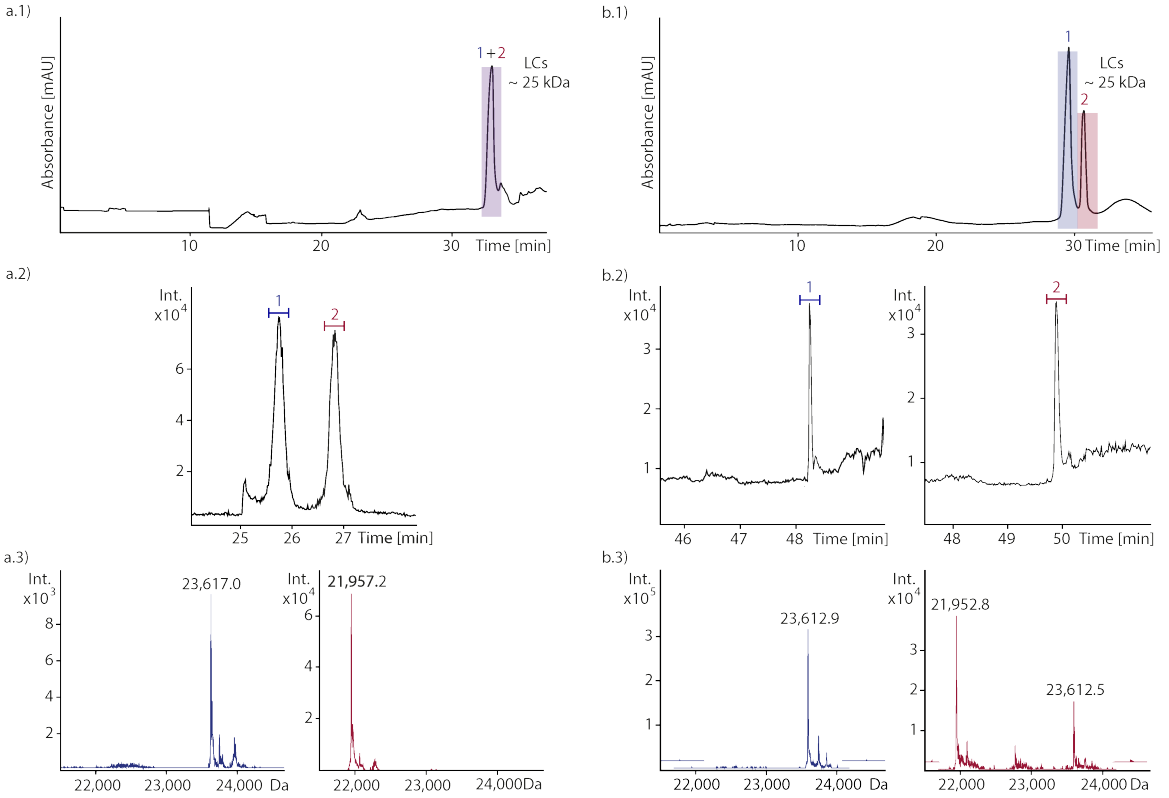

Figure 4.8: Analysis of LCs of a bispecific antibody with the CE(SDS)-CZE-MS system. Single peak obtained in the ^{1}D CE(SDS) separation of the two LCs of the reduced bispecific mAb4 with the commercial SDS-MW-gel buffer (a.1). Transferring the peak to the ^{2}D CZE-MS, the separation of both LCs (a.2) and their associated mass (a.3) could be obtained. Separation of the two LCs in the ^{1}D CE(SDS) with the optimized SDS-MW gel buffer (b.1). Both LCs were transferred (n = 3) to the ^{2}D CZE-MS in separate runs (b.2) for MS identification (b.3). Separation conditions for the commercial buffer: injection of -10 kV for 40 s (10 mg/mL in 1.5% (v/v) SDS). Separation conditions for the optimized buffer: injection of -15 kV for 30 s (14.9 mg/mL in 2% (v/v) SDS), UV detection at 214 nm and methanol:water (50:50, v/v) with 0.5% (v/v) formic acid as sheath liquid. Other conditions are as in Figure 4.4

To confirm these results, the composition of the SDS-MW gel buffer was optimized to improve the separation efficiency in the LC region of mAb4. Several separation gel buffer

compositions were studied in a 1D set-up (materials and methods). The addition of 5% (v/v) 2-propanol as organic modifier instead of glycerol [21] showed a significantly improved resolution of the LC species, where also some further variants could be observed (see Figure 4.7 b). The number of peaks separated from the single LC peak increased with the amount of organic modifier. Since the buffer was optimized for the separation in the LC region, the resolution improvement could not be observed for the total mass range. In the 2D set-up, after baseline separation of the LCs in the ^{1}D CE(SDS) was achieved (Figure 4.8 b.1), both peaks were transferred (n = 3) to the ^{2}D in separate runs and MS-characterized (Figure 4.8 b.2 and b.3). Contrary to expectations, the first migrating peak was identified as LC with the higher molecular mass. This reveals again that mass estimation with CE(SDS)-UV/LIF can be incorrect, whereas the presented 2D system enables an accurate mass determination. With the prospect of the development of increasingly complex biopharmaceutical protein structures, the analytical methods need to be improved. Therefore, the CE(SDS)-CZE-MS system can be a powerful tool, strongly extending CE(SDS) analysis.

Analysis of soybean proteins with CE(SDS)-CZE-MS system

As presented, the CE(SDS)-CZE-MS system is most promising for the application in the biopharmaceutical field but can be applied in general to all kinds of proteins that are separated via SDS-PAGE or CE(SDS). This is demonstrated by the analysis of soybean storage proteins (Figure 4.9). Due to the size distribution of the reduced proteins, they are often analyzed via SDS-PAGE [37–40], CE(SDS), or with lab-on-a-chip instruments [41]. Here, proteins were extracted from defatted soybean flour, reduced, and analyzed with the CE(SDS)-CZE-MS system. It was possible to analyze two main peaks observed in the CE(SDS) separation that are attributed to the seed storage protein glycinin (11S). Glycinin is a hexameric protein consisting of six monomer units. Each monomer consists of an acid subunit (around 40 kDa) linked via a disulfide bond with a basic subunit (around 20 kDa) [38]. For peak 1, most probably the basic subunits of glycinin, it was possible to obtain ten different masses. For peak 2, most likely the acidic subunits of glycinin, seven different masses were obtained. Several research groups analyzed soybean proteins with SDS-PAGE, stating different mass regions for the subunits of the main storage soybean protein glycinin and β-conglycinin (7S) [42]. This demonstrates that the mass estimation with SDS-PAGE or CE(SDS) is not exactly enough and leaking of reproducibility. Our system offers additional information on proteoforms providing highly resolved and exact mass data for the subunits of glycinin. Nevertheless, even with exact mass determination, only a tentative assignment of the soybean protein subunits was possible.

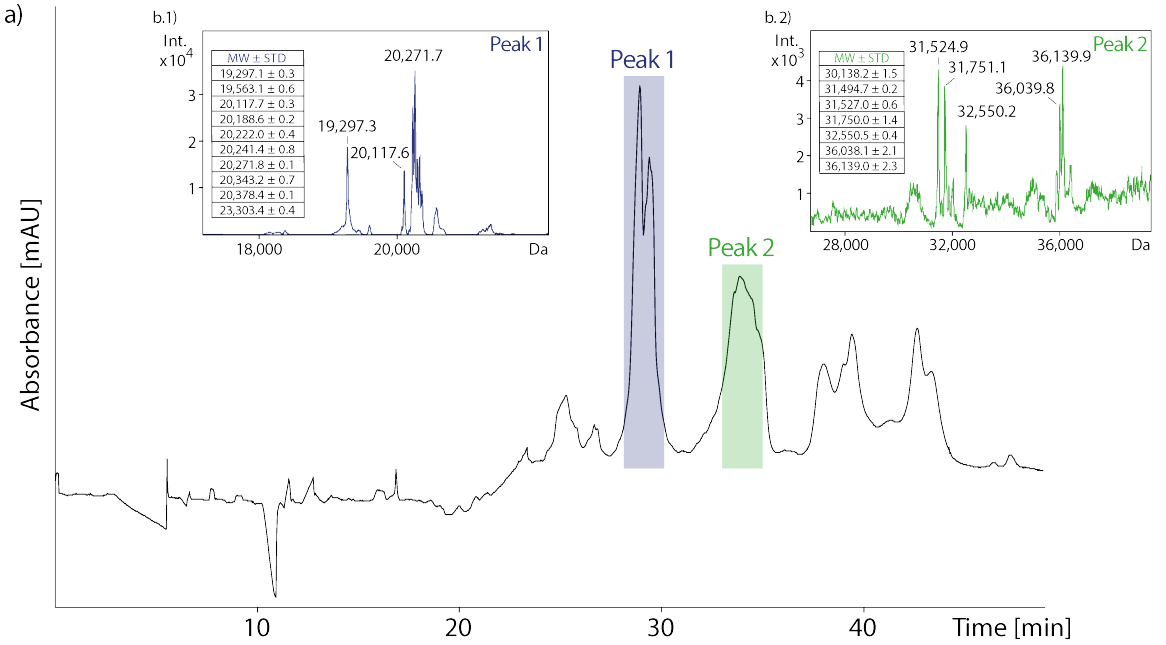

Figure 4.9: Analysis of soybean proteins with the CE(SDS)-CZE-MS system. CE(SDS)-UV separation (at 214 nm) of reduced, extracted soybean protein (a) from defatted soybean flour. Deconvoluted mass spectra were obtained in the ^{2}D for peak 1 (b.1, blue) and peak 2 (b.2, green) by using an injection of − 15 kV for 60 s, methanol:water (50:50, v/v) with 0.5% (v/v) formic acid as sheath liquid and 0.3 bar nebulizer gas. Other conditions are as in Figure 4.4. Mean values and related standard deviation for masses obtained from peak 1 (n = 4) and peak 2 (n = 3) are shown in the tables

4.1.5 Conclusion

In conclusion, we describe the functionality, validation, and application of a capillary electrophoresis-based 2D system for the analysis of CE(SDS)-separated proteins by MS. An online, in-capillary SDS-removal strategy, consisting of the injection of methanol and a cationic surfactant, was implemented in this system. To the best of our knowledge, we present in this work the first hyphenation of generic CE(SDS) with MS. In the ^{1}D, the separation can be performed applying generic CE(SDS) methods, which allows the use of already defined applications. We applied the CE(SDS)-CZE-MS system to several mAbs and soybean proteins. The ability to characterize several proteoforms from only one single CE(SDS) peak via MS demonstrates that the commonly used standard addition approach is inappropriate for identification. Besides the additional approaches in the biopharmaceutical field, further applications are seen in the analysis of proteins from various sources like biological fluids, agriculture, and food products, if they are available at appropriate concentrations. The CE(SDS)-CZE-MS system enables a detailed insight and understanding of proteins, especially for mAbs, and may revolutionize SDS protein analysis.

Acknowledgments
The authors gratefully acknowledge Dr. Laura Sánchez-Hernández for helpful discussions and Kevin Jooß for the support in data interpretation.

Author's contributions
JR, CM, and JS developed the methods and performed experiments, analyzed data, and wrote the paper. SK and BM conceived the approach and wrote the paper. CN initiated and supervised the project, conceived the approach, and wrote the paper.

Funding information
This study was funded by F. Hoffmann-La Roche Ltd.

4.1.6 Compliance with ethical standards

Conflict of interest
The authors declare that they have no conflict of interest.

References

(1) Gennaro, L. A., Salas-Solano, O., and Ma, S. (2006). Capillary electrophoresis-mass spectrometry as a characterization tool for therapeutic proteins. *Anal. Biochem. 355*, 249–258.

(2) Hunt, G., and Nashabeh, W. (1999). Capillary Electrophoresis Sodium Dodecyl Sulfate Nongel Sieving Analysis of a Therapeutic Recombinant Monoclonal Antibody: A Biotechnology Perspective. *Anal. Chem. 71*, 2390–2397.

(3) Lacher, N. A., Wang, Q., Roberts, R. K., Holovics, H. J., Aykent, S., Schlittler, M. R., Thompson, M. R., and Demarest, C. W. (2010). Development of a capillary gel electrophoresis method for monitoring disulfide isomer heterogeneity in IgG2 antibodies. *Electrophoresis 31*, 448–458.

(4) Michels, D. A., Brady, L. J., Guo, A., and Balland, A. (2007). Fluorescent derivatization method of proteins for characterization by capillary electrophoresis-sodium dodecyl sulfate with laser-induced fluorescence detection. *Anal. Chem. 79*, 5963–5971.

(5) Salas-Solano, O., Tomlinson, B., Du, S., Parker, M., Strahan, A., and Ma, S. (2006). Optimization and validation of a quantitative capillary electrophoresis sodium dodecyl sulfate method for quality control and stability monitoring of monoclonal antibodies. *Anal. Chem. 78*, 6583–6594.

(6) Creamer, J. S., Oborny, N. J., and Lunte, S. M. (2014). Recent advances in the analysis of therapeutic proteins by capillary and microchip electrophoresis. *Anal. Methods 6*, 5427–5449.

(7) Zhao, S. S., and Chen, D. D. Y. (2014). Applications of capillary electrophoresis in characterizing recombinant protein therapeutics. *Electrophoresis 35*, 96–108.

(8) El Deeb, S., Watzig, H., Abd El-Hady, D., Sanger-van de Griend, C., and Scriba, G. K. E. (2016). Recent advances in capillary electrophoretic migration techniques for pharmaceutical analysis (2013-2015). *Electrophoresis 37*, 1591–1608.

(9) Tamizi, E., and Jouyban, A. (2015). The potential of the capillary electrophoresis techniques for quality control of biopharmaceuticals-a review. *Electrophoresis 36*, 831–858.

(10) Gahoual, R., Beck, A., Leize-Wagner, E., and Francois, Y.-N. (2016). Cutting-edge capillary electrophoresis characterization of monoclonal antibodies and related products. *J. Chromatogr., B: Anal. Technol. Biomed. Life Sci. 1032*, 61–78.

(11) Rundlett, K. L., and Armstrong, D. W. (1996). Mechanism of signal suppression by anionic surfactants in capillary electrophoresis-electrospray ionization mass spectrometry. *Anal. Chem. 68*, 3493–3497.

(12) Kachuk, C., Stephen, K., and Doucette, A. (2015). Comparison of sodium dodecyl sulfate depletion techniques for proteome analysis by mass spectrometry. *J. Chromatogr., A 1418*, 158–166.

(13) Sanchez-Hernandez, L., Montealegre, C., Kiessig, S., Moritz, B., and Neusüß, C. (2016). In-capillary approach to eliminate SDS interferences in antibody analysis by capillary electrophoresis coupled to mass spectrometry. *Electrophoresis 38*, 1044–1052.

(14) Lu, J. J., Zhu, Z., Wang, W., and Liu, S. (2011). Coupling sodium dodecyl sulfate-capillary polyacrylamide gel electrophoresis with matrix-assisted laser desorption ionization time-of-flight mass spectrometry via a poly(tetrafluoroethylene) membrane. *Anal. Chem. 83*, 1784–1790.

(15) Kotia, R. B., and Raghani, A. R. (2010). Analysis of monoclonal antibody product heterogeneity resulting from alternate cleavage sites of signal peptide. *Anal. Biochem. 399*, 190–195.

(16) Kaschak, T., Boyd, D., and Yan, B. (2011). Characterization of glycation in an IgG1 by capillary electrophoresis sodium dodecyl sulfate and mass spectrometry. *Anal. Biochem. 417*, 256–263.

(17) Schlecht, J., Jooß, K., and Neusüß, C. (2018). Two-dimensional capillary electrophoresis-mass spectrometry (CE-CE-MS): coupling MS-interfering capillary electromigration methods with mass spectrometry. *Anal. Bioanal. Chem. 410*, 6353–6359.

(18) Ross, A. R. S., Lee, P. J., Smith, D. L., Langridge, J. I., d. Whetton, A., and Gaskell, S. J. (2002). Identification of proteins from two-dimensional polyacrylamide gels using a novel acid-labile surfactant. *Proteomics 2*, 928–936.

(19) König, S., Schmidt, O., Rose, K., Thanos, S., Besselmann, M., and Zeller, M. (2003). Sodium dodecyl sulfate versus acid-labile surfactant gel electrophoresis: comparative proteomic studies on rat retina and mouse brain. *Electrophoresis 24*, 751–756.

(20) Root, B. E., Zhang, B., and Barron, A. E. (2009). Size-based protein separations by microchip electrophoresis using an acid-labile surfactant as a replacement for SDS. *Electrophoresis 30*, 2117–2122.

(21) Liu, Y., Reddy, M. P., Ratnayake, C. K., and Koh, E. V. Methods and compositions for capillary electrophoresis (CE): United States patent pat., US007381317B2, 27.06.2003.

(22) Kler, P. A., Sydes, D., and Huhn, C. (2015). Column-coupling strategies for multi-dimensional electrophoretic separation techniques. *Anal. Bioanal. Chem. 407*, 119–138.

(23) Kohl, F. J., Sánchez-Hernández, L., and Neusüß, C. (2015). Capillary electrophoresis in two-dimensional separation systems: Techniques and applications. *Electrophoresis 36*, 144–158.

(24) Xu, X., Liu, K., and Fan, Z. H. (2012). Microscale 2D separation systems for proteomic analysis. *Expert Rev. Proteomics 9*, 135–147.

(25) Grochocki, W., Markuszewski, M. J., and Quirino, J. P. (2015). Multidimensional capillary electrophoresis. *Electrophoresis 36*, 135–143.

(26) Kohl, F. J., Montealegre, C., and Neusüß, C. (2016). On-line two-dimensional capillary electrophoresis with mass spectrometric detection using a fully electric isolated mechanical valve. *Electrophoresis 37*, 954–958.

(27) Neuberger, S., Jooß, K., Ressel, C., and Neususs, C. (2016). Quantification of ascorbic acid and acetylsalicylic acid in effervescent tablets by CZE-UV and identification of related degradation products by heart-cut CZE-CZE-MS. *Anal. Bioanal. Chem. 408*, 8701–8712.

(28) Jooß, K., Hühner, J., Kiessig, S., Moritz, B., and Neusüß, C. (2017). Two-dimensional capillary zone electrophoresis-mass spectrometry for the characterization of intact monoclonal antibody charge variants, including deamidation products. *Anal. Bioanal. Chem. 409*, 6057–6067.

(29) Hühner, J., and Neusüß, C. (2016). CIEF-CZE-MS applying a mechanical valve. *Anal. Bioanal. Chem. 408*, 4055–4061.

(30) Hühner, J., Jooß, K., and Neusüß, C. (2017). Interference-free mass spectrometric detection of capillary isoelectric focused proteins, including charge variants of a model monoclonal antibody. *Electrophoresis 38*, 914–921.

(31) Montealegre, C., and Neusüß, C. (2018). Coupling imaged capillary isoelectric focusing with mass spectrometry using a nanoliter valve. *Electrophoresis 39*, 1151–1154.

(32) Höcker, O., Montealegre, C., and Neusüß, C. (2018). Characterization of a nanoflow sheath liquid interface and comparison to a sheath liquid and a sheathless porous-tip interface for CE-ESI-MS in positive and negative ionization. *Anal. Bioanal. Chem. 410*, 5265–5275.

(33) Liu, H., Gaza-Bulseco, G., and Lundell, E. (2008). Assessment of antibody fragmentation by reversed-phase liquid chromatography and mass spectrometry. *J. Chromatogr., B: Anal. Technol. Biomed. Life Sci. 876*, 13–23.

(34) Vlasak, J., and Ionescu, R. (2011). Fragmentation of monoclonal antibodies. *mAbs 3*, 253–263.

(35) Lasorsa, A., Losacco, M., Iacobazzi, R. M., Porcelli, L., Azzariti, A., Natile, G., and Arnesano, F. (2016). Probing the interaction between cisplatin and the therapeutic monoclonal antibody trastuzumab. *RSC Adv. 6*, 29229–29236.

(36) Moritz, B., and Stracke, J. O. (2017). Assessment of disulfide and hinge modifications in monoclonal antibodies. *Electrophoresis 38*, 769–785.

(37) Li, L., Wang, C., Qiang, S., Zhao, J., Song, S., Jin, W., and Wang, B. (2016). Mass Spectrometric Analysis of N-Glycoforms of Soybean Allergenic Glycoproteins Separated by SDS-PAGE. *J. Agric. Food Chem. 64*, 7367–7376.

(38) Yaklich, R. W. (2001). ß-Conglycinin and Glycinin in High-Protein Soybean Seeds. *J. Agric. Food Chem. 49*.

(39) Sathe, S. K., Lilley, G. G., Mason, A. C., and Weaver, C. M. (1987). High-resolution sodium dodecyl sulfate polyacrylamide gel electrophoresis of soybean (Glycin max L.) seed proteins. *Cereal Chem. 64*, 380–384.

(40) Mujoo, R., Trinh, D. T., and Ng, P. K. (2003). Characterization of storage proteins in different soybean varieties and their relationship to tofu yield and texture. *Food Chem. 82*, 265–273.

(41) Blazek, V., and Caldwell, R. A. (2009). Comparison of SDS gel capillary electrophoresis with microfluidic lab-on-a-chip technology to quantify relative amounts of 7S and 11S proteins from 20 soybean cultivars. *Int. J. Food Sci. Technol. 44*, 2127–2134.

(42) Liu, S., Zhou, R., Tian, S., and Gai, J. (2007). A Study on Subunit Groups of Soybean Protein Extracts under SDS-PAGE. *J. Am. Oil Chem. Soc. 84*, 793–801.

4.2 Improved CE(SDS)-CZE-MS method utilizing an 8-port nanoliter valve

This chapter has been published and adapted with permission from:

Römer, J., Kiessig, S., Moritz, B., and Neusüß, C. (2021).
Electrophoresis, 42, 374-380; DOI: 10.1002/elps.202000180

4.2.1 Abstract

Capillary sieving electrophoresis utilizing SDS (CE(SDS)) is one of the most applied methods for the analysis of antibody (mAb) size heterogeneity in the biopharmaceutical industry. Inadequate peak identification of observed protein fragments is still a major issue. In a recent publication, we introduced an electrophoretic 2D system, enabling online mass spectrometric detection of generic CE(SDS)-separated peaks and identification of several mAb fragments. However, an improvement regarding system stability and handling of the approach was desired. Here, we introduce a novel 8-port valve in conjunction with an optimized decomplexation strategy. The valve contains four sample loops with increased distances between the separation dimensions. Thus, successively coinjection of solvent and cationic surfactant without any additional detector in the second dimension is enabled, simplifying the decomplexation strategy. Removal efficiency was optimized by testing different volumes of solvents as presample and cationic surfactant as postsample zone. 2D measurements of the light and heavy chain of the reduced NIST mAb with the 8-port valve and the optimized decomplexation strategy demonstrates the increased robustness of the system. The presented novel set-up is a step toward routine application of CE(SDS)-CZE-MS for impurity characterization of proteins in the biopharmaceutical field.

4.2.2 Introduction

Capillary sieving electrophoresis utilizing SDS (CE(SDS)) with UV or LIF detection is the most efficient and, thus, standardized method for size heterogeneity analysis of biotherapeutics like antibodies (mAbs) [1]. The identification of observed protein fragments is of outstanding importance to assure drug efficacy and safety. However, direct characterization of peaks in CE(SDS) is not possible since neither fraction collection of the small volumes nor direct ESI-MS is possible due to strong ionization suppression of proteins by SDS [2] and other separation gel components. There are several ways to cope with the challenges of hyphenating MS interfering electrophoretic separation methods summarized by Schlecht et al. [3]. In order to maintain the original separation method, two-dimensional heart-cut approaches can be applied, like presented in several set-up and applications [3, 4]. None of these approaches was utilized for the CE(SDS) application so far. Hence, we recently introduced a 2D capillary electrophoretic separation system utilizing a 4-port nanoliter valve [5] for online mass spectrometric detection of CE(SDS)-separated peaks [6]. The generic CE(SDS) separation dimension, as first dimension (^{1}D), is hyphenated via the 4-port nanoliter valve with an MS-compatible CZE method as second dimension (^{2}D), for separating interfering substances from the peak of interest prior to introduction into the MS. One crucial part of this CE(SDS)-CZE-MS approach is the decomplexation of the SDS-protein

complex in the ^{2}D. An in-capillary decomplexation strategy was developed in our group, by testing several cationic compounds, revealing that the cationic surfactant CTAB and SDS form a more stable complex than SDS with proteins, releasing the free protein [7]. Thus, in relation to the SDS-protein sample, that is transferred via sample loop from the ^{1}D to the ^{2}D, a presample zone of solvent (methanol) and a postsample zone of CTAB is utilized for decomplexation in the ^{2}D. Therefore, the zones were hydrodynamically injected via the second CZE dimension and positioned with the help of C^{4}D. In this way, several mAb fragments and soybean proteins separated by CE(SDS) were characterized by MS [6]. However, robustness was limited due to frequent current leakage and breakdown, most probably caused by insufficient distance between the separation dimensions and inaccurate positioning of the decomplexation zones in the ^{2}D.

Here, we present a novel 8-port nanoliter valve with increased distances between separation dimensions and additional loops, allowing successive transfer of the SDS-decomplexation zones into the ^{2}D. The decomplexation strategy is adapted to the new design and optimized regarding measurement stability and signal intensity. The performance of the new set-up is demonstrated by the CE(SDS)-CZE-MS analysis of the light chain (LC) and heavy chain (HC) of the reduced mAb of the National Institute of Standard and Technologies (NIST) and compared to previous results obtained with the 4-port valve.

4.2.3 Materials and methods

Chemical and samples

Methanol (HPLC-MS grade), acetic acid (HAc), and formic acid (FAc) were obtained from Carl Roth GmbH und Co. KG (Karlsruhe, Germany). Ethanol (HPLC grade) was purchased by Fisher Scientific (Schwerte, Germany). Sodium hydroxide (NaOH), hydrochloric acid (HCl), and 1-butanol were obtained from Merck (Darmstadt, Germany). DTT, SDS (10% in water), CTAB, glutaraldehyde solution (50% in water), PVA (99%, average molecular weight (MW) 89,000–98,000), and Tris were purchased from Sigma Aldrich (Steinheim, Germany). All solutions were prepared using ultrapure water (18 MΩ cm at 25 °C, SG Ultra Clear UV from Siemens Water Technologies, USA). ESI Tuning mix solution was acquired from Agilent Technologies (Waldbronn, Germany). SDS-MW gel buffer was obtained from Sciex (AB Sciex, Darmstadt, Germany). Sample solution of mAb 1 was provided by F. Hoffmann-La Roche (Basel, Switzerland) and NIST mAb was obtained from the NIST. Reduction of mAbs was carried out by adding 0.5 M DTT and heating for 10 min at 70 °C in a Thermomixer (Eppendorf, Wesseling-Berzdorf, Germany), followed by centrifugation at 14,100 g during 90 s (Eppendorf). For decomplexation optimization by injection via valve, mAb 1 was diluted in SDS-MW gel buffer to obtain a final concentration of 1 mg/mL. For the 2D analysis, NIST mAb was diluted in SDS solution with a final concentration of 1 mg/mL.

Technical set-up of 2D system with an 8-port valve

An 8-port-valve was designed consisting of eight symmetrically positioned ports on the stator and four symmetrically positioned sample loops (4 x 20 nL) on the rotor. The stator is made of polyether ether ketone (PEEK) and the rotor of Valcon E (polyaryletherketone (PAEK)/PTFE-based composite) as described before [6]. The valve was custom made by VICI AG International (Schenkon, Switzerland; part number: C5M-4354-CU1), equipped with 360 μm fittings and a multi position electric microactuator. With this microactuator the rotor can be switched into each of the four desired positions. The ^{1}D (position 1) and the ^{2}D (position 3) are placed on the opposite sides and, thus, the loops for the pre- (position 2) and postsample zones (position 4) are chosen to be contiguous to the separation dimensions (Figure 4.10).

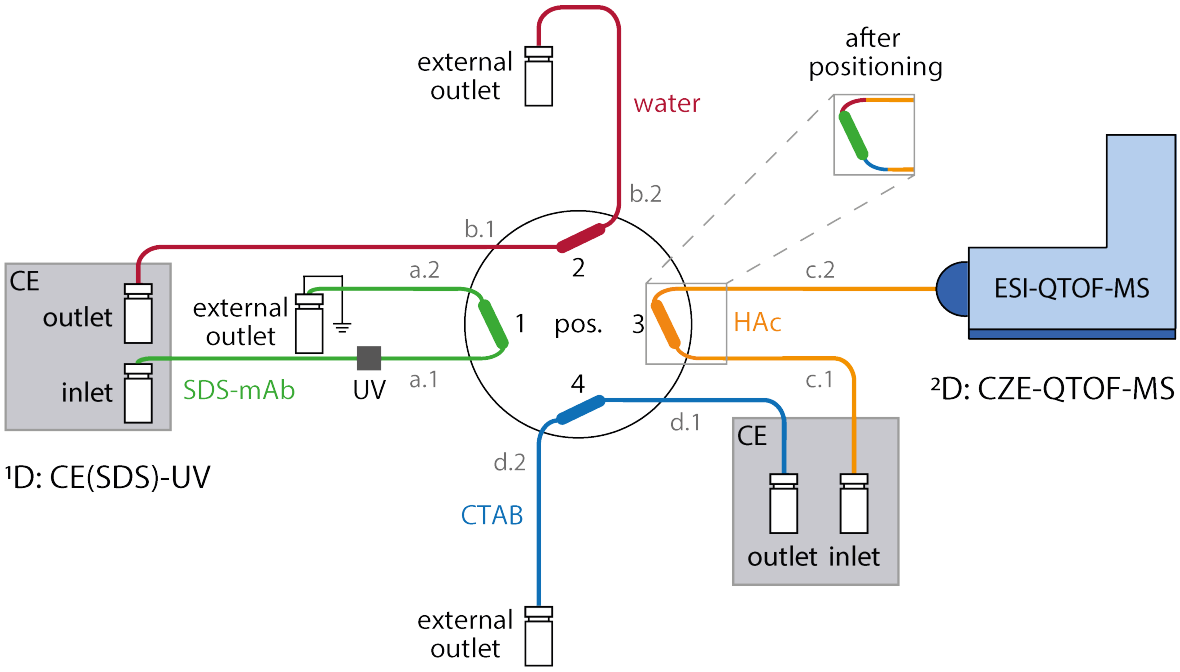

Figure 4.10: Set-up of the optimized CE(SDS)-CZE-MS system. Detailed scheme of the 8-port nanoliter valve, where the analysis is performed in the first CE(SDS) dimension (green, position 1). For each decomplexation zone, consisting of water (red, position 2) and the cationic surfactant CTAB (blue, position 4), separate connections are utilized and positioned between both separation dimensions. The second CZE-MS dimension (orange, position 3) is located vis-à-vis the CE(SDS) dimension. For zone and sample transfer into the CZE-MS dimension, filled loops are switched to positon 3 via the multiposition electric microactuator. Capillary lengths: a.1: 35 cm, a.2: 12 cm; b.1 and d.1: 60 cm, b.2 and d.2: 20 cm; c.1 and c.2: 35 cm.

For the ^{1}D and both zone dimensions, fused silica capillaries (Polymicro Technologies, Phoenix, AZ, USA) and for the ^{2}D, PVA coated capillaries, prepared in-house as described before [8], all with 50 μm id, are connected to the valve. The inlet position of an Agilent HP^{3D}CE instrument (Agilent Technologies, Waldbronn, Germany) is utilized for applying

voltage and pressure in the ^{1}D and the outlet position for pressure application in the presample zone dimension. The grounding of the ^{1}D dimension is assured by placing a platinum electrode inside the outlet vial with the electrode being connected to an external HV-power supply. Instrument control was performed with the ChemStation software. The separation in the ^{1}D is tracked via an ECD2600 EX UV-VIS detector (ECOM spol. s r.o., Prague, Czech Republic) at a wavelength of 214 nm. A detection window is positioned 4.3 cm in front of the valve on the first capillary of the ^{1}D. The inlet of a second Agilent CE instrument (HP^{3D}CE) is utilized for flushing and applying voltage in the ^{2}D and the outlet for the pressure application in the postsample zone dimension. To ensure safety of the user and integrity of the instruments, the valve itself is additionally grounded. An orthogonal electrospray interface (ESI, model G1607A from Agilent Technologies) is used for coupling of CE and MS. For MS detection a Compact Q-TOF (Bruker Daltonics, Bremen, Germany) is employed. MS control and data analysis are carried out using Data Analysis software (Bruker, Bremen, Germany). ESI is performed in positive ion mode (4.5 kV). The flow rate of dry gas is set at 4.0 L/min and a temperature of 170 °C with a nebulizer gas pressure of 0.2 bar. As sheath liquid, a mixture of methanol : water (50:50, v/v) with 0.5% (v/v) FAc is used, delivered with a flow rate of 4 μL/min. Spectra are acquired in a mass range of 700 – 3,500 m/z. External calibration of the MS is performed at the beginning of every day.

Preconditioning of CE(SDS)-CZE-MS system

In the ^{1}D, capillaries were conditioned prior to use by flushing 0.1 M NaOH, 0.1 M HCl and water at 3 bar for 3 min. For method development by injection via valve, capillaries were filled with mAb 1 in SDS-MW gel buffer at 3 bar and 2 bar for 10 min each. Meanwhile the ^{1}D was flushed with mAb 1 in gel, the presample zone dimension was flushed with water, the postsample zone dimension with CTAB solved in ethanol: water: butanol (2:2:1) for 10 min at 2 bar. The capillaries of the ^{2}D were flushed at 2 bar for 5 min with water and 25 min with 1 M HAc. For the 2D analysis, capillaries of the ^{1}D were flushed after the conditioning step with SDS-MW gel buffer at 3 bar and 2 bar for 30 min each, followed by applying -15 kV for 5 min. Other capillaries were kept filled with air until the separation in the ^{1}D was completed. After the analysis in the ^{1}D was stopped, both zone dimensions and the ^{2}D were flushed with water, CTAB and 1 M HAc at 3 bar for 2 min, respectively.

SDS-removal strategy optimization and validation

The transfer of the presample zone into the ^{2}D was performed by switching the loop filled with water to position 3 and applying pressure for several seconds. For transferring the postsample zone into the ^{2}D, the loop filled with 0.4% w/v CTAB solved in ethanol: water: butanol (2:2:1) was switched to position 3 and negative pressure was applied for several

seconds. After the pre- and postsample zone were transferred, the sample loop filled mAb 1 sample diluted in SDS-MW gel buffer was positioned in between these zones into the ^{2}D by switching the valve to position 3 without further pressure application utilizing the valve as injector (no separation over the ^{1}D). After successful positioning of the decomplexation zones and mAb 1 sample, the capillaries of the ^{1}D and of the zone dimensions were flushed with air for 2 min at 5 bar, followed by setting the separation voltage in the ^{2}D to +10 kV. After each analysis, capillaries were flushed with air for 5 min at 5 bar at position 3 and 1 to prevent possible clogging. For zone length optimization, different injection times for the pre- and postsample zone and each combination were surveyed. Additionally, a comparison to the 4-port valve decomplexation strategy was done by utilizing methanol as presample zone and CTAB (solved in methanol: water, 1:1) as postsample zone with the 8-port-valve.

Analysis of mAb with CE(SDS)-CZE-MS system
NIST mAb was injected electrokinetically at −15 kV for 60 s in the ^{1}D and separated by applying −15 kV. As soon as the CE(SDS) peak maxima was detected, the migration time and the effective length of the capillary were used to calculate the migration velocity. With the migration velocity and the known distance from the UV detector to the middle of the sample loop in the valve, the stop time for the CE(SDS) peak to arrive in the sample loop was determined. As soon as the stop time was reached, the separation voltage was set to 0 kV and the zone dimensions and ^{2}D were flushed as described before. After transferring the decomplexation zones and the CE(SDS)-separated protein fragment into the ^{2}D, capillaries of the zone dimensions and ^{1}D were flushed with air at 5 bar for 2 min before applying voltage in the ^{2}D. The analysis were performed for the NIST LC (n = 3) and the HC (n = 3). After each measurement, capillaries were flushed with air at 5 bar for 5 min at the end (position 3) and starting position (position 1) to prevent possible clogging.

4.2.4 Results and discussion

Set-up and principle
With the here presented 8-port valve, each separation and zone dimension has its own connection and loop. They can be transferred into the ^{2}D separately, by filling the loops, switching the valve, and applying pressure in the ^{2}D. This allows the precise placement of defined volumes relative to the SDS-protein sample. Another major advantage of the 8-port valve design is the enlargement of the distances between the loops and, thus, between the dimensions. In the commercially available 4-port valve, the distance between the ^{1}D and ^{2}D is around 1 mm. Now, the distances between neighboring dimensions are about 3 mm and by utilizing the opposite positions for the ^{1}D and ^{2}D, the distance is 5 mm. Thus, even if SDS gel is allocated between rotor and stator as a result of flushing and switching the valve

several times, current leakage is less observed than before. Especially, when all other loops are kept filled with air during voltage application in the ^{1}D or ^{2}D. The breakthrough voltage was tested by filling the ^{2}D with 1M HAc and applying voltage (5, 10, 15, 20, 25, 30 kV) for 10 min each (data not shown). Stable current was observed up to 25 kV, at 30 kV a break down and damage of the power supply was observed. For this reason, additional grounding of the valve was implemented to assure integrity of the instruments and safety for the user. With this set-up, separation voltages up to 25 kV can be utilized with the 8-port valve. Nevertheless, the voltage during the CE(SDS) separation utilized as ^{1}D was kept at -15 kV as commonly used in routine analysis. Due to the low surface tension of SDS-containing solutions, they have a high tendency to allocate between rotor and stator. The bigger distances between loops support that current leakage is less frequently observed. However, the separation voltage in the ^{2}D was kept at 10 kV to lower the risk of current breakdown. With this operating method, the analysis stability is still improved compared to the 4-port valve set-up. For other approaches without SDS, higher separation voltages in the ^{1}D and ^{2}D might be feasible with the here presented 8-port valve to speed up the analysis and increase separation efficiency.

SDS-removal strategy optimization and validation

Different than in our work presented before, decomplexation zones are now transferred separately and do not need to be hydrodynamically injected via the ^{2}D. This assures a more precise decomplexation zone positioning in relation to the SDS protein sample without the necessity of a C^{4}D detector. Due to known problems with the formation of bubbles of SDS-containing solutions upon application of pressure, sample transfer of the SDS-protein complex from the sample loop into the ^{2}D was aspired without pressure application. For this reason, the pre- and postsample zones were positioned prior to sample transfer. Applying the previous SDS-removal strategy performed with the 4-port valve [6, 7], with methanol as presample zone and CTAB solution in methanol: water 1:1 as postsample zone, the current was instable or even broke down completely. To understand these current instabilities, offline solubility experiments were performed. When mixing equal amounts of methanol, SDS-MW gel, and CTAB (0.4% solved in methanol: water, 1:1) precipitation was observed. Various combinations and ratios of water/1-alcohol mixtures were tested in a similar way. By substituting methanol with water and solving CTAB in a mixture of ethanol: water: butanol (2:2:1), hardly any precipitation was observed. For this reason, water was used as presample zone and CTAB solved in ethanol: water: butanol (2:2:1) as postsample zone for the SDS-removal strategy with the 8-port-valve. For zone length optimization, different injection times for water (30, 35, and 40 s) and for 0.4% w/v CTAB (20, 25, and 30 s) solved in ethanol: water: butanol (2:2:1) and each combination ($n = 3$) were

surveyed. Interestingly, utilizing water and CTAB solved in ethanol: water: butanol (2:2:1), no current instabilities were observed and MS signals of the decomplexed mAb were obtained for all 27 measurements. Besides measurement stability and robustness, the decomplexation strategy with the highest removal efficiency was determined. In addition to the quality of the resulting mass spectrum (absence of noise and adducts), both peak intensity and area can be considered for the evaluation of the removal efficiency. Therefore, both signal intensities and areas of the extracted ion electropherograms (EIE) peaks, resulting from the sum of the eight most abundant m/z for the LC or HC of mAb 1, were evaluated. Optimal decomplexation conditions resulting in the highest peak area were found both for LC and HC in utilizing 35 s water as presample and 25 s CTAB as postsample zone (Figure 4.11).

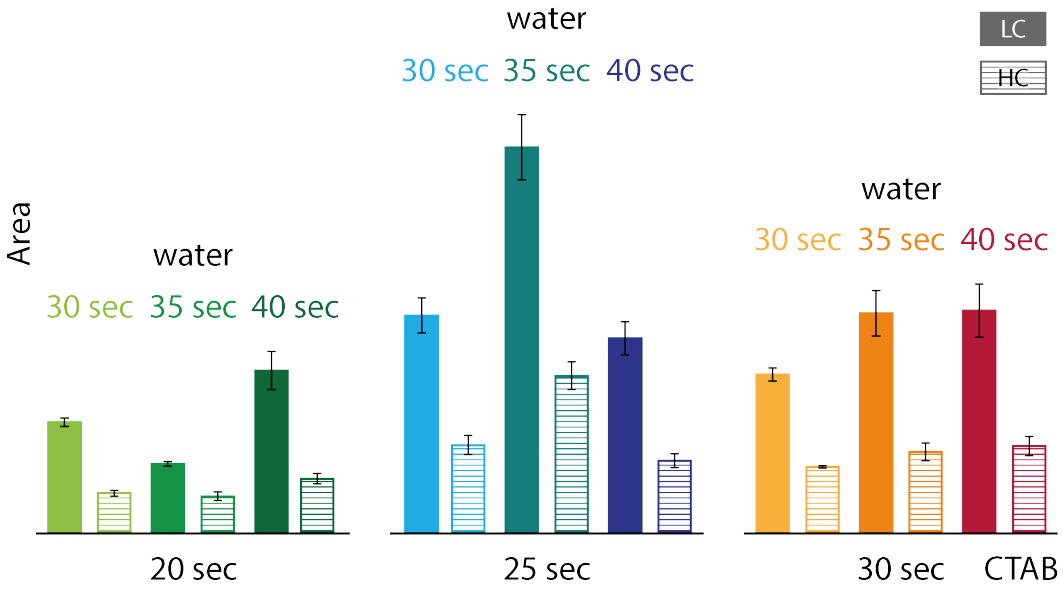

Figure 4.11: Peak area obtained with the EIEs (sum of the eight most abundant m/z) for LC and HC of reduced mAb 1 applying different zone length of water and CTAB (0.4% in ethanol: water: butanol, 2:2:1). Injection of mAb 1 in SDS-MW gel buffer into the ^{2}D was performed via valve. Zone length of water and CTAB were positioned via valve applying pressure for several seconds (water: 30; 35; or 40 s at 50 mbar and CTAB: 20; 25, or 30 s at −50 mbar). Highest peak areas were found for both LC and HC utilizing 35 s water as pre- and 25 s CTAB as postsample zone. Error bars represent standard deviation (n = 3).

Standard deviations of the obtained signal areas for every decomplexation strategy (n = 3) were determined, ranging from 7 to 24% (mean value = 16%) for the LC and 4 to 24% (mean value=18%) for the HC. The optimum regarding peak intensity of the LC was found for 40 s water in combination with 25 s CTAB and for the HC 35 s water and 25 s CTAB as pre- and postsample zone. The standard deviation for peak intensities ranged between 4 and 26% (mean value = 14%) for the LC and 1 to 23% (mean value = 8%) for the HC.

For a direct comparison to the decomplexation strategy used with the 4-port valve, methanol and CTAB (solved in methanol: water, 1:1) were applied as pre- and postsample zone with the 8-port valve, too. Here, only one zone length combination, namely 30 s of methanol and 20 s of CTAB (solved in methanol: water, 1:1), was tested, due to observed current instabilities as described before. Otherwise, the same set-up was utilized as performed for the decomplexation optimization by injecting reduced mAb 1 in SDS-MW gel buffer via valve. For the same transfer time into the ^{2}D, obtained peak intensities with water and CTAB (solved in ethanol: water: butanol, 2:2:1) were higher for the LC (25%) and for the HC (20%) compared to the peak intensities obtained with methanol and CTAB (solved in methanol: water, 1:1). Important to note here is that utilizing methanol and CTAB (in methanol: water, 1:1) for decomplexation, a higher number of runs, here five, was necessary for obtaining three runs with stable current in the ^{2}D and MS signals, demonstrating poor robustness and stability. The resulted peak areas obtained with methanol and CTAB (in methanol: water, 1:1) were 24% for the LC and 18% for the HC higher, than the peak areas obtained with water and CTAB (in ethanol: water: butanol, 2:2:1) at the same transfer time into the ^{2}D. This is related to the poor peak shape that was obtained with methanol and CTAB (in methanol: water, 1:1). Hence, higher standard deviations in between successful measurements (n = 3) for the area were observed compared to the new decomplexation strategy: for the LC, here 20% than 8%, and for the HC, here 39% than 15%. All in all, the experiments by injection via valve with the 8-port valve demonstrate that the optimized decomplexation strategy results in a higher method robustness and stability compared to the methanol decomplexation strategy used before. Additionally, better peak shapes and intensities were obtained for the same transfer times into the ^{2}D.

Analysis of mAb with CE(SDS)-CZE-MS system

To evaluate the overall performance in a two-dimensional approach, CE(SDS)-CZE-MS analysis were performed with the presented 8-port-valve and optimized decomplexation in terms of peak intensity and area. The obtained results with the optimized decomplexation strategy regarding peak intensity were compared to partly published CE(SDS)-CZE-MS measurements of the NIST mAb LC and HC (c = 1 mg/mL) performed with the 4-port valve and its corresponding methanol decomplexation strategy [6]. The comparison of the runs with both CE(SDS)-CZE-MS systems is demonstrated by the EIEs (sum of the eight most abundant m/z) with the mean intensity (n = 3) for LC (Figure 4.12 A.1) and HC (Figure 4.12 B.1). For the EIEs of the LC (Figure 4.12 A.1), it can be seen that the 4-port valve approach (dark gray, peak 1) resulted in a higher peak intensity (factor 1.5) but lower peak area (26%) compared to the 8-port valve approach (dark blue, peak 2) and their related decomplexation strategy. Comparing the averaged mass spectra (Figure 4.12 A.2), almost

the same intensity for both approaches was found. Regarding the deconvoluted masses (Figure 4.12 A.3), about 81% of the intensity obtained with the 4-port valve approach was preserved with the 8-port valve approach at the same spectra quality.

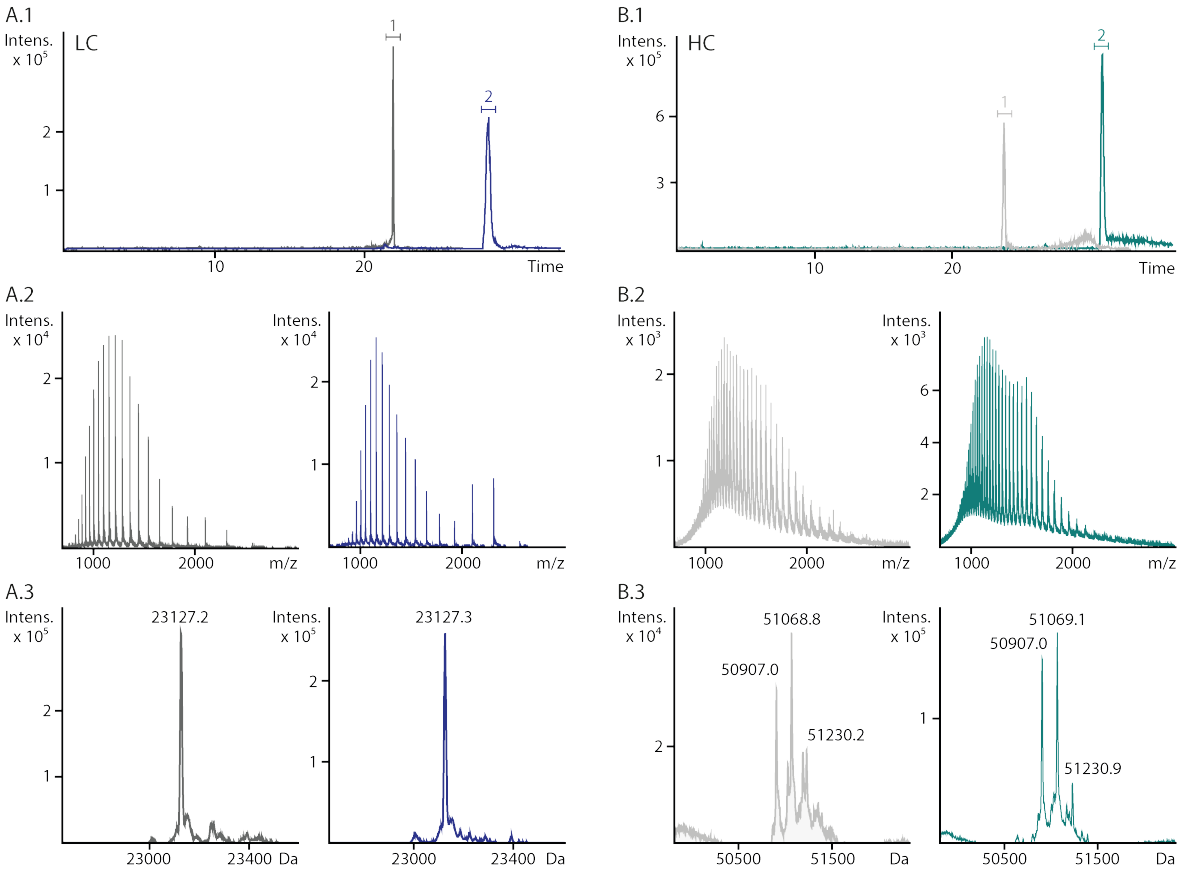

Figure 4.12: Comparison of CE(SDS)-CZE-MS measurements of the reduced NIST mAb LC (A.1-A.3) and HC (B.1-B.3) with the 4- and 8-port valve and their related decomplexation strategy. LC and HC (1 mg/mL) were analyzed (each n = 3) with both approaches and the representative EIEs (sum of the eight most abundant m/z) and MS signals are presented. The EIEs obtained in the second CZE-MS dimension of the LC is shown in A.1, where peak 1 (dark gray) was obtained with the 4-port valve approach and peak 2 (dark blue) with the 8-port valve approach. The averaged mass spectra for both LC peaks can be seen in A.2 and the related deconvoluted mass in A.3. The EIEs obtained in the second CZE-MS dimension of the HC is shown in B.1, where peak 1 (light gray) was obtained with the 4-port valve approach and peak 2 (cyan) with the 8-port valve approach. The averaged mass spectra for both HC peaks can be seen in B.2 and the related deconvoluted masses in B.3. For both approaches, a 20 nL sample loop was utilized to transfer the peak of interest from the ^{1}D to the ^{2}D.

Comparing the results obtained for the HC (Figure 4.12 B.1) with the 8-port valve approach (cyan, peak 2), an increase regarding the EIEs intensity (factor 1.5) and area (factor 2.2), averaged mass spectra intensity (Figure 4.12 B.2, factor 3.3) and the intensity of the deconvoluted masses (Figure 4.12 B.3, factor 3.9) was observed compared to the 4-port

valve approach (light gray, peak 1). Additionally, the mass spectra quality was improved as demonstrated by less adducts and artifacts (Figure 4.12 B.3).
Comparing the averaged EIE peak areas (Figure 4.13 A, n = 3) of the LC (dark blue) and HC (cyan) obtained with the 8-port valve approach to the 4-port valve approach (LC, dark gray and HC, light gray), an increase of a factor of 2.8 for the LC and a factor of 2.6 for the HC could be obtained.

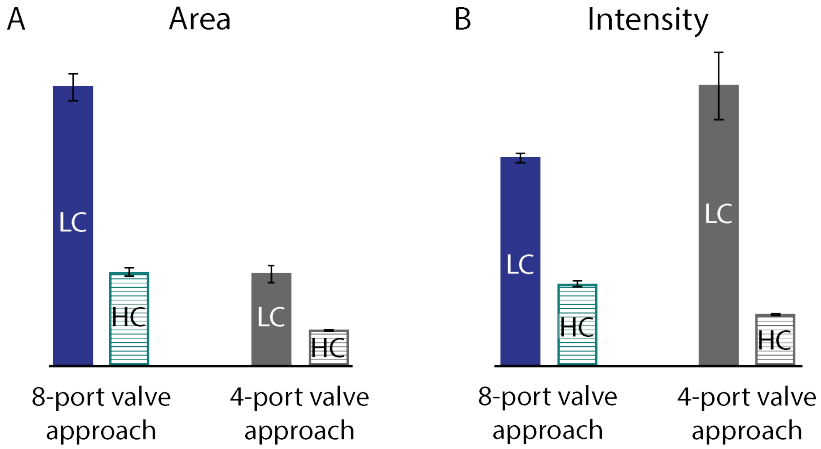

Figure 4.13: Mean value of the peak areas (A) and heights (B) resulting from the EIEs (sum of the eight most abundant m/z) obtained for reduced NIST mAb LC and HC performing 2D measurements with the 8-port valve (LC, dark blue and HC, cyan) and 4-port valve approach (LC, dark gray and HC, light gray). For both approaches, a 20 nL sample loop was utilized to transfer the peak of interest (here LC or HC) from the ^{1}D to the ^{2}D. Error bars represent standard deviation (n = 3).

Optimized decomplexation with the 8-port valve resulted in an averaged peak intensity (Figure 4.13 B) increase of a factor of 1.6 for the HC (cyan) compared to the 4-port valve approach (light gray). For the LC, our 8-port valve approach (dark blue) resulted in a peak intensity of 70% compared to peak intensities obtained with the 4-port valve approach (dark gray). Even if lower peak intensities were observed on average for the LC with the 8-port valve approach, standard deviation was improved from 24 to 12%.
Another interesting point is the comparison of the success rate of both CE(SDS)-CZE-MS set-up. Here, the analysis was stated as successful, if the current in both dimensions was stable and standard deviation was less than 25% regarding MS signal intensity. Comparing the number of performed 2D runs to obtain three successful measurements each for the LC and HC analysis, 14 measurements with the 4-port valve set-up were necessary. This results in a success rate of 43% (6 of 14 runs). With the 8-port valve set-up, nine successful runs were obtained by performing 12 measurements. This leads to a success rate of 75% with the 8-port valve and optimized decomplexation, demonstrating an almost doubled success rate and, thus, an increased measurement stability.

4.2.5 Conclusion

We presented a new designed 8-port valve for the improved set-up and handling of our previously described CE(SDS)-CZE-MS system. Decomplexation zones are now positioned successively via separate zone dimensions. This allows precise positioning for the addition of decomplexation agents before and after the transferred CE(SDS) peak. It turned out that the use of water as presample and CTAB (in ethanol: water: butanol, 2:2:1) as postsample zone resulted in most stable conditions. Best removal efficiency, represented by the highest peak areas, was found by utilizing 35 s at 50 mbar of water as presample zone in combination with 25 s at −50 mbar of CTAB as postsample zone for both LC and HC. Compared to the previous decomplexation strategy (methanol and CTAB in methanol: water, 1:1), the here developed approach reached better signal intensities both for the LC (25%) and HC (20%) by injection via valve. CE(SDS)-CZE-MS measurements of the NIST mAb LC and HC with the 8-port valve and optimized decomplexation strategy were performed and compared to results obtained with the 4-port valve approach. Even if lower signal intensities of the LC EIEs were observed, it was possible to preserve about the same signal intensity for the mass spectra and for the deconvoluted mass (81%) at same signal quality. An increase of the intensity regarding the HC EIEs (factor 1.5), mass spectra (factor 3.3), and deconvoluted mass (factor 3.9) was observed compared to the 4-port valve approach. Additionally, the mass spectra quality for the HC was improved demonstrated by masses showing less adducts and artifacts. Especially, an increase of current stability in the ^{2}D could be achieved. Comparing the 2D measurement for the analysis of the NIST LC and HC performed with the 8-port valve to the 4-port valve, an almost doubled total measurement stability was obtained. Thus, the measurements with the 8-port valve and optimized decomplexation strategy are a significant step toward a routine application of this new technology. The here presented 8-port valve can be utilized for other two-dimensional separation approaches as well. For approaches without SDS, higher separation voltages up to 25 kV in the ^{1}D and ^{2}D might be feasible, to speed up the analysis and increase separation efficiency. Due to the symmetrical and equally sized loops, another interesting approach for the presented valve is seen in 2D multiple heart-cut analysis.

The authors want to thank Alexander Stolz and Jens Meixner for valuable comments and proofreading of the manuscript. This study was funded by F. Hoffmann-La Roche Ltd.

The authors have declared no conflict of interest.

References

(1) Sänger-van de Griend, C. E. (2019). CE-SDS method development, validation, and best practice-An overview. *Electrophoresis 40*, 2361–2374.

(2) Rundlett, K. L., and Armstrong, D. W. (1996). Mechanism of signal suppression by anionic surfactants in capillary electrophoresis-electrospray ionization mass spectrometry. *Anal. Chem. 68*, 3493–3497.

(3) Schlecht, J., Jooß, K., and Neusüß, C. (2018). Two-dimensional capillary electrophoresis-mass spectrometry (CE-CE-MS): coupling MS-interfering capillary electromigration methods with mass spectrometry. *Anal. Bioanal. Chem. 410*, 6353–6359.

(4) Kler, P. A., Sydes, D., and Huhn, C. (2015). Column-coupling strategies for multidimensional electrophoretic separation techniques. *Anal. Bioanal. Chem. 407*, 119–138.

(5) Kohl, F. J., Montealegre, C., and Neusüß, C. (2016). On-line two-dimensional capillary electrophoresis with mass spectrometric detection using a fully electric isolated mechanical valve. *Electrophoresis 37*, 954–958.

(6) Römer, J., Montealegre, C., Schlecht, J., Kiessig, S., Moritz, B., and Neusüß, C. (2019). Online mass spectrometry of CE (SDS)-separated proteins by two-dimensional capillary electrophoresis. *Anal. Bioanal. Chem. 411*, 7197–7206.

(7) Sanchez-Hernandez, L., Montealegre, C., Kiessig, S., Moritz, B., and Neusüß, C. (2016). In-capillary approach to eliminate SDS interferences in antibody analysis by capillary electrophoresis coupled to mass spectrometry. *Electrophoresis 38*, 1044–1052.

(8) Neuberger, S., Jooß, K., Ressel, C., and Neususs, C. (2016). Quantification of ascorbic acid and acetylsalicylic acid in effervescent tablets by CZE-UV and identification of related degradation products by heart-cut CZE-CZE-MS. *Anal. Bioanal. Chem. 408*, 8701–8712.

4.3 Online top-down mass spectrometric identification of CE(SDS)-separated antibody fragments by two-dimensional capillary electrophoresis

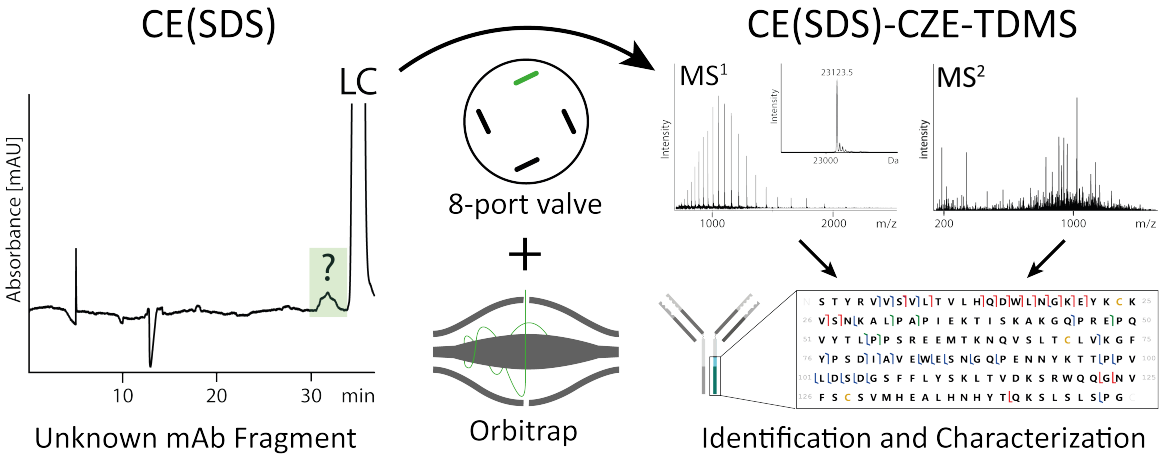

Figure 4.14: Graphical abstract: Principle of the two-dimensional top-down approach

This chapter has been accepted by the Journal of Pharmaceutical and Biomedical Analysis and adapted with permission:

Römer, J., Stolz, A., Kiessig, S., Moritz, B., and Neusüß, C. (2021);
DOI: 10.1016/j.jpba.2021.114089

4.3.1 Abstract

Size heterogeneity analysis by capillary sieving electrophoresis utilizing sodium dodecyl sulfate (CE(SDS)) with optical detection is a major method applied for release and stability testing of monoclonal antibodies (mAbs) in biopharmaceutical applications. Identification of mAb-fragments and impurities observed with CE(SDS) is of outstanding importance for the assessment of critical quality attributes and development of the analytical control system. Mass spectrometric (MS) detection is a powerful tool for protein identification and characterization. Unfortunately, CE(SDS) is incompatible with online MS-hyphenation due to strong ionization suppression of SDS and other separation buffer components. Here, we present a comprehensive platform for full characterization of individual CE(SDS)-separated peaks by CE(SDS)-capillary zone electrophoresis-top-down-MS. The peak of interest is transferred from the first to the second dimension via an 8-port valve to remove MS-incompatible components. Full characterization of mAb byproducts is performed by intact mass determination and fragmentation by electron transfer dissociation, higher-energy collisional dissociation, and ultraviolet photodissociation. This enables online determination of intact mass as well as sequence verification of individual CE(SDS)-separated peaks simultaneously. A more substantiated characterization of unknown CE(SDS) peaks by exact localization of modifications without prior digestion is facilitated. High sensitivity is demonstrated by successful mass and sequence verification of low abundant, unknown CE(SDS) peaks from two stressed mAb samples. Good fragmentation coverages are obtained by MS^2, enabling unequivocal identification of these mAb-fragments. Also, the differentiation of reduced/non-reduced intra-protein disulfide bonds is demonstrated. In summary, a reliable and unambiguous online MS^2 identification of unknown compounds of low-abundant individual CE(SDS) peaks is enabled.

4.3.2 Introduction

For the analysis of size heterogeneity of monoclonal antibodies (mAbs), capillary sieving electrophoresis utilizing sodium dodecyl sulfate (CE(SDS)) is one of the most important analytical method in the biopharmaceutical industry. CE(SDS) can be seen as a further development of sodium dodecyl sulfate-polyacrylamide gel electrophoresis, with the possibility of online detection and quantification. Besides providing increased resolution, precision, linearity, repeatability, and robustness, it also enables a higher degree of automatization [1]. CE(SDS) is routinely used for product characterization, release, and stability studies [2]. For stability studies, mAbs are stored under recommended storage conditions, or they are stressed by e.g. elevated temperature, mechanical stress or light [3, 4]. In general, it is of outstanding importance to identify mAb modifications to evaluate production and

storage conditions, thus ensuring the safety and efficacy of the biopharmaceutical product throughout its shelf life. The commonly used detection with ultraviolet (UV) or laser-induced fluorescence (LIF) in CE(SDS) does not provide details about the identity of unknown peaks. Mass spectrometric (MS) detection can provide essential information for identification, such as the intact mass via full scan mass spectrometry (MS^1) and sequence information via tandem mass spectrometry (MS^2) experiments. So far, only offline approaches, including fraction collection from reversed-phase liquid chromatography (RPLC) separation with additional MS analysis [5, 6] are utilized to obtain mass spectrometric information attributed to CE(SDS)-separated mAb-fragments. Only a single publication using fraction collection of CE(SDS)-separated proteins with subsequent offline cleanup and hyphenation with matrix-assisted laser desorption ionization (MALDI) MS via a polytetrafluoroethylene membrane was reported so far [7]. Recently, we introduced a two-dimensional (2D) electrophoretic system CE(SDS)-CZE-MS, enabling online mass spectrometric detection of CE(SDS)-separated proteins utilizing a 4-port nanoliter valve [8]. The fundamental method was improved regarding stability and in-capillary SDS-protein decomplexation employing an 8-port nanoliter valve [9].

The identification and exact localization of modifications in biotherapeutics is traditionally performed by bottom-up workflows, i.e. the analysis of proteolytic peptides, including their sequence verification by MS^2. Although this technique is still widely applied, several issues remain even with optimized workflows. Sample preparation is time-consuming, and the conditions during tryptic digestion are known to introduce artifacts [10–12]. Additionally, full characterization of minor variants or differentiation of closely related proteoforms remains challenging [13, 14]. In recent years, top-down MS (TDMS) has been increasingly used for biopharmaceuticals [15–17]. Here, the undigested protein is subjected to gas-phase fragmentation to obtain sequence information. In contrast to bottom-up approaches, TDMS provides additional full mass information about the protein, combinatory post-translational modifications (PTMs) can be revealed, and closely related proteoforms can be differentiated unambiguously [13]. Besides high-performance liquid chromatography-mass spectrometry (HPLC-MS), CE-MS has been increasingly used for top-down proteomics as reviewed by Shen et al. [18]. CE-MS advantages are high separation efficiency for intact proteins, high sensitivity and low sample consumption [19]. However, top-down applications using CE-MS for the analysis of biopharmaceuticals are rare. Biacchi et al. applied capillary zone electrophoresis (CZE) with UV detection for fraction collection of IdeS digested and reduced mAb. The fractions were collected on a MALDI target plate and subsequently analyzed by intact mass measurement as well as intact protein fragmentation [20]. Bush et al. impressively demonstrated the application of CZE-MS in combination with top-down analysis for the in-depth characterization of biopharmaceutical human interferon

β-1 proteoforms [21]. They were able to identify 138 proteoforms, including glycoforms and non-enzymatic modifications. Here, we present the CE(SDS)-CZE-TDMS system as a sensitive and comprehensive platform, enabling online top-down characterization of CE(SDS)-separated proteins for the first time. Coupling of the system to an Orbitrap Fusion Lumos MS is performed via a nanoflow sheath liquid (SL) interface [22]. The evaluation and suitability of the system are demonstrated by online CE(SDS)-CZE-MS^1 and CE(SDS)-CZE-MS^2 characterization of the intact light chain (LC) of the NIST mAb. Furthermore, we are able to identify unknown degradation products of stressed NIST mAb and a second mAb.

4.3.3 Materials and methods

Materials and reagents

Methanol (HPLC-MS grade), 2-propanol (IPA, HPLC-MS grade), acetonitrile (ACN, HPLC-MS grade) acetic acid (glacial, HAc) and formic acid ($\geq$ 98%, FAc) were obtained from Carl Roth GmbH + Co. KG (Karlsruhe, Germany). Ethanol (HPLC grade) was purchased by Fisher Scientific (Schwerte, Germany). Sodium hydroxide (NaOH), hydrochloric acid (HCl), 1-butanol (HPLC grade), urea (Ph Eur) were obtained from Merck (Darmstadt, Germany). Dithiothreitol (DTT, BioUltra), SDS (BioUltra, 10% in water), CTAB (BioUltra), glutaraldehyde solution (50% in water), PVA ($\geq$ 99%, average molecular weight (MW) 89,000 – 98,000) and tris(hydroxymethyl)aminomethan were purchased from Sigma Aldrich (Steinheim, Germany). All solutions were prepared using ultrapure water (18 MΩ cm at 25 °C, SG Ultra Clear UV from Siemens Water Technologies, Günzburg, Germany). SDS-MW gel buffer was obtained from AB Sciex (Darmstadt, Germany). From the National Institute of Standard & Technologies (NIST, Gaithersburg, MD, USA) the NIST mAb (Reference Material 8671) was obtained and sample solution of stressed mAb 1 (40 °C for 8 weeks, deglycosylated) was provided by F. Hoffmann-La Roche (Basel, Switzerland).

Sample preparation

Reduction of NIST mAb for HPLC-MS parameter optimization was performed with 1 M DTT at 70 °C for 10 min in presence of 8 M urea to assure stable and full reduction and denaturation of the LC and heavy chain (HC) [23]. For CE(SDS)-CZE-MS analysis, a part of NIST mAb was stressed at 40 °C for 10 weeks. Reduction of stressed and unstressed NIST mAb and stressed mAb 1 for CE(SDS)-CZE-MS measurements was carried out with 1 M DTT at 70 °C for 10 min. After reduction, samples were centrifuged for 90 s at 14,100 g. For injection via valve experiments (no separation in ^{1}D), reduced NIST mAb was diluted in SDS-MW gel buffer to obtain a final concentration of 1 mg/mL. For the CE(SDS)-CZE-MS measurements, reduced NIST mAb was diluted to a final concentration of 1 mg/mL or 0.03 mg/mL, stressed NIST to 5 mg/mL and stressed mAb 1 to 15.8 mg/mL with SDS solution.

Method development of fragmentation parameters (HPLC-MS)
All MS experiments were performed on an Orbitrap Fusion Lumos Tribrid mass spectrometer (Thermo Fisher Scientific, San Jose, CA, USA) with an Ultimate 3000 HPLC instrument (Thermo Fisher Scientific, San Jose, CA, USA). MS^2 fragmentation parameters were optimized by HPLC-MS measuring the reduced LC of the NIST mAb. All MS^2 spectra were acquired in positive ion mode with a spray voltage set to 3,500 V and an ion transfer tube temperature of 300 °C. For the MS^1 survey scan, Orbitrap scan range was 700 – 2,500 m/z at a resolution of 7,500. Maximum injection time was set to 150 ms with an Automatic Gain Control (AGC) target at 1 x 10^6 and 3 μscans. For the MS^2 experiments, Orbitrap scan range was 150 – 2,000 m/z at a resolution of 120,000 with a maximum injection time of 200 ms and 7 μscans. Each utilized fragmentation technique, here electron transfer dissociation (ETD), higher-energy collisional dissociation (HCD) and ultraviolet photodissociation (UVPD), was optimized separately. For each fragmentation technique, different precursor ions and fragmentation parameters were tested. For the final HPLC-MS method, HCD, ETD and UVPD were combined with optimized parameters. Detailed information of the method development and parameters as well as chromatographic conditions can be found in the supporting information (SI).

Set-up of CE(SDS)-CZE-MS system
For the here presented top-down analysis of CE(SDS)-separated mAb-fragments, our recently presented 8-port nanoliter valve and its optimized method was adapted [9]. In brief, it is a polyether ether ketone 8-port nanoliter valve, that was custom made by VICI AG International (Schenkon, Switzerland). Capillaries are connected to the ports on the stator via 360 μm fittings and placed in two HP^{3D}CE Agilent Technologies CE instruments (Waldbronn, Germany), utilizing the inlet for the separation dimensions (voltage and pressure application) and the outlet for the decomplexation zone dimensions (only pressure application) (see Figure 4.15). Two ports are connected via 20 nL loops on the rotor made of polytetrafluoroethylene. Every sample loop can be switched to each of the four position by the multi position electric microactuator. Thus, four independent dimensions are given with the possibility to transfer 20 nL from one to another. The other two dimensions were utilized for the SDS-removal strategy for SDS-protein decomplexation by transferring successively water and CTAB into the ^{2}D, as previously described [9, 24]. Hyphenation of the 2D system with the Orbitrap was achieved by a nanoflow sheath liquid interface with a two capillary approach, that was recently reported by our group [22].

A PVA-coated capillary (40 cm, 50 μm ID) with an etched tip was used for separation. The capillary is inserted into a borosilicate emitter (5.5 cm length, 1 mm outer diameter, 30 μm tip inner diameter) from BioMedical Instruments (Zöllnitz, Germany). Sheath liquid (50% IPA + 0.5% FAc) was provided via a second capillary (150 μm inner diameter, fused silica) that was inserted into the emitter.

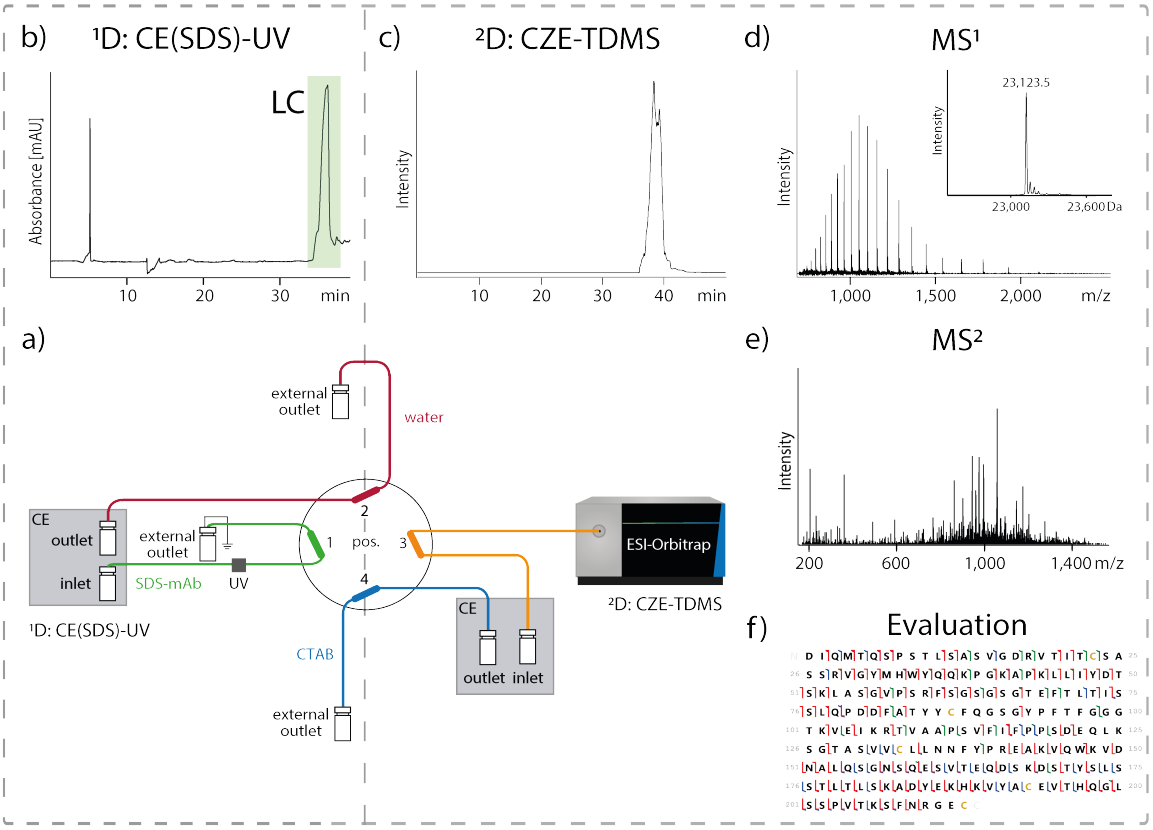

Figure 4.15: Set-up and procedure of CE(SDS)-CZE-TDMS approach. Detailed scheme of the CE(SDS)-CZE system with 8-port nanoliter valve hyphenated with the Orbitrap mass spectrometer (a). CE(SDS) analysis is performed in the first dimension (^{1}D, (a) green, position 1 and (b) CE(SDS) separation). For each decomplexation zone, consisting of water ((a) red, position 2) and the cationic surfactant cetyltrimethylammonium bromide (CTAB, (a) blue, position 4) separate ports of the valve are used and positioned between the separation dimensions. The second CZE-MS dimension (^{2}D, (a) orange, position 3 and (c) CZE-TDMS separation) is located vis-à-vis the CE(SDS) dimension. Hyphenation with the Orbitrap mass spectrometer is done via a nanoflow sheath liquid interface. For zone and sample transfer into the CZE-TDMS dimension, filled loops are switched via the multi position electric microactuator. MS^1 and MS^2 experiments are performed to obtain the mass spectra of the intact mAb-fragment (d) and fragmentation spectrum (e) for identification and fragmentation coverage determination (f).

Preconditioning of CE(SDS)-CZE-MS system and general procedure
Capillaries of the ^{1}D CE(SDS) separation were conditioned prior to each measurement by flushing with 0.1 M NaOH, 0.1 M HCl and water at 3 bar for 3 min. For the injection via valve experiments (no separation in the ^{1}D), the capillaries of the ^{1}D were flushed with reduced NIST mAb (1 mg/mL) in SDS-MW gel buffer with 3 bar and 2 bar for 10 min each. At the same time, both decomplexation dimensions were flushed with water or CTAB solved in ethanol : water : butanol (2:2:1) for 10 min at 2 bar. Capillaries of the ^{2}D were flushed at 2 bar for 5 min with water and 25 min with 1 M HAc.
For the 2D measurements (separation over the ^{1}D), the preconditioning in the ^{1}D was followed by SDS-MW gel buffer at 3 bar and 2 bar for 30 min each and application of -15 kV for 5 min. Decomplexation zone dimensions were kept filled with air and the CZE-MS dimension flushed with water at 50 mbar until the separation in the ^{1}D was completed. Meanwhile, the separation capillary is positioned behind the SL capillary. Continuous flow of the SL was provided, to guarantee stable spray conditions and removal of water coming from the ^{2}D. After the analysis in the ^{1}D was stopped, both zone dimensions and the ^{2}D were flushed with water, CTAB and 1 M HAc at 3 bar for 2 min, respectively. After transferring the decomplexation zones by switching the valve and applying pressure (water: 35 s at 50 mbar and CTAB: 25 s at -50 mbar) into the ^{2}D, the SDS-mAb filled loop was positioned between these zones. After positioning, all capillaries except of the ^{2}D were flushed with air at 5 bar for 2 min. Meanwhile, SL capillary was pulled back and the separation capillary was positioned 0.8 mm in front of the emitter tip. Spray voltage was set between 1,300-1,800 V and separation voltage of 10 or 15 kV in the ^{2}D was applied. After completing the measurement, capillaries were flushed with air at 5 bar for 5 min at the end and starting position to prevent clogging of all dimensions.

Characterization of intact light chain in SDS-MW gel buffer
For compatibility check of the 2D decomplexation method with the new set-up and the developed top-down method, injection via valve experiments were performed. Here, the ^{1}D including the sample loop was filled with NIST mAb in SDS-MW gel buffer with a final concentration of 1 mg/mL. After transferring the decomplexation zones mAb-SDS filled loop was positioned between these zones and spray and separation voltage in the ^{2}D was applied as described before. Here, MS^{1} and MS^{2} experiments (a combination of all three fragmentation techniques) were performed, as described before.

Characterization of intact CE(SDS)-separated light chain
2D analysis of the LC of the reduced NIST mAb at 1 mg/mL and 0.03 mg/mL were performed, to evaluate the performance of the CE(SDS)-CZE-MS set-up. Reduced NIST

mAb was injected electrokinetically at −15 kV for 60 s in the ^{1}D and separated by applying −15 kV. The migration time and the effective length of the capillary were used to calculate the migration velocity. With the migration velocity and the known distance from the UV detector to the middle of the sample loop in the valve, the stop time for the CE(SDS) peak to arrive in the sample loop was determined. As soon as the stop time was reached, the separation voltage was set to 0 kV and the zone dimensions and ^{2}D were flushed as described before. After transferring the decomplexation zones and the CE(SDS)-separated LC of the reduced NIST mAb into the ^{2}D, capillaries of the zone dimensions and ^{1}D were flushed with air and spray and separation voltage were applied as mentioned before. MS^1 and MS^2 analysis were performed for the NIST LC (n = 3) for both concentration levels (precursor ions stated in Table 5 in SI).

Characterization of unknown degradation product of NIST mAb and mAb 1

For identification and characterization of the unknown mAb-fragments of the reduced and stressed NIST mAb and mAb 1, pre-injection of a water plug was applied to perform sample stacking and increase sensitivity [25]. Therefore, different volumes of water plugs in a CE(SDS)-UV approach were tested (data not shown). Highest intensity was found for the pre-injection of a water plug at 2 bar for 7 s. This result was implemented in the 2D approach, followed by −15 kV for 30 s sample injection in the CE(SDS) dimension. After separation of the stressed antibodies in the CE(SDS) dimension, unknown mAb-fragments were transferred into the ^{2}D and analyzed as described before. For both mAb-fragments, first MS^1 experiments were performed to obtain the intact mass of the mAb-fragments and m/z values for MS^2 precursor selection. Precursor selection for MS^2 analysis of stressed NIST mAb-fragment with the mass of 16,807.5 Da and mAb 1, can be found in Table 5 in the SI.

Data analysis

MS^1 data were analyzed using Freestyle 1.5 (Thermo Fisher Scientifc, San Jose, CA, USA) and deconvolution was performed with PMI Intact Mass v3.4 (Protein Metrics, Cupertino, CA, USA). Extracted ion electropherograms were created by summing up the intensities of the eight most abundant charge states for mAb LC and mAb-fragments and smoothed with the moving mean algorithm (7 data points) in Freestyle. High resolution averaged MS^2 data were deconvoluted with Xtract algorithm embedded in Freestyle. Assignment of the MS^2 fragments to mAb sequence was performed with PMI Byonic v3.8.13 (Protein Metrics, Cupertino, CA, USA) using primary sequences published for the NIST mAb [26] and mAb 1 sequence provided by F. Hoffmann-La Roche (Basel, Switzerland). Fragment maps were created using ProSight Lite v1.4 (Northwestern University, Evanston, IL, USA) with a fragment ion tolerance of 15 ppm.

4.3.4 Results and discussion

Method development of fragmentation parameters (HPLC-MS)
For the fragmentation of the LC of the reduced NIST mAb, ETD, HCD and UVPD techniques were evaluated by HPLC-MS. Best fragmentation coverage was found for ETD for the precursor ion 926.0 m/z (z = 25) with 20 ms reaction time, an AGC target of 5 x 10^5 and a reagent target of 5 x 10^5. For HCD, 964.6 m/z (z = 24) was selected with an AGC target at 1 x 10^6 and collision energy of 15%. UVPD was carried out selecting the precursor 1,006.5 m/z (z = 23) with an AGC target of 5 x 10^5 and 20 ms activation time. A detailed description of optimized parameters can be found in the material and methods and in the SI. These parameters were combined with an additional survey scan to the final MS^2 method resulting in an averaged fragmentation coverage of 55 ± 3% (n = 3) for the NIST mAb LC.

Characterization of intact light chain in SDS-MW gel buffer
After method development by HPLC-MS with good fragmentation coverages for the NIST mAb LC, the CE(SDS)-CZE-TDMS system was hyphenated to the Orbitrap mass spectrometer via a nanoflow sheath liquid interface. First experiments with injection via valve (no separation over the first CE(SDS) dimension) were performed, to identify system compatibility independent from the transfer precision of the peak of interest from the first CE(SDS) dimension into the second CZE dimension. MS^1 and MS^2 experiments from the reduced LC of the NIST mAb diluted in SDS-MW gel buffer were performed (n = 3). The implemented SDS-removal strategy in the ^{2}D enabled characterization of the SDS-containing LC transferred from the ^{1}D. MS^1 measurements revealed method compatibility for the LC (data not shown). For MS^2 measurements, an averaged fragmentation coverage of 64 ± 7% (n = 3) was achieved, resulting in a higher coverage than obtained by HPLC-MS^2 (55% ± 3%), while only 1% of sample amount is needed for analysis. This impressively demonstrates the high mass sensitivity of CZE-MS applying the nanoflow sheath liquid interface and the general MS^2 method compatibility with our 2D set-up.

Characterization of intact CE(SDS)-separated light chain
The general set-up and procedure of our CE(SDS)-CZE-TDMS approach is shown in Figure 4.15. MS^1 and MS^2 experiments (n = 3) of the CE(SDS)-separated LC of the reduced NIST mAb were performed at a concentration of 1 mg/mL and 0.03 mg/mL to evaluate signal intensity and fragmentation coverage. Deconvolution of MS^1 spectra resulted in the averaged intact mass 23,126.64 ± 0.47 Da (n = 3) for the 1 mg/mL sample. This obtained mass is in accordance with the masses found by HPLC-MS measurements, injection via valve experiments and literature [8, 27]. For 0.03 mg/mL, an averaged intact mass of 23,123.18 ± 0.24 Da (n = 3) was determined. Mass spectra of the NIST mAb LC at

0.03 mg/mL showed a different charge state distribution, shifted to lower z-values compared to the 1 mg/mL sample. Also, intact mass determination revealed a mass difference of 3.5 Da in the 0.03 mg/mL dilution compared to masses observed in the 1 mg/mL sample. Averaged fragmentation coverage of the LC by CE(SDS)-CZE-MS^2 experiments was 58 ± 10% (n = 3) for 1 mg/mL and 13 ± 9% (n = 4) for 0.03 mg/mL reduced NIST mAb (see Figure 4.16), respectively.

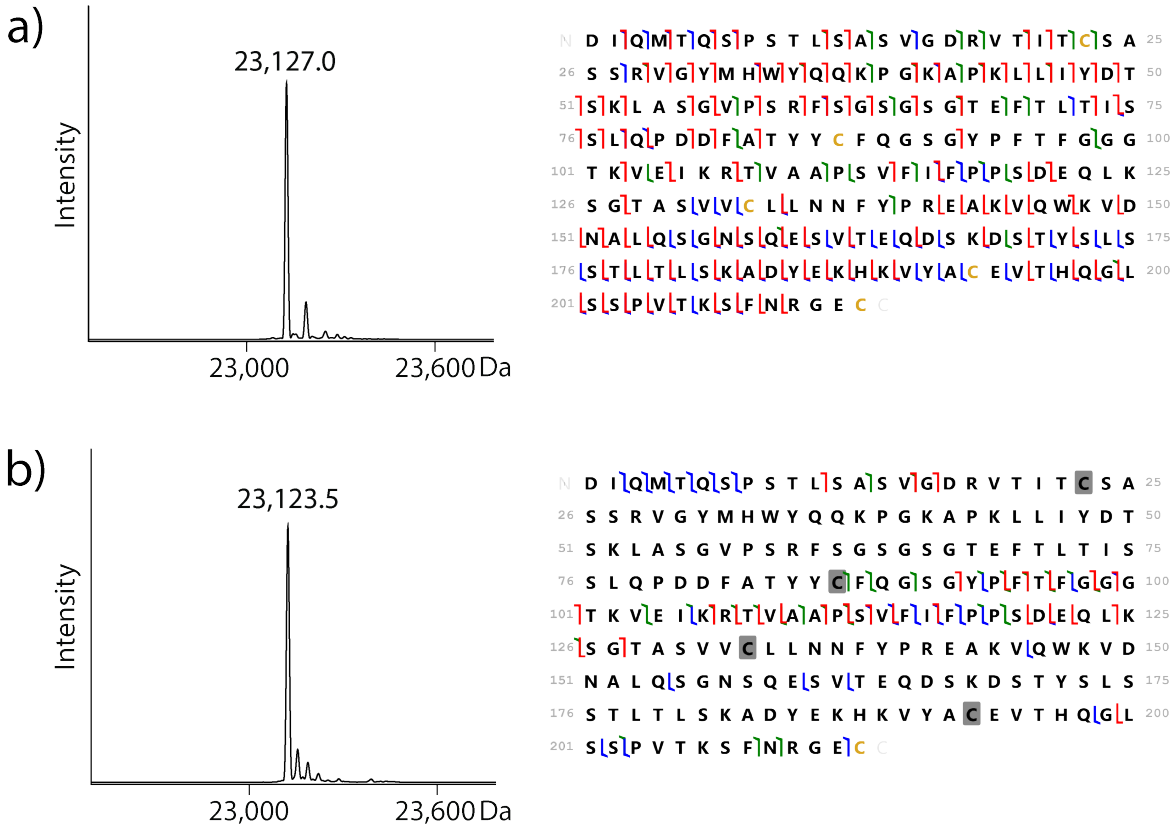

Figure 4.16: MS^1 and MS^2 analysis of NIST LC. 1 mg/mL (a) and 0.03 mg/mL (b) of NIST LC were analyzed with MS^1 experiments to obtain the intact mass and MS^2 experiments for top-down analysis. For the 1 mg/mL sample, the averaged intact mass of the LC with reduced disulfide bonds and fragmentation coverages of 58 ± 10% (n = 3) were obtained. For the 0.03 mg/mL sample, the averaged intact mass of the LC with (partly) intact intra-disulfide bonds and fragmentation coverage of 13 ± 9% (n = 3) was obtained.

Here, significantly lower fragmentation coverages are obtained by top-down measurements for the LC in the 0.03 mg/mL dilution. Only few fragments were observed, all of them on the N-terminal and C-terminal ends and between the cysteines that are not natively connected by disulfide bonds. Intact mass, fragmentation coverage and p-values clearly indicate the presence of intra-molecular disulfide bonds (see Figure 4.16 b). These intra-molecular disulfide bonds might be due to either incomplete reduction or reformation of

one or two disulfide-bonds in the LC [28]. In fact, these species with -2 and -4 Da were also observed as minor forms besides the main form of fully reduced LC in the 1 mg/mL dilution. Since the same reduction protocol was used for all concentrations, this phenomena is likely to be connected to the concentration of the mAb. Selective adsorption or sample loss of fully reduced LC as well as an incomplete reduction or reformation of disulfide bonds when using lower mAb concentrations is possible. In a previous study, the same antibody was analyzed in the same concentrations on a quadrupole time-of-flight (Q-TOF) instrument with comparable spectral quality and deconvolution precision [8]. In this study however, intact masses after deconvolution were the same for both concentrations and the effect of partial reduction at lower sample concentrations was not observed. It is not the scope of this study to reveal the potential reasons behind this phenomenon, however, the fact that identification and localization of disulfide bonds is possible, shows the potential of the here presented platform. Averaged fragmentation coverage obtained with the 2D separations (separation in the ^{1}D) of the NIST mAb LC 1 mg/mL are comparable to the fragmentation coverage resulted from injection-via-valve experiments. This demonstrates the compatibility of the 2D system and the good transfer precision of the CE(SDS)-separated peak of interest from the ^{1}D (first CE(SDS) dimension) into the ^{2}D (second CZE dimension).

Characterization of unknown degradation products of NIST mAb and mAb 1

An unknown peak ($\leq$ 1% of total UV-peak area) of temperature stressed NIST mAb, migrating before the LC, was analyzed with our 2D system (see Figure 4.17 a). MS^1 spectra obtained for this CE(SDS) peak revealed several masses (see Figure 4.17 b). The most prominent peak with the averaged mass of 16,807.5 Da was chosen for MS^2 experiments. Thereby, this mass could be assigned to the C-terminal fragment crystallizable (Fc) part (amino acids 301 - 449) of the HC with an additional C-terminal loss of lysine. Fc fragmentation and C-terminal lysine cleavage are commonly observed for mAbs [29, 30]. An averaged fragmentation coverage of 22 $\pm$ 5% (n = 3) was achieved (Figure 4.17 c). A fragmentation mechanism is proposed in Figure 4.17 d, as reported previously [31, 32]. Additionally, fragments that were observed in MS^1 experiments were assigned (on MS^1 level only) to the same Fc part by additional N-terminal losses of amino acids. The mAb-fragment with the averaged intact mass of 14,694.6 Da with Δm = 2,112.9 Da compared to the 16,807.5 Da mAb-fragment corresponds to the N-terminal loss of the amino acids STYRVVSVLTVLHQDWLN. The 13,577.0 Da mAb-fragment with Δm = 1,117.6 Da compared to 14,694.6 Da correlates with an additional N-terminal loss of the amino acids GKEYKCKVSN.

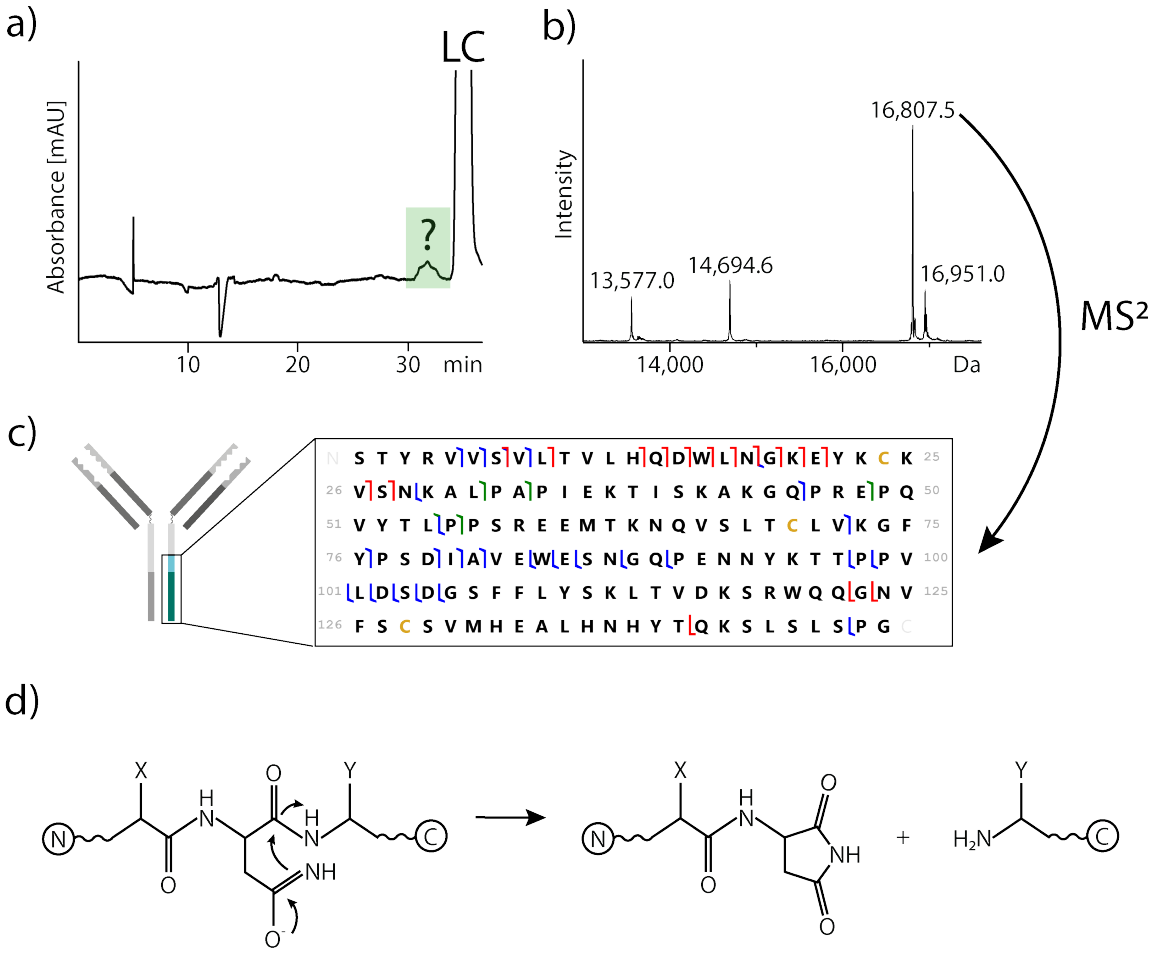

Figure 4.17: CE(SDS)-CZE-TDMS analysis of a stressed (8 weeks at 40 °C) and reduced NIST mAb-fragment. After CE(SDS) separation (a) underlying masses of the highlighted CE(SDS) peak were obtained by MS^1 experiments (b). The peak with the averaged mass of 16,807.5 Da was further analyzed by MS^2 and could be assigned to the C-terminal Fc part of the HC (c) with a fragmentation coverage of 22 ± 5%. The suggested cleaving mechanism [31, 32] is shown in (d).

A CE(SDS) peak (∼ 1.5% of total peak area), migrating before the LC of the temperature stressed mAb 1, was analyzed as well. MS^1 measurements revealed that two mAb-fragments were co-migrating in the first CE(SDS) dimension with intact masses of 13,019.5 Da and 13,089.0 Da. This was in accordance with related Q-TOF measurements (data not shown). The 13,089.0 Da mAb-fragment was further analyzed via top-down measurements (see Figure 4.18 a). It could be assigned to the C-terminal Fc fragment (amino acids 335 - 451) of the HC caused by β-elimination of serine 1 with subsequent hydrolytic cleavage of the protein (see Figure 4.18 b) [31]. A fragmentation coverage of 47 ± 10% (n = 3) was achieved. By the mass difference of $\Delta m = 70$ Da, the second peak (13,019.5 Da) was identified as the same Fc fragment with additional N-terminal loss of serine 2 by the same mechanism.

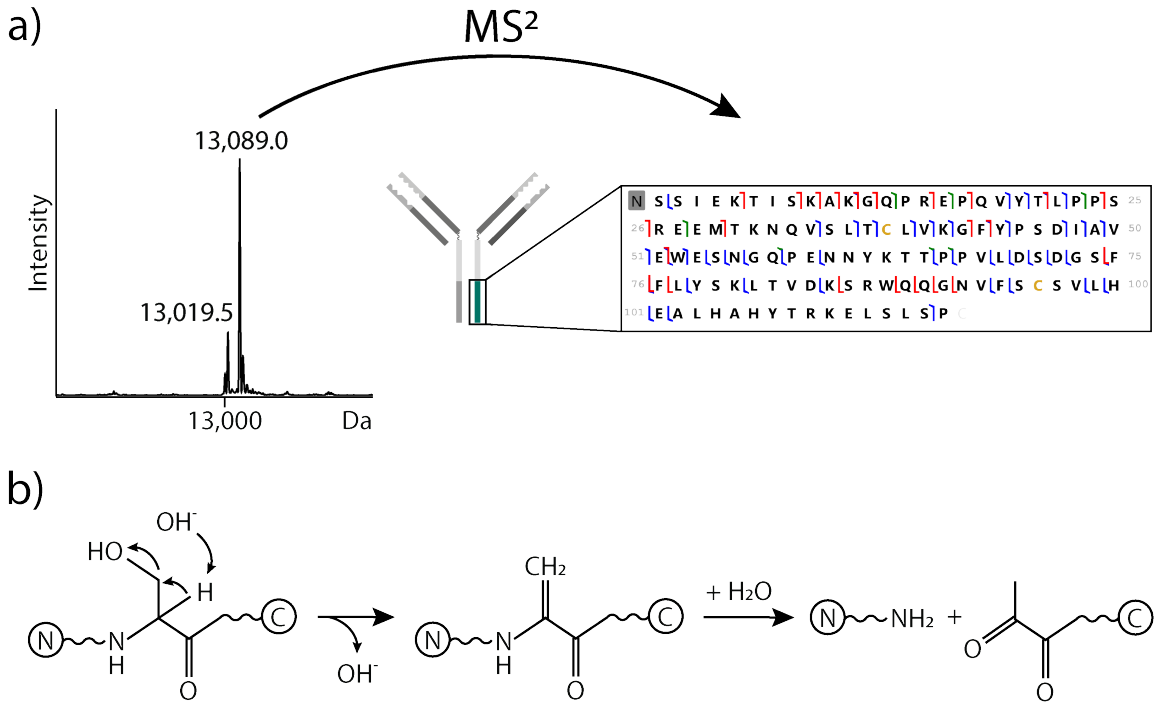

Figure 4.18: CE(SDS)-CZE-TDMS analysis of a reduced fragment of stressed mAb 1 (10 weeks at 40 °C). Masses were obtained by MS^1 experiments. The peak with the averaged mass of 13,089.0 Da was further analyzed by MS^2 experiments (n = 3) (a). It could be assigned to the C-terminal Fc part of the HC with the suggested cleaving mechanism [31](b). An averaged fragmentation coverage of 47 ± 10% (n = 3) was obtained.

The obtained results show the high value of TDMS data in combination with intact mass information. Intact mass information alone often only allows an unproven assumption of mAb-fragments or other modifications like PTMs. The high fragmentation coverage of our top-down data by combining HCD, ETD and UVPD enable a sophisticated confirmation of these assumptions and enable a comprehensive identification of single CE(SDS) peaks.

4.3.5 Conclusion

We have developed a sophisticated CE(SDS)-CZE-TDMS platform for the online identification and in-depth characterization of CE(SDS)-separated proteins. The platform allows characterization of low abundant CE(SDS)-peaks as demonstrated by both, dilution experiments of LC and the unequivocal identification of unknown fragments of two mAbs. These minor mAb-fragments were only present in the range of $\leq$ 1% total peak area, demonstrating the characterization possibilities in biopharmaceutical relevant concentrations. The conjunction of intact mass determination with combined HCD, ETD and UVPD MS^2 spectra proved its high potential for peak identification. Especially in case of small changes in intact mass such as deamidation and disulfide bonds, the obtained MS^1 does often not

unambiguously reveal these modifications. The identification and characterization of not fully reduced LC species impressively underlines the verification capabilities of the platform. Our system allows, for the first time, the online identification and characterization of unknown peaks in CE(SDS) in great detail. This helps to reduce induced artifacts, while minimizing the sample amount for a single analysis and unambiguity in assignment of identified mAb-fragments to the CE(SDS) analysis. The platform can help to support CE(SDS) routine analysis in quality control and process development to confidently identify and characterize various mAb-fragments, proteoforms and in general proteins in the low/middle mass range.

CRediT authorship contribution statement

Jennifer Römer: Conceptualization, Investigation, Writing - Original Draft, Visualization; Alexander Stolz: Conceptualization, Investigation, Writing - Original Draft, Visualization; Bernd Moritz: Funding acquisition, Writing - Review & Editing; Steffen Kiessig: Funding acquisition, Writing - Review & Editing; Christian Neusüß: Conceptualization, Supervision, Writing - Review & Editing

Acknowledgments

The authors would like to thank Oliver Höcker and Johannes Schlecht for their preliminary work on the nanoflow-sheath liquid interface.

Declaration of Competing Interest

The authors declare that they have no known competing financial interests or personal relationships that could have appeared to influence the work reported in this paper.

Funding

This work was kindly supported by F. Hoffmann-La Roche Ltd and the German Federal Ministry of Education and Research [grant numbers 13FH140IN6, 16PGF0346].

4.3.6 Supporting information for Online top-down mass spectrometric identification of CE(SDS)-separated antibody fragments by two-dimensional capillary electrophoresis

Optimization of Fragmentation Parameters

For top-down analysis of mAb-fragments, the MS^2 method was optimized via HPLC-MS of the LC from the reduced NIST mAb. Here, an UltiMate 3000 (Thermo Fisher Dionex, San Jose, CA, USA) equipped with a MAbPac RP guard column (2.1 x 10 mm; 4 μm particles, Thermo Fisher Scientific, San Jose, CA, USA) and a MAbPac RP separation column (1 x 100 mm; 4 μm particles, Thermo Fisher Scientific, San Jose, CA, USA) was utilized. Injection volume was 2 μL and column oven was set at 80 °C. A binary gradient was applied, where solvents A was water with the addition of FAc (99.9 : 0.1, v/v) and solvent B was acetonitrile with water and FAc (90.0 : 9.9 : 0.1, v/v/v). The separation gradient consisted of linear ramps at 150 μL/min from 5.5 to 22% B in 1 min, keeping 22% for 0.5 min, followed by 22 to 44% B in 8.5 min and 44% to 100% in 1 min. This gradient was followed by keeping 100% B for 2 min, a linear gradient from 100% to 5% in 0.5 min and final 5.5% B for 2.5 min.

For each fragmentation technique, AGC (automatic gain control) target and precursor optimization was performed (n = 3). AGC targets for HCD, ETD and UVPD were set at 2×10^5, 5 x 10^5 and 1 x 10^5 for the same precursor, here 1,006.5 m/z (n = 3).

For the comparison of precursor ion fragmentation with HCD, different precursors were tested (see Table 4) while keeping the AGC target constant at 1×10^6. Additionally, four different collision energies (12 ± 5, 10, 15 and 17%) were evaluated at constant AGC target (2 x 10^5) and precursor (1,006.5 m/z).

Besides the AGC target of the precursor, the AGC target for the ETD reagent was tested at four different levels (2×10^5, 5 x 10^5, 7×10^5 and 1 x 10^6), while keeping the reaction time (20 ms), the precursor (964.6 m/z) and its AGC target constant (5 x 10^5). Different precursors were evaluated (see Table 4), while keeping its AGC target (5 x 10^5), the reaction time (20 ms) and the AGC target of the ETD reagent (5×10^5) constant. Additionally, the reaction time at 5, 10, 20 and 30 ms, keeping AGC target for the precursor (2 x 10^5 for 1,006.5 m/z) and for the ETD reagent (7×10^5) unchanged.

For UVPD, reaction times were set at 5, 10, 15, 20, 30, 50 ms, while utilizing the precursor 1,006.5 m/z and its AGC target at 1 x 10^6. Additionally, three different precursors were selected (see Table 4), keeping AGC target (1 x 10^6) and reaction time constant (20 ms). The final chosen fragmentation precursor ions for each analyte can be found in Table 5.

Table 4: Precursor ions chosen for fragmentation parameter optimization for each fragmentation technique

Precursor ion (m/z) for		
HCD	ETD	UVPD
964.6	926.0	964.6
1,006.5	964.6	1,006.5
1,052.2	1,006.5	1,285.8
1,102.3	1,052.2	
1,157.4	1,102.3	
1,218.2	1,157.4	
1,285.8		

Table 5: Precursor ions chosen for fragmentation depending on analysis

Analysis	Precursor ion (m/z) and charge state (z) for		
	HCD	ETD	UVPD
LC of 1 mg/mL NIST mAb	964.6 (z = 24)	926.0 (z = 25)	1,006.5 (z = 23)
LC of 0.03 mg/mL NIST mAb	1,361.2 (z = 17)	1,285.6 (z = 18)	1,361.2 (z = 17)
Unknown mAb-fragment of NIST mAb	934.8 (z = 18)	934.8 (z = 18)	934.8 (z = 18)
Unknown mAb-fragment of mAb 1	1,007.8 (z = 13) or 935.9 (z = 14)	1,007.8 (z = 13) or 873.5 (z = 15)	1,007.8 (z = 13)

References

(1) Shi, Y., Li, Z., and Lin, J. (2012). Advantages of CE-SDS over SDS-PAGE in mAb purity analysis. *Anal. Methods 4*, 1637.

(2) Sänger-van de Griend, C. E. (2019). CE-SDS method development, validation, and best practice-An overview. *Electrophoresis 40*, 2361–2374.

(3) Hawe, A., Wiggenhorn, M., van de Weert, M., Garbe, J. H. O., Mahler, H.-C., and Jiskoot, W. (2012). Forced degradation of therapeutic proteins. *J. Pharm. Sci. 101*, 895–913.

(4) Nowak, C., K Cheung, J., M Dellatore, S., Katiyar, A., Bhat, R., Sun, J., Ponniah, G., Neill, A., Mason, B., Beck, A., and Liu, H. (2017). Forced degradation of recombinant monoclonal antibodies: A practical guide. *mAbs 9*, 1217–1230.

(5) Kubota, K., Kobayashi, N., Yabuta, M., Ohara, M., Naito, T., Kubo, T., and Otsuka, K. (2017). Identification and characterization of a thermally cleaved fragment of monoclonal antibody-A detected by sodium dodecyl sulfate-capillary gel electrophoresis. *J. Pharm. Biomed. Anal. 140*, 98–104.

(6) Wang, W.-H., Cheung-Lau, J., Chen, Y., Lewis, M., and Tang, Q. M. (2019). Specific and high-resolution identification of monoclonal antibody fragments detected by capillary electrophoresis-sodium dodecyl sulfate using reversed-phase HPLC with top-down mass spectrometry analysis. *mAbs 11*, 1233–1244.

(7) Lu, J. J., Zhu, Z., Wang, W., and Liu, S. (2011). Coupling sodium dodecyl sulfate-capillary polyacrylamide gel electrophoresis with matrix-assisted laser desorption ionization time-of-flight mass spectrometry via a poly(tetrafluoroethylene) membrane. *Anal. Chem. 83*, 1784–1790.

(8) Römer, J., Montealegre, C., Schlecht, J., Kiessig, S., Moritz, B., and Neusüß, C. (2019). Online mass spectrometry of CE (SDS)-separated proteins by two-dimensional capillary electrophoresis. *Anal. Bioanal. Chem. 411*, 7197–7206.

(9) Römer, J., Kiessig, S., Moritz, B., and Neusüß, C. (2020). Improved CE(SDS)-CZE-MS method utilizing an 8-port nanoliter valve. *Electrophoresis 42*, 374–380.

(10) Krokhin, O. V., Antonovici, M., Ens, W., Wilkins, J. A., and Standing, K. G. (2006). Deamidation of -Asn-Gly- sequences during sample preparation for proteomics: Consequences for MALDI and HPLC-MALDI analysis. *Anal. Chem. 78*, 6645–6650.

(11) Hao, P., Ren, Y., Alpert, A. J., and Sze, S. K. (2011). Detection, evaluation and minimization of nonenzymatic deamidation in proteomic sample preparation. *Mol. Cell. Proteomics 10*, O111.009381.

(12) Thornalley, P. J., and Rabbani, N. (2014). Detection of oxidized and glycated proteins in clinical samples using mass spectrometry–a user's perspective. *Biochim. Biophys. Acta 1840*, 818–829.

(13) Schaffer, L. V. et al. (2019). Identification and Quantification of Proteoforms by Mass Spectrometry. *Proteomics 19*, e1800361.

(14) Siuti, N., and Kelleher, N. L. (2007). Decoding protein modifications using top-down mass spectrometry. *Nat. Methods 4*, 817–821.

(15) Macht, M. (2013). Top-down characterization of biopharmaceuticals. *TrAC 48*, 62–71.

(16) Zhang, H., Cui, W., and Gross, M. L. (2014). Mass spectrometry for the biophysical characterization of therapeutic monoclonal antibodies. *FEBS Lett. 588*, 308–317.

(17) Srzentić, K. et al. (2020). Interlaboratory Study for Characterizing Monoclonal Antibodies by Top-Down and Middle-Down Mass Spectrometry. *J. Am. Soc. Mass Spectrom. 31*, 1783–1802.

(18) Shen, X., Yang, Z., McCool, E. N., Lubeckyj, R. A., Chen, D., and Sun, L. (2019). Capillary zone electrophoresis-mass spectrometry for top-down proteomics. *TrAC 120*, DOI: 10.1016/j.trac.2019.115644.

(19) Lubeckyj, R. A., McCool, E. N., Shen, X., Kou, Q., Liu, X., and Sun, L. (2017). Single-Shot Top-Down Proteomics with Capillary Zone Electrophoresis-Electrospray Ionization-Tandem Mass Spectrometry for Identification of Nearly 600 Escherichia coli Proteoforms. *Anal. Chem. 89*, 12059–12067.

(20) Biacchi, M., Said, N., Beck, A., Leize-Wagner, E., and François, Y.-N. (2017). Top-down and middle-down approach by fraction collection enrichment using off-line capillary electrophoresis - mass spectrometry coupling: Application to monoclonal antibody Fc/2 charge variants. *J. Chromatogr., A 1498*, 120–127.

(21) Bush, D. R., Zang, L., Belov, A. M., Ivanov, A. R., and Karger, B. L. (2016). High Resolution CZE-MS Quantitative Characterization of Intact Biopharmaceutical Proteins: Proteoforms of Interferon-beta1. *Anal. Chem. 88*, 1138–1146.

(22) Höcker, O., Knierman, M., Meixner, J., and Neusüß, C. (2020). Two capillary approach for a multifunctional nanoflow sheath liquid interface for capillary electrophoresis-mass spectrometry. *Electrophoresis*, DOI: 10.1002/elps.202000169.

(23) Scheffler, K., and Damoc, E. Antibody subunit analysis workflow on a quadrupole-Orbitrap mass spectrometer: from optimized sample preparation to data analysis: Application note 72854, ed. by Thermo Fisher Scientific.

(24) Sanchez-Hernandez, L., Montealegre, C., Kiessig, S., Moritz, B., and Neusüß, C. (2016). In-capillary approach to eliminate SDS interferences in antibody analysis by capillary electrophoresis coupled to mass spectrometry. *Electrophoresis 38*, 1044–1052.

(25) Zhang, C.-X., and Meagher, M. M. (2017). Sample Stacking Provides Three Orders of Magnitude Sensitivity Enhancement in SDS Capillary Gel Electrophoresis of Adeno-Associated Virus Capsid Proteins. *Anal. Chem. 89*, 3285–3292.

(26) Tarlov, M. J., and Choquett, S. J. Report of Investigation Reference Material 8671: NISTmAb, Humanized IgG1k Monoclonal Antibody: Lot No. 14HB-D-002 ed. by National Institute of Standards & Technology, `https://www-s.nist.gov/srmors/certificates/8671.pdf`.

(27) Formolo, T., Ly, M., Levy, M., Kilpatrick, L., Lute, S., Phinney, K., Marzilli, L., Brorson, K., Boyne, M., Davis, D., and Schiel, J. In *State-of-the-Art and Emerging Technologies for Therapeutic Monoclonal Antibody Characterization Volume 2. Biopharmaceutical Characterization: The NISTmAb Case Study*, Schiel, J. E., Davis, D. L., and Borisov, O. V., Eds.; ACS Symposium Series, Vol. 1201; American Chemical Society: Washington, DC, 2015, pp 1–62.

(28) Wu, S., Shen, M., Murphy, S., and van den Heuvel, Z. An Integrated Workflow for Intact and Subunits of Monoclonal Antibody Accurate Mass Measurements: Application Note: Biotherapeutics and Biosimilars, USA.

(29) Gao, S. X., Zhang, Y., Stansberry-Perkins, K., Buko, A., Bai, S., Nguyen, V., and Brader, M. L. (2011). Fragmentation of a highly purified monoclonal antibody attributed to residual CHO cell protease activity. *Biotechnol. Bioeng. 108*, 977–982.

(30) Liu, H., Ponniah, G., Zhang, H.-M., Nowak, C., Neill, A., Gonzalez-Lopez, N., Patel, R., Cheng, G., Kita, A. Z., and Andrien, B. (2014). In vitro and in vivo modifications of recombinant and human IgG antibodies. *mAbs 6*, 1145–1154.

(31) Vlasak, J., and Ionescu, R. (2011). Fragmentation of monoclonal antibodies. *mAbs 3*, 253–263.

(32) Patel, K., and Borchardt, R. T. (1990). Chemical pathways of peptide degradation. III. Effect of primary sequence on the pathways of deamidation of asparaginyl residues in hexapeptides. *Pharm. Res. 7*, 787–793.

5 Summary

Size-based protein separation by CE(SDS) is indispensable for process and quality control in the biopharmaceutical industry and is commonly applied for purity assessment on behalf of drug approval. To overcome the challenge of uncertain peak identification of CE(SDS)-separated fragments and impurities, here, the first online hyphenation with mass spectrometry is presented. This hyphenation is achieved by introducing a second electrophoretic, MS-compatible CZE dimension after the first generic CE(SDS) separation. Both dimensions are hyphenated via a 4-port nanoliter valve that is commercially available from VICI AG International. As soon as the peak of interest of the CE(SDS) separation reaches the sample loop, the separation is stopped. Due to the very stable SDS-protein complex that can not be separated electrophoretically in the CZE dimension alone, a decomplexation with a solvent and a cationic surfactant is required. Therefore, simultaneously to the separation in the ^{1}D, methanol as presample and CTAB (solved in methanol : water (1:1)) as postsample zone are injected and positioned via a C^{4}D detector in the second CZE dimension. The peak of interest is then transferred via a heart-cut approach between the decomplexation zones in the ^{2}D. With this set-up, it was possible to demonstrate the proof of principle. The LOD was determined by measuring the LC of the NIST mAb at different concentrations, revealing the possibility of intact mass determination at biopharmaceutical relevant concentrations. Universal application of the mass spectrometric CE(SDS) protein characterization is presented by soybean protein analysis. By analyzing several mAb fragments, the suitability and power of the 2D system for pertinent biopharmaceutical questions are proven. The intact mass determination facilitate identification of these fragments directly from generic CE(SDS) separation for the first time. In addition, the analysis allows a deeper insight, revealing migration order shifts and detection of several fragments, migrating simultaneously in the CE(SDS) dimension. Detection of these proteoforms resulting from only one CE(SDS) peak demonstrates the necessity of a more detailed investigation that can only be achieved by mass spectrometry hyphenation.

One major drawback of this 4-port nanoliter valve approach is the system and measurement instability due to frequently occurring current leakage. This current leakage is mainly related to the utilized 4-port nanoliter valves material and design, with distances of less than 1 mm between the separation dimensions. Additionally, the exact positioning of the CE(SDS) peak from the ^{1}D in between the decomplexation zones in the ^{2}D is crucial for successful decomplexation and directly related to MS signal intensity. So far, good timing and experience were the only possibilities to minimize imprecise positioning and reduce the error rate. For these main reasons, further development of the nanoliter valve and method adaptation was the primary aim of the second part of this work to improve system and

measurement stability. Therefore, an 8-port nanoliter valve was developed and designed. Realization and manufacturing were performed in collaboration with VICI AG International. Here, the distances between the separation dimensions are increased to 3.14 mm (for 20 nL sample loops), rotors made of different materials and two additional dimensions are added to allow independent and successively decomplexation zone transfer into the ^{2}D. While determining the decomplexation zones' right transfer volume, additional solvents were tested as presample and postsample zones. The developed decomplexation strategy itself and its implementation in the 2D approach was tested with the new 8-port nanoliter valve set-up and compared with the 4-port nanoliter approach. Comparing the decomplexation strategies without separation over the first CE(SDS) dimension, MS-signal intensities could be improved for the LC and HC with the new approach. Regarding the complete CE(SDS)-CZE-MS measurements, around the same mass spectra signal intensities for the LC and an increase for the HC were obtained with the 8-port valve approach. Significantly, current stability in the ^{2}D could be doubled, which was a fundamental improvement for further experiments presented in the third part of this work.

To allow immediate and unambiguous identification and characterization of CE(SDS)-separated peaks, the optimized system was hyphenated with top-down mass spectrometry. For this reason, first method development and optimization for MS^1 and MS^2 experiments, utilizing HCD, ETD, and UVPD fragmentation was performed by HPLC-MS for the NIST mAb LC. Then, after successful hyphenation of the 2D system with the Orbitrap MS via nanoflow sheath liquid interface, method compatibility of the developed top-down MS method with the decomplexation strategy was tested. Therefore, reduced NIST mAb in SDS gel was directly injected via valve from the ^{1}D into the ^{2}D between the successively positioned decomplexation zones. Here, good sequence coverage was obtained by MS^2 experiments for the NIST mAb LC. After successful compatibility verification, complete 2D measurements were performed with NIST mAb LC at two different concentrations. It was possible to prove that concentration down to 0.03 mg/mL of NIST mAb LC can be analyzed by top-down MS analysis. Furthermore, the presence of intra disulfide bonds was verified by intact mass determination and MS^2 fragmentation. In the last part, the identification and characterization of stress-induced fragments of two different mAbs were performed. Both mAb fragments were identified as Fc fragments of the HC, and the cleavage mechanism could be suggested. This identification was only feasible by MS^2 top-down measurements and not possible by intact mass analysis alone, representing the value of the third part of this work.

The here presented work demonstrates the first online mass spectrometric characterization of generic CE(SDS)-separated proteins. It is shown that intact mass determination strongly supports the identification of these proteins and mAb fragments. The observation of

unexpected migration order shift and several masses of proteoforms by analyzing only one CE(SDS) peak confirm the ambiguity of optical detection alone. Top-down experiments verify the strength of direct identification of mAb fragments and PTMs like the presence of disulfide bonds, which can not be distinguished by intact mass determination alone. This direct and unambiguous identification of CE(SDS)-separated proteins provides a detailed insight. It facilitates the understanding of protein stability and fragmentation, thereby supporting the production, safety and efficacy assurance of biopharmaceuticals.

6 Zusammenfassung in deutscher Sprache

Größenabhängige Trennung von Proteinen mittels CE(SDS) ist ein wichtiger Bestandteil in der Prozess- und Qualitätskontrolle in der biopharmazeutischen Industrie. Sie dient meist der Reinheits- und Stabilitätsbestimmung und wird für die Charakterisierung von Biopharmazeutika bei der Zulassung verwendet. Um die Peakidentifikation von CE(SDS)-getrennten Fragmenten und Verunreinigungen zu ermöglichen, wird hier die erste Kopplung von CE(SDS)-Trennung mit der Massenspektrometrie präsentiert. Diese Kopplung wird durch eine zweite elektrophoretische, MS-kompatible CZE-Trenndimension ermöglicht, die zwischen der CE(SDS)-Trennung und dem Massenspektrometer geschaltet ist. Beide Trenndimensionen sind durch ein Nanoliterventil, hier ein kommerziell erhältliches 4-Wegeventil der VICI AG International, miteinander verbunden. Sobald der zu analysierende CE(SDS)-Peak die Probenschlaufe des Ventils erreicht hat, wird die Trennung gestoppt. Da der SDS-Protein-Komplex sehr stabil ist, kann er nicht durch die alleinige elektrophoretische Trennung in der CZE-Dimension aufgetrennt werden. Deshalb ist es notwendig, in der ^{2}D eine Dekomplexierungsstrategie mit einem Lösungsmittel und einem kationischen Tensid anzuwenden. Dazu wird parallel zur Trennung in der ^{1}D Methanol und CTAB in der ^{2}D injiziert und durch einen C^{4}D-Detektor positioniert. Der zu analysierende SDS-Peak wird mittels Heart-cut zwischen die positionierten Dekomplexierungszonen in der ^{2}D transferiert. Mit diesem Aufbau ist es gelungen, die Machbarkeit aufzuzeigen und eine Nachweisgrenze zu bestimmen. Die Nachweisgrenze wurde durch die Messung der leichten Kette des NIST Antikörpers bei verschiedenen Konzentrationen bestimmt, bei der sich herausstellte, dass eine Intaktmassenbestimmung in biopharmazeutisch relevanten Konzentrationen ermöglicht wird. Die universelle Anwendung der massenspektrometrischen Charakterisierung von CE(SDS)-getrennten Proteinen mit Hilfe des 2D-Systems wurde durch die Analytik von Sojabohnenproteinen verdeutlicht. Durch die Analyse von mehreren Antikörperfragmenten konnte der große Nutzen des 2D-Systems bei biopharmazeutischen Fragestellungen aufgezeigt werden. Zum ersten Mal wird durch direkter Intaktmassenbestimmung von CE(SDS)-getrennten Proteinen die Identifikation unterstützt. Dieser detailreiche Einblick in die CE(SDS)-Trennung ermöglicht die Beobachtung unerwarteter Migrationsreihenfolgen und die Migration von verschiedenen Fragmenten zur gleichen Zeit. Besonders die unzureichende Trennung von Proteofomen mittels CE(SDS) verdeutlicht die Notwendigkeit einer detaillierteren Detektion, die durch Massenspektrometrie ermöglicht wird.

Einer der größten Herausforderungen die sich bei der Verwendung des 4-Wegeventils herausstellte, das im ersten Teil dieser Arbeit verwendet wurde, ist die unzureichende System- und Messstabilität durch auftretenden Kriechstrom. Dieser Kriechstrom ist ein Resultat aus der Materialwahl und der Geometrie des kommerziell erhältlichen 4-Wegeventils, bei dem

die Distanzen zwischen den Trenndimensionen unter 1 mm betragen. Zudem trägt eine ungenaue Positionierung der CE(SDS)-getrennten Proteinen der ^{1}D inmitten der Dekomplexierungszonen in der ^{2}D zur Reduzierung der Dekomplexierungseffizienz und somit zur Abnahme der MS-Signalintensität bei. Bisher konnte nur durch gutes Timing und mit gewissen Erfahrungswerten eine unpräzise Positionierung und somit die Fehlerquote minimiert werden. Aus diesen Gründen wurde in dem zweiten Teil dieser Arbeit die Weiterentwicklung des Nanoliterwegeventils und die entsprechende Methodenanpassung verfolgt, um die System- und Messstabilität zu verbessern. Dafür wurde ein 8-Wegenanoliterventil entwickelt und entworfen. Die Umsetzung und Herstellung wurde in Zusammenarbeit mit VICI AG International realisiert. Bei diesem Ventil sind die Abstände zwischen den Trenndimensionen auf 3,14 mm (für die 20 nL Probeschleifen) erhöht. Zudem wurden Rotoren aus verschiedenen Materialien angefertigt und zwei zusätzliche Dimensionen hinzugefügt, um einen unabhängigen und schrittweisen Transfer der Dekomplexierungszonen in die ^{2}D zu ermöglichen. Während der Bestimmung der richtigen Transfervolumen wurden zusätzlich verschiedene Lösungsmittel als Dekomplexierungszonen getestet. Die optimierte Dekomplexierungsstrategie an sich und unter Einbindung in den 2D-Ansatz wurde mit dem 8-Wegeventil getestet und mit dem 4-Wegeventilansatz verglichen. Bei dem alleinigen Betrachten der Dekomplexierungsstrategie mit dem entwickelten 8-Wegeventil, ohne Trennung in der ersten CE(SDS)-Dimension, konnte die MS-Signalintensität für die leichte und schwere Kette des NIST Antikörpers verbessert werden. Bezüglich der gesamten CE(SDS)-CZE-MS-Trennung wurden vergleichbare MS-Signalintensitäten für die leichte Kette und eine Verbesserung bei der schweren Kette mit dem 8-Wegeventil erzielt. Insbesondere konnte die Stromstabilität in der ^{2}D verdoppelt werden. Dies stellt eine fundamentale Verbesserung und die Grundlage für die weiteren Experimente im dritten Teil dieser Arbeit dar.
Um eine direkte und eindeutige Identifizierung und Charakterisierung der CE(SDS)-getrennten Proteine zu ermöglichen, wurde das optimierte Systems mit Top-down-Massenspektrometrie gekoppelt. Dafür wurde zuerst die Methodenentwicklung und -optimierung der MS^{1}- und MS^{2}-Methoden, mittels HCD-, ETD- und UVPD-Fragmentierung, durch HPLC-MS-Messungen der leichten Kette des NIST-Antikörpers durchgeführt. Nach der Methodenentwicklung und erfolgreicher Kopplung des 2D-Systems mit dem Orbitrap-MS durch ein nanoflow-sheath-liquid Interface, wurde die Methodenkompatibilität der entwickelten Top-down-Methode und der Dekomplexierungsstrategie getestet. Dazu wurde der reduzierte NIST-Antikörper mit SDS-Gel verdünnt und direkt über die Probenschleife von der ^{1}D in die ^{2}D, in mitten der davor positionierten Dekomplexierungszonen, injiziert. Hierbei wurde eine gute Sequenzabdeckung durch MS^{2}-Messungen für die leichte Kette des NIST-Antikörpers in zwei Konzentrationen erzielt. Es war möglich die leichte Kette des NIST-Antikörpers bei einer Probenkonzentration von 0,03 mg/mL zu analysieren. Des Weiteren konnte die Präsenz

von intakten Intra-Disulfidbrücken mittels Intaktmasse und MS^2-Fragmentierung bestätigt werden. Im letzten Teil wurden stressinduzierte Fragmente von zwei unterschiedlichen Antikörpern identifiziert und charakterisiert. Beide Antikörperfragmente konnten als Fc-Fragmente der schweren Kette identifiziert und der dazugehörige Spaltungsmechanismus vorgeschlagen werden. Diese Identifikation wurde nur durch die MS^2 Top-down-Messungen ermöglicht und wäre durch alleinige Intaktmassenbestimmung nicht realisierbar gewesen. Dies verdeutlicht die Bedeutung des dritten Teils dieser Arbeit.
Die hier präsentierte Arbeit zeigt die erste, online massenspektrometrische Charakterisierung von generisch CE(SDS)-getrennten Proteinen. Durch diese Intaktmassenbestimmung wird die Identifikation von Proteinen und Antikörperfragmenten deutlich unterstützt. Die Beobachtung von unerwarteten Migrationsreihenfolgen und die Messung von mehreren Intaktmassen von unterschiedlichen Proteoformen bei gleicher Migrationszeit, verdeutlichen die Limitierungen der optischen Detektion. Durch Top-down-Experimente konnte die Stärke der direkten Identifikation von Antikörperfragmenten und deren PTMs, wie die Präsenz von Disulfidbrücken, verdeutlicht werden, welche durch alleinige Intaktmassenbestimmung nicht möglich ist. Die direkte und eindeutige Identifikation der CE(SDS)-getrennten Proteine ermöglicht einen detaillierten Einblick. Dieser trägt zu einem besseren Verständnis der Proteinstabilität und -fragmentierung bei, das für den Herstellungsprozess und zur Sicherstellung der Wirksamkeit und Sicherheit von Biopharmazeutika von großer Bedeutung ist.

Eidesstattliche Erklärung

Ich habe die vorliegende Arbeit selbstständig verfasst, keine anderen als die angegebenen Quellen und Hilfsmittel benutzt und bisher keiner anderen Prüfungsbehörde vorgelegt. Von den in §27 Abs. 5 vorgesehenen Rechtsfolge habe ich Kenntnis genommen.

Bad Waldsee, den 20.05.2021

Jennifer Römer